Mechanism of exploding agents in food tablets

Xavier Mesnier

Department of Chemical and Biological Engineering

The University of Sheffield

A thesis submitted in partial fulfilment of the requirements for the degree of Doctor of Philosophy

March 2014

ABSTRACT

The complete reconstitution of food powders, from a solid to a homogeneous solution, is primordial for consumers. As a result food companies are putting more and more effort into understanding the mechanisms of powder reconstitutions: wetting, dissolution and disintegration. This thesis focuses on the disintegration of food powders and more specifically of food tablets such as stock cubes. Disintegration is the process of breaking down a powder aggregate, in this case a tablet, into multiple fragments thereby increasing the surface area of powder in contact with water. This results in a faster tablet dissolution. The disintegration of tablets can be improved with the use of certain types of ingredients called disintegrants. Such ingredients are very commonly used in pharmaceutical preparations; however these are new to the food industry. The purpose of this thesis is to investigate the possible use of food grade disintegrants, obtained from a natural source if possible, to decrease the reconstitution time of food tablets.

In order to do this, first the dissolution and disintegration of tablets of a food model powder, maltodextrin, were characterised experimentally. The results were then compared to a model developed in this thesis to obtain a better understanding of the dissolution and disintegration processes, prior to the incorporation of disintegrants. Subsequently, different food grade natural ingredients were selected and characterised to understand their mechanisms of action. The dissolution and disintegration of tablets of maltodextrin tablets containing different disintegrants were then investigated to decide which one was the most suitable. Finally, a novel method to study simultaneously both

dissolution and disintegration is presented. The method has proven to give valuable insights towards a better understanding of the reconstitution of food tablets.

Finally, recommendations to as which disintegrants, which concentration and which incorporation methods best suitable for a fast tablet dissolution and disintegration are given. Furthermore, the novel method developed in this work shows that the enhancement of the tablet disintegration can improve greatly the reconstitution time of food tablets.

ACKNOWLEDGEMENT

Firstly I would like to express my sincere gratitude to my academic supervisors, Professor Agba Salman and Professor Mike Hounslow for their support during my PhD study and continuous interest and enthusiasm for my work. I would also like to thank Nestle for funding this work and especially Professor Stefan Palzer, Dr. Gerhard Niederreiter, Dr. Tim Althaus and Dr. Laurent Forny for their support and valuable insight into my work.

I also would like to thank all the technicians from the department, Oz McFarlane, Mark McIntosh, Stuart Richards, Usman Younis for building the piece of equipment central to this research and for being always ready to help. A very special thought goes to Clif Wray and his family.

Obviously I would like to thank my fellow PPG colleagues for their help, encouragement and for making this experience unforgettable. A special thank to Selassie (Dr. D) for being so helpful and patient with teaching me about cameras and image analysis. Washino, thank you so much, for all your help in coding and maths, I am looking forward to visiting you in Japan. James, thanks buddy, I believe that our friendly competition helped us to go through the PhD in a more enjoyable way, I am glad you decided to do a PhD as well. A big thank you to Kate for proof reading my work so many times and to Menan for his valuable help in the lab. Finally, a massive thank you to all the PPG members for sharing this journey in the office, in the lab and in the pub.

For their continuous support and being so understanding, thank you to my family, mum, dad, my brothers and their growing family. Love you all.

PUBLICATIONS

Listed below are the publications resulting from this thesis.

Journal paper

- Mesnier, X., Althaus, T.O., Forny, L., Niederreiter, G., Palzer., Hounslow, M., Salman, A., *A novel method to quantify tablet disintegration.* Powder Technology, 2013. **238**(0): p. 27-34

Conference papers

- Mesnier, X., Forny, L., Niederreiter, G., Palzer, S., Hounslow, M.J., Salman, A.D., *A novel method to quantify tablet disintegration*. 5th International granulation workshop, Lausanne, 2011. Paper N°44
- Mesnier, X., Althaus, T., Forny, L., Niederreiter, G., Palzer, S., Hounslow, M.J., Salman, A.D., *Determination of dissolution regimes for tablets of maltodextrin*. 7th International Conference for Conveying and Handling of Particulate Solids - CHOPS 2012

CONTENTS

LIST OF FIGURES

.

LIST OF TABLES

NOMENCLATURE

Latin letters	Description
A	Surface upper and lower sides of a cylindrical tablet
a_w	Water activity
C	Concentration
C_s	Saturation concentration
C_1	Time for liquid penetration into tablets
$\mathcal{D}$	Diffusion coefficient
D_a	Diameter of the agitator
Dt	Tablet diameter
$d_{50,3}$	Volume based median size
F	Breaking force
F_d	Disintegration force
F_∞	Maximum disintegration force
H	Tablet thickness
h_c	Tablet thickness at minimum punch separation
h_l	Thickness of the diffusion layer
h_{24}	Tablet thickness after 24 hours of production
J	Number particles flux
k	Noyes and Whitney constant
K	Gordon and Taylor constant
K_e	Expansion rate constant
k_b	Bonding capacity constant
k_c	Mass transfer coefficient
m	Disintegration exponent
m_t	Tablet mass
n	Number density of particles
N	Rotational speed
p	Partial vapour pressure

p^{sat}	Saturation vapour pressure
Re	Reynolds number
S	Tablet surface area
Sh	Sherwood number
t	Time
T_g	Glass transition temperature
u_i	Velocity of the moving front
V	Tablet volume
V_0	Initial tablet volume
V_m	Volume of the dissolution medium

Greek letters	Description
ε	Tablet porosity
μ	Dynamic viscosity
ρ_a	Tablet apparent density
ρ_f	Fluid density
ρ_t	True density
$\bar{\sigma}$	Tensile strength of material at zero porosity
σ_t	Tablet tensile strength
τ	Total stress for disintegration
τ_p	Stress exerted by swelling of disintegrants
τ_w	Stress exerted by water
v	Volume of a single particle

CHAPTER 1 - INTRODUCTION

1.1 Dehydrated food products

Food products are often offered to consumers in a dehydrated form to decrease their transport cost and increase their shelf life. The most common products are instant beverages such as instant coffee, dehydrated soups or infant formulas, and kitchen aids such as stock cubes. In most cases, these products are agglomerated which is the process of sticking together primary particles to form larger aggregates. The aim of the agglomeration process is to enhance the powder properties such as flowability and dissolution speed. Dehydrated food products are presented in different forms such as fine powder, agglomerates or tablets (Figure 1-1).

Figure 1-1: Example of a dehydrated food product: coffee

In the food industry the consumers' expectations regarding products quality are extremely high. A fast, easy and complete re - hydration or reconstitution of the dehydrated products is required. Products dispensed in a tablet form have the advantage of delivering a constant amount of product. Tablets are made of several ingredients which originally exist in a powder form and are compressed together to produce uniform products. Thus the consumer can benefit in that the taste, flavour and appearance of the re-hydrated product will always be the same.

In general, the aim is to produce fast dissolving products and thus research and development in the food industry have focused on how to reduce the dissolution time. The dissolution is a multistep phenomenon starting with wetting and followed by a combination of transport of water and solid material into and out of the tablet resulting in the transformation of a solid into a solution (Marabi 2008). The dissolution is often accompanied with disintegration which is the process of breaking up the tablet into smaller pieces. This process increases the dissolution rate by increasing the surface area available for dissolution to occur. Such a process is helped by the use of disintegrants. More details about disintegrants are given in Chapter 2. Disintegrants are commonly used in the pharmaceutical industry; however, the food industry has only recently shown an interest for their potential use.

1.2 Aims

The work carried out in this thesis aims at studying the possible use of disintegrants to reduce the dissolution time of food tablets. The following questions will be answered:

- Can natural ingredients displaying a disintegrant function be found and used in food tablets? Indeed, the negative consumer's perception towards E-numbers and ingredients holding a "chemical name", such as the disintegrants used in the pharmaceutical industry, pushes to find and investigate new natural sources for disintegrants.
- Is the use of disintegrants in food tablets beneficial for the overall reconstitution of the products?
- Can we provide further understanding into the tablet disintegration process? As it will be highlighted in the literature review (Chapter 2), the disintegration process is still not well understood.
- What is the relationship between dissolution and disintegration, and how do they affect each other?
- Can a simple model be developed to predict the overall reconstitution of a tablet in water?

1.3 Outlook

The thesis is organised in 4 main parts. In the first main part, the introduction, literature review and materials & method (Chapters 1 to 3) give the necessary background information for the reader to understand the thoughts behind this work.

In the second part (Chapter 4), the dissolution of the main material used in this study is investigated. This part gives important insights to understand the dissolution of a food model tablet before any disintegrants are introduced. Chapter 4 is based on two subparts; first the experimental results are explained and are then compared to a mathematical model specially developed for this work.

In the third part (Chapters 5 and 6), different disintegrants are sourced and characterised (Chapter 5) before being introduced in food tablets. Chapter 6 investigates the influence of these disintegrants and their concentrations on the dissolution time and on the tablets properties.

In the fourth part (Chapter 7 and 8), a novel method to study both tablet dissolution and disintegration is introduced (Chapter 7). The results and insight obtained with this novel method are explained in Chapter 8.

Finally, Chapter 9 will conclude this work and open to the future work which should be carried out to further the knowledge in tablet dissolution and disintegration based on the work done in this thesis.

CHAPTER 2 – LITERATURE REVIEW

2.1 Introduction

In this chapter, the work which has been carried out by other authors in the field of tablet dissolution and disintegration is reviewed. The dissolution and disintegration of maltodextrin, a polymer carbohydrate, which is used as a food model in this study, are also reviewed. The chapter will highlight the fact that the understanding in this field is far from being complete and that research into food tablets dissolution and disintegration is limited.

2.2 Tablet reconstitution in water

The reconstitution of a food tablet in water involves the complete transformation of a solid product into a solute state. From a consumer's point of view, the tablet reconstitution is complete when the product's original state is obtained, such as coffee or stock. This means that when a homogenous liquid is obtained, without any lumps or non-dissolved powder. The tablet reconstitution is a multistage action based on the following processes: wetting and sinking, disintegration and finally dissolution. Wetting of the solid and sinking into the bulk of the solvent are the first necessary steps. Disintegration and dissolution will occur next, simultaneously, and both will affect each other (Forny, Marabi et al. 2011). The following sections introduce each process and emphasise the disintegration and dissolution processes which are of interest in this work.

2.2.1 Wetting

Wetting is often considered as a separate subject to dissolution as it is not only of interest to its link with the dissolution process. When the solvent, water in this context, comes into contact with the surface of the solid, in this case a tablet, a three phase interaction, solid-liquid-gas, occurs. In order to optimise the dissolution behaviour, it is better to have a favourable interaction between the liquid and solid phase. Good wetting and spreading of the solvent is thus an elementary aspect of rapid dissolution (Fukami, Yonemochi et al. 2006). The wetting of liquid over a solid surface is the result of molecular interactions between these two phases. A surface which is covered by a hygroscopic material such as a carbohydrate will present favourable wetting properties. To characterize the wettability of a solid it is common practice to look at the contact angle, a

measure of the equilibrium of surface tensions between the three phases. Many parameters such as density, porosity, surface charges, surface activity, polarity were shown to influence the wetting ability of a material (Marabi 2008). In this study, maltodextrin is used as the model product. It is a polymer carbohydrate which presents favourable wetting characteristics.

2.2.2 Dissolution basics

Any chemical reaction has kinetic and thermodynamic aspects. For dissolution to occur, the main reactants must in a favourable condition for the process to occur. The advantage of dealing with food powders is that, generally, their dissolution is thermodynamically favourable; an obvious exception being fat. In this work, a carbohydrate was chosen for its ability to dissolve in water. The thermodynamics of the dissolution process will not be approached as the interest is not focused on whether a material will dissolve but on how fast will it dissolve. Therefore; in the following section, the kinetics of dissolution will be discussed.

A short history of the research into dissolution is given before focusing on the dissolution of polymers as the material of interest in this work is a polymer carbohydrate.

2.2.2.1 Kinetics

Dissolution is a heterogeneous process since it takes place on the solid–liquid phase boundaries. It generally involves three main steps (Marabi 2008):

- (i) Supply of solvent at the surface of the system

- (ii) Transition of the solid into solute state at the interaction of solid-solvent

- (iii) Transport of the solute away from the solid by diffusion or convection

The slowest of these steps exercises a dominating influence upon the rate of dissolution.

The first to study the kinetics of the dissolution process were Noyes and Whitney. They carried out the first dissolution experiments in 1897 (Dokoumetzidis and Macheras 2006). They noticed that the rate of dissolution is proportional to the difference between the instantaneous concentration in solution C, at time t, and the saturation concentration, Cs. The following mathematical expression was defined to summarise their finding:

$$\frac{dC}{dt} = k(C_s - C) \qquad \text{Eq. 2-1}$$

where k is a constant.

Noyes and Whitney hypothesized the dissolution mechanism is based on the existence of a thin diffusion layer around the solid-liquid interface through which the molecules diffuse to the bulk aqueous solution. The rate at which the molecules diffuse is the limiting rate for the dissolution process.

Later on, in 1900, Brunner and von Tolloczko furthered the research of Noyes and Whitney and Eq. 2.1 by introducing the surface area S to give (Siepmann and Siepmann 2013);

$$\frac{dC}{dt} = K_1 S(C_s - C) \qquad \text{Eq. 2-2}$$

In this case k becomes $k=K_1S$, with K_1 becoming the resulting constant.

Finally, a more complete equation of Nernst and Brunner was published in 1904 (Siepmann and Siepmann 2013). In this work, the Fick's second law was introduced to complete the diffusion layer theory to give:

$$\frac{dC}{dt} = \frac{DS}{V_m h_l}(C_s - C) \qquad \text{Eq. 2-3}$$

Where D is the diffusion coefficient, h_l the thickness of the diffusion layer and V_m the volume of the dissolution medium.

The different works introduced above are based on the fact that the diffusion layer model is the physical explanation for the dissolution process. In this model,

the dissolution kinetics are limited by the diffusion of the dissolved molecules through a film surrounding the solid surface. Other approaches and models were developed but the diffusion layer model remains the most attractive (Dokoumetzidis and Macheras 2006).

The dissolution of tablets has been extensively studied in the pharmaceutical industry and numerous parameters were found to have an influence on the dissolution time. Liquid properties such as viscosity, surface tension, temperature etc. and on the other hand powder properties such as particle size, density, porosity, chemical composition etc., were found to significantly influence the kinetics of powder dissolution (Costa and Sousa Lobo 2001).

The dissolution of a polymeric material involves additional mechanisms to the ones introduced above. It includes solvent diffusion inside the polymer and polymer chain disentanglement which is also a transport process (Miller-Chou and Koenig 2003). When the solvent (water in this case) diffuses inside the polymer, a gel layer is created due to the transition from the glassy to the rubbery state of the polymer. Polymer dissolution presents also an induction time after which the polymer starts to dissolve.

Polymer dissolution can be either limited by the disentanglement rate of the polymer chains or by one of the transport mechanisms; diffusion of water inside the polymer or the diffusion of the polymer chains away from the surface.

Ueberreiter (1968) summarized the dissolution process of a polymer by representing the surface layers in 6 stages: starting from the pure polymer, infiltration layer, the solid swollen layer, the gel layer, the liquid layer and finally pure solvent. Figure 2-1 gives a representation of these different layers in a tablet.

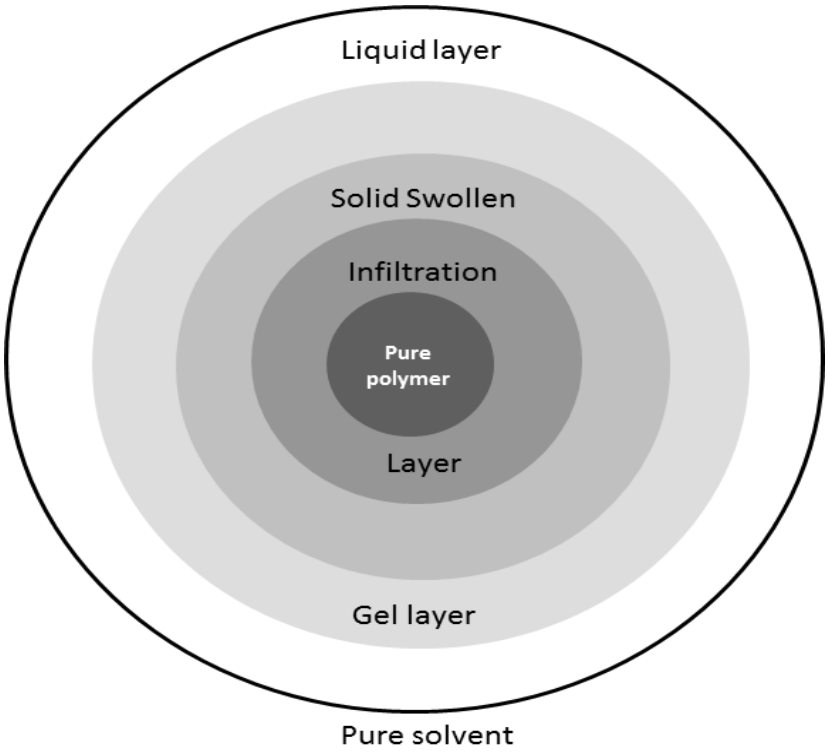

Figure 2-1: Different layers in the dissolution of a polymer tablet according to Ueberreiter (1968)

According to Ueberreiter (1968), the infiltration layer represents the filling up of the free volume within the solid polymer by the solvent molecules. In this step, the solvent starts diffusing within the polymer but no polymer transfer is yet occurring. In the next layer, the solid swollen layer, the polymer starts swelling due to the entrapment of solvent in between the polymer chains. However, at this stage the polymer is still in the glassy state. Next, the polymer passes from the glassy to rubbery state and the gel layer is formed. This layer is surrounded by a liquid layer containing the solvent and the detached solid. The last layer is composed of pure solvent.

However, some polymers do not follow this type of dissolution. Another mechanism was proposed where no gel layer is formed. In this case, small blocks of polymer erode and leave the surface. This phenomena was first reported by Asmussen and Raptis (Miller-Chou and Koenig 2003).

The effect of different parameters on the dissolution of polymers has been reported in the literature. The influence of polymer molecular weight has been investigated. It was found that polymers with high molecular weight present slower dissolution than polymers with a lower molecular weight (Cooper, Krasicky et al. 1985). This was explained by the fact that the dissolution time is controlled by chain disentanglement which is longer for high molecular weight polymers. Other parameters such as structure and composition were also investigated.

The dissolution of polymers has been extensively studied in the pharmaceutical industry as such components are used in the controlled release of drugs in the digestive system (Kazarian and Weerd 2007). The polymer forms a rubbery phase upon wetting. Due to the increase in free volume, the drug starts diffusing from within the tablet to the outside environment. The type of polymer used and its characteristic swelling upon wetting can be used to control the timescale of drug delivery. Bettini et al., (1994) studied the swelling, erosion and gel formation of a hydrophilic matrix and proposed a model in which the matrix dissolution was described by the movement of the boundaries between the glassy core and rubbery gel and dissolution medium. In addition, a front corresponding to the dissolution of the drug inside the matrix has been identified. This explanation was then confirmed by Colombo et al (1995). However, an alternative explanation of the fronts was provided by Gao and Meury (Gao and Meury 1996). In their work

the fronts were studied with the use of an optical technique and an additional front was recognised as being the true penetrating front where water penetrates the glassy polymer but no gel has formed yet. It means in this case that there is a lapse of time between the water ingress and the occurrence of the glass transition. This explanation is in agreement with the work of Ueberreiter (1968). Additionally, experiments conducted by Kazarian and Weerd (2007) tend to work in favour of the explanation by Gao and Meury (1996) but no consensus has been reported.

2.2.2.2 Experimental assessment of dissolution

In the pharmaceutical industry polymer dissolution would be related to the drug dissolution which can be followed by conductivity measurements (Brielles, Chantraine et al. 2008) or using the conventional USP method (U.S. Pharmacopeia or European Pharmacopeia). In this technique, the sample is introduced into standard cells and the mixing regime is determined. The dissolution of the drug molecule is then followed by spectrophotometric measurements as a function of time.

However, one of the main characteristics of the polymer dissolution which has been studied is the rate of front movement. Most of the attention has been spent on the swelling rate as it is believed to control the diffusion of the drug inside the tablet and thus its release from the tablet. Mikac et al., (2010) studied the swelling of xanthan tablets using Magnetic Resonance Imaging (MRI). Different authors have employed simpler imaging techniques such as photo or video and image analysis to measure dimensional changes during dissolution. Coloured drugs or coloured solvents are usually employed to facilitate the front's detection. In these

experiments, the tablet is often fixed in between two slides of glass; water is thus only penetrating the tablets from the lateral surface (Zuleger, Fassihi et al. 2002).

Other techniques based on a penetration probe in the gel layer of a swollen tablet have been utilised (Zuleger, Fassihi et al. 2002). They have been used to investigate the gel thickness and structure by measuring the resistance to the probe penetration (Sriamornsak, Thirawong et al. 2007).

Kravtchenko et al. (1999) developed a simple method for determining the dissolution kinetics of soluble polymer powders. The amount of hydrocolloid dissolved was followed via the torque on a modified rotational viscometer.

2.2.2.3 Modelling of the dissolution process

The various approaches to model the dissolution of amorphous polymers have taken into account phenomena such as the viscoelasticity of the polymer, disentanglement of polymer chains and external transfer limitations (Miller-Chou and Koenig 2003). When modelling the dissolution of polymers, several parameters should be considered. First, due to the uptake of water, the polymers swell resulting in a change in the dimensions, concentration and molecular mobility. Second, the polymer dissolves, thus the matrix composition is changing with time as well as the diffusion parameters.

The way polymer dissolution has been modelled can be grouped into three main approaches:

1. Phenomenological models using Fickian equations (Tu and Ouano 1977; Moore, Croy et al. 2000). These models are based on Ficks equation of diffusion together with expressing mathematically the moving boundaries during the dissolution process.
2. Models with external mass transfer as the controlling resistance to dissolution (Lee and Peppas 1987; Lee and Lee 1991). In these types of models the assumption is made that the dissolution is controlled by the resistance offered by the layer surrounding the polymer.
3. Stress relaxation models and molecular theories (Herman and Edwards 1990). In these types of models the dissolution is controlled by the relaxation of the polymer.

A complete review of the different models present in the literature to model polymer dissolution has been carried out by Miller, Chou and Koenig (2003).

The dissolution of food powders has mainly been studied through the dissolution behaviour of bulk powder which is of interest when investigating the dissolution of instants product such as coffee, infant milk and soups. However, almost no work has been published on the dissolution behaviour of food tablets. In general custom made apparatus are developed in these studies in comparison with the standardized methods used in the pharmaceutical industry (Marabi, Mayor et al. 2008).

2.2.2.4 Dissolution of maltodextrin

Very few papers deal with the dissolution of maltodextrin. Papadimitriou (1992) evaluated different grades of maltodextrin (different Dextrose Equivalent number) for tabletting and their dissolution rates. They noticed that the compression load during tabletting did not have any influence on the release rate of a drug included in the formulation. However, the stirring speed during dissolution in an U.S.P. apparatus was found to influence the release rate of drugs. In addition, the comparison of dissolution of maltodextrin with or without magnesium stearate used as a lubricant showed that the addition of magnesium stearate resulted in a slower drug release rate. Magnesium stearate is apolar and acts by covering the particles of maltodextrin. During dissolution, water is repulsed and the penetration of water inside the polymer matrix takes longer (Chouk, Gururajan et al. 2009).

2.2.3 Disintegration process

The main role of the disintegration process is to expose a larger surface area of solid to the solvent to increase the dissolution rate by breaking down the original structure of the tablet into small fragments (Melia and Davis 1989a) (Figure 2-2).

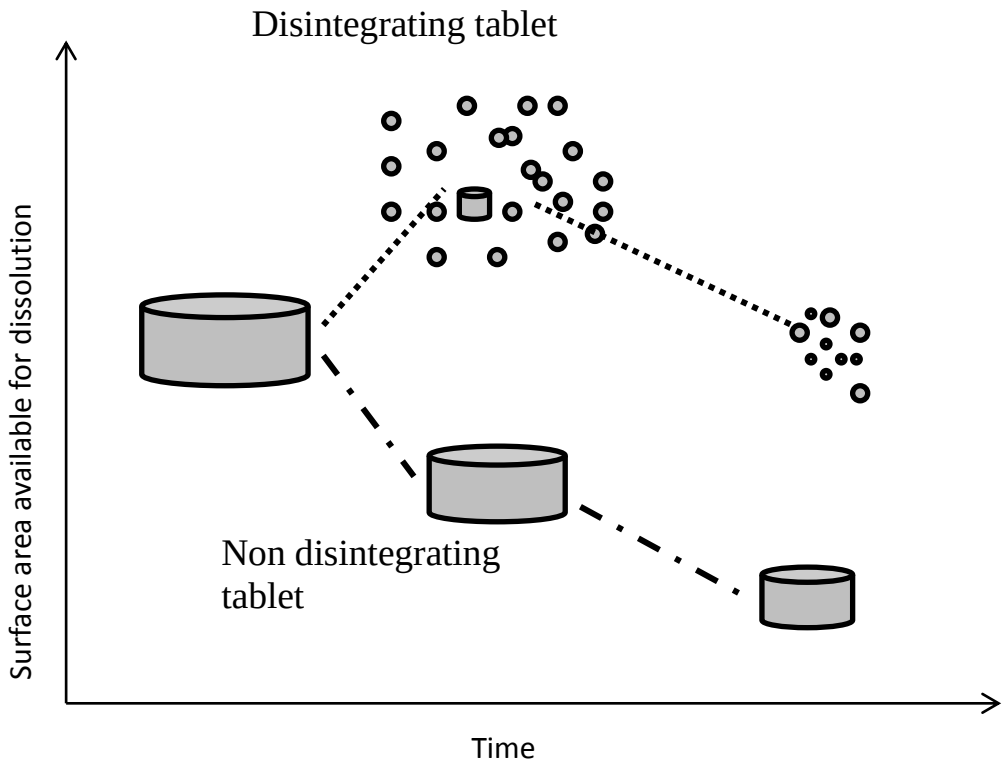

Figure 2-2: Difference in surface area available for dissolution in the case of disintegrating or non disintegrating tablets

In the pharmaceutical industry, the disintegration of tablets is enhanced by the use of disintegrants. A definition of disintegrants is given in the Handbook of Pharmaceutical excipients (2004): " Disintegrants are substances or mixture of substances added to the drug formulation that facilitate the breakup or disintegration of tablets content into smaller particles that dissolve more rapidly than in the absence of disintegrants". This definition is specific to the pharmaceutical industry as it refers to drug formulation. Disintegrants have been very lately introduced into the food industry, mainly in the formulation of neutraceutical products (Dhere and Patwekar 2011). Disintegrants are generally

derived from two types of product: starch and microcrystalline cellulose. Recently superdisintegrants have been introduced. They are more effective agents and can be used at lower concentrations in the tablet formulation (Zimmer, Belniak et al. 2011). Common superdisintegrants used in the pharmaceutical industry are: Ac-Di-Sol (FMC biopolymer, Croscarmellose Sodium), Primojel (DMV-Fonterra, Sodium Starch Glycolate), Explotab (JRS pharma, Sodium Starch Glycolate), etc.

Disintegrants are added either prior to granulation (intragranular) or prior to tablet compression together with granulated material (extragranular) or in direct tablet compression. It is commonly believed by powder technologists that disintegrants present in the extragranular fraction facilitate the breakup of the tablet to granules. Adversely, disintegrants present in the intragranular fraction help the disintegration of the granules to fine primary particles. A combination of both methods should allow complete disintegration of first to granules and then to fine particles (Gordon, Chatterjee et al. 1990).

The disintegration process has been extensively studied in the pharmaceutical industry. However, it was mainly studied to quantify the time required for a particular formulation to disintegrate (Fukami, Yonemochi et al. 2006). Few papers relate the mechanisms involved in the disintegration process and try to understand the type of forces which are implied to overcome the bonding force inside a tablet.

Several mechanisms of disintegrants have been postulated but their effect on tablet disintegration is still not well understood (Fukami, Yonemochi et al. 2006). The different possible mechanisms which have been reported are:

- Swelling: disintegrant particles swell in contact with water and induce stress inside the matrix causing it to breaking down. (Melia and Davis 1989b; Weitschies, Hartmann et al. 2001; Fukami, Yonemochi et al. 2006).
- Wicking: disintegrants which have a fibrous structure absorb water quickly. During the course of the water ingress into the tablet, physical bonding inside the tablet is broken (Fukami, Yonemochi et al. 2006).
- Deformation: When exposed to water, particles in the tablet swell to precompression size leading to localised stresses. This mechanism differs from swelling by the fact that the stress is not only due to the use of disintegrants (Luginbühl and Leuenberger 1994).
- Repulsion: when water is drawn into pores due to capillary action or due to the disintegrant, repulsive electrical forces are created which lead to particle repulsion (Luginbühl and Leuenberger 1994). However, this last mechanism has not been well supported by researchers as pointed out by Zhao and Augsburger (2006).

Based on the chemical composition and physical state of disintegrants, it can be assumed that not only one of these mechanisms is taking part in disintegration but several which act simultaneously.

Despite all the theories which have been proposed, there is still a lack of understanding of the mechanism of disintegration. However, the swelling of

disintegrants is apparently the most widely accepted mechanism for tablet disintegration as most of the disintegrants swell in contact with water but at different degrees (Chang, Shinwari et al. 1998; Zhao and Augsburger 2006). Irrespectively of the mechanism involved in the disintegration, the water uptake is the first step necessary for tablet disintegration. The water uptake can be caused by the capillary forces inside the pores or by diffusion of water in the case of a hydrophilic material. The ability of the constituent to draw water inside the tablet is an essential parameter for disintegration and dissolution (Iyad, Mayyas et al. 2008). Thus the hygrocapacity of the disintegrants is a very important parameter to study when comparing the action of different disintegrants.

Different parameters believed to have an influence on the disintegration process have been studied: porosity, pore size distribution, physico-chemistry of the ingredients (ie. is it a polar or apolar material?). These parameters are related to the processing conditions and the different types of ingredients. Other parameters related to the disintegrants themselves have been found to influence the disintegration, such as particle size, swelling capacity, rate and extent of water uptake (Bolhuis, Zuurman et al. 1997; Yunxia, Yorinobu et al. 1999; Yamamoto, Fujii et al. 2009). The disintegrant efficiency is related to factors which influence the water accessibility to the disintegrants in tablets. Such factors are tablet solubility, tablet hygroscopicity, tablet porosity and incorporation method (Johnson, Wang et al. 1991; Villiers 2003).

Due to the high hygroscopicity of disintegrants, several studies have been conducted on the influence of storage conditions. It has been shown that storage at high relative humidities decreases the disintegrant efficiency (Villiers 2003). This could be explained by the fact that less water will be absorbed by

disintegrants when dissolution occurs as they have been in contact with water previously. In this case, water molecules are already linked to the disintegrants preventing more water from bonding to it. Thus the swelling of disintegrants, leading to the breaking up of tablets, which is caused by the sorption of water, cannot occur anymore or will occur to a much lesser extent (Villiers 2003).

Ferrero et al., (1997) studied the effect of the concentration of superdisintegrants on the porosity and disintegration time of tablets of microcrystalline cellulose. They reported that the disintegrant particles form a continuous network or skeleton in the tablet which tends to increase the plastic deformation during compression leading to high density tablets. It was suggested that there is a concentration limit over which this network can be formed (close to 7.6% in their case). However, at higher concentrations they noticed that the disintegration time was increasing. The same phenomena has been reported by Gonninssen et al., (2008) and by Bolhuis (1997) and was explained by the fact that the swollen disintegrants formed a gel which blocked the water from penetrating inside the pores.

2.2.3.1 Tablet disintegration characterisation

When comparing and studying the efficiency of different types of disintegrants, two main techniques have been used.

Firstly, the disintegration time is determined using a tablet disintegration tester unit according to the US or European pharmacopeia method (Luginbühl and Leuenberger 1994; Ferrero, Muñoz et al. 1997). In this test, tablets are placed on a mesh under different conditions of temperature and agitation in a fixed volume

of liquid. The disintegration time is determined as the time for the tablet to disintegrate and pass through the mesh screen. This technique provides a disintegration time which is useful when comparing different drug formulations as it is in the pharmaceutical industry. However, it does not provide any details about the mechanisms implied in the disintegration of tablets.

Secondly, many authors tried to relate the disintegration process with the amount of water penetrating into the tablet with time (Pesonen, Paronen et al. 1989; Luginbühl and Leuenberger 1994; Brielles, Chantraine et al. 2008). Tablets are located on a porous holder above a liquid. The liquid penetration from the bottom is followed with time by use of an imaging system (water is usually dyed to help the image analysis) or by weighing the amount of water leaving the solution when penetrating the tablet. Usually data is analyzed using the Washburn equation to describe the capillary flow in the tablet pores. The determination of the wetting kinetics have been reported to depend on the porosity of the tablet and wettability of the pores for non-dissolving material (Luginbühl and Leuenberger 1994).

The comparison and characterisation of disintegrants has also been assessed via the study of moisture sorption, hydration and swelling capacity (Adebayo, Brown-Myrie et al. 2008).

2.2.3.2 Modelling of the tablet disintegration

As a lot of uncertainties remain surrounding the action of disintegrants, very few papers present models to explain the disintegration process. Caramella et al (1988) presented a model where they expressed the disintegration force F_d with time *t*, with the following equation:

$$\frac{F_d}{F_\infty} = 1 - \exp(-k_e t^m) \qquad \text{Eq. 2-4}$$

where F_∞ is the maximum disintegration force, the parameter k_e is the expansion rate constant and *m* is an exponent which varies as a function of the composition of the tablet tested.

This model is based on the assumption that disintegration occurs in layers parallel to the surface of the largest area of the tablet. And thus, disintegration is limited by either the detachment of these layers from the surface of the tablet or the transport of the layer away from the solid – liquid interface. The values of k_e and m indicate, according to the authors, which process from detachment or transport is limiting the tablet disintegration. It is worth mentioning that this model was developed for non-soluble components. This model is very specific to the research conducted and does not provide any physical explanation of the disintegration process.

Later, Peppas and Colombo (1989) introduced another model based on the physical characteristics of the disintegration process. This model was again developed for non-dissolving material. The model is based on experimental measurement of the force during disintegration. A tablet is placed on a porous

support and entrapped in a cylinder. A plate is placed on the top surface and thus water is only allowed to penetrate from the bottom of the tablet through the porous support. A transducer is located on the top plate to measure the force exerted during the disintegration process.

The stress exerted during the disintegration process has been expressed by the following equation:

$$\tau = \frac{F_d}{A} = C_1 + \tau_w + \tau_p \qquad \text{Eq. 2-5}$$

where τ is the total stress which is measured as the force F_d throughout the tablet surface A. τ_w expresses the stress exerted by the water when entering the pores of the tablet. τ_p expresses the stress generated by the swelling of the disintegrants when in contact with water. An additional parameter C_1 has been introduced according to the authors to take into consideration that there is a period of time required for the water to fill into the pores and during which no force is measured. The authors describe it as a constant with a negative value.

The authors fitted equation 2-5 and presented a good correlation with the experimental results obtained from the method presented above. It shows that the force developed is a linear function of the quantity of water penetrating the tablet.

2.2.3.3 Disintegration of maltodextrin tablets

Mollan and Celik (1993) studied the disintegration of maltodextrin tablets. They noticed that the compression force during tabletting had relatively no impact on the disintegration time. Moreover they noticed that for tablets made from a compression pressure higher than 75MPa, no correlation could be drawn between the crushing strength and disintegration time. It was concluded that the maltodextrin tablet disintegration was not controlled by the tablet porosity. They noticed the formation of a gel layer around the tablet.

Another study investigated the disintegration of maltodextrin but not in a tablet form this time. Gonnissen et al. (2008) attempted to spray dry a mixture containing maltodextrin and a superdisintegrant among other ingredients. It was noticed that an increasing amount of maltodextrin in the formulation had a negative impact on the disintegration time. However, this study showed that during the spray drying most of the disintegrants were lost due to sticking to the walls of the spray drier and thus it was difficult to draw any conclusions.

2.3 Chemical and physical properties of food powders

According to the supra-molecular structure of food powders, three different types of water soluble materials can be distinguished: amorphous (such as polymer carbohydrates), crystalline (such as salt and sugar) and semi-crystalline which are partly amorphous and contain a crystalline region (starch for example) (Palzer 2010).

In the crystalline state, the atoms are well arranged in a regular lattice. In the amorphous state, molecules are in a disordered form in comparison to the crystalline state. The formation of an amorphous or crystalline material is strongly related to the molecular mobility. The molecular mobility is a function of the free volume which is available for the motion of molecules. The free volume corresponds to the voids and holes in a molecular matrix. If the temperature of a system is increased the molecular mobility and the free volume will also increase. However, it will increase differently for crystalline and amorphous materials. The molecules in a crystalline material, when heated, will vibrate around their position until the melting point is reached where the structure breaks down. This process is reversible if the solution is cooled down slowly. The free volume in an amorphous matrix will increase while heated and allow the rotation of molecules. The product passes from the glassy to the rubbery state. This transition is called glass transition and characterised by the glass transition temperature. However, this process does not happen at a specific temperature but rather between an interval whose onset or midset are taken as the glass transition temperature (Roos 1995a).

Amorphous products are commonly formed through rapid cooling of a liquid melt in which the molecules do not have time to reorganize. The molecules are "frozen" in their original position. In the glassy state, there is not enough energy for molecules to move and arrange themselves in an organised order (Palzer 2010).

Crystalline and amorphous substances are characterised by different material properties such as hygroscopicity, hygrosensivity and mechanical properties. These properties will influence the way material interacts with other components and especially with water which is of interest in a dissolution and disintegration study.

The hygrocapacity of a powder describes its ability to bind with water. The water can be absorbed into the material molecular matrix and/or adsorbed on the free surface area of the material. It is usually demonstrated by building the sorption isotherm of a powder at a certain temperature. The sorption isotherm relates the amount of water present in a product at different water activities. The water activity (a_w) corresponds to the partial vapour pressure (p) exerted by a food product divided by the saturation vapour pressure of water (p^{sat}) at the same temperature.

$$a_w = \frac{p}{p^{sat}} \qquad \text{Eq. 2-6}$$

The water activity is an indicator of the availability of free water in a food product. At equilibrium, the water activity of a product equals the relative humidity in the surrounding air (Roos and Benjamin 2003). The amount of water absorbed by the hydrophilic powder is a function of its water activity and thus the relative humidity of the surrounding air. The water content of food product at a given water activity is not only a function of the chemical composition, the supra-molecular and micro structure, but also temperature (Palzer 2007).

Amorphous food substances adsorb increasing amounts of water with increasing relative humidity. This water is stored within the free volume inside the amorphous product. The water stored has a plastifying effect which means that the viscosity and elasticity of the material decreases with increasing water content (Palzer 2009). On the contrary, crystalline powders do not absorb significant amounts of water while increasing the relative humidity in the surrounding air. This is due to the fact that only a limited amount of water can be embedded in the molecular matrix. However, once a specific relative humidity level is reached (the value varies for different crystalline materials), the crystal starts to dissolve layer by layer (Roos and Benjamin 2003). For amorphous products, it is not possible to determine a relative humidity at which it will dissolve. When an increasing amount of water is added to an amorphous product, during dissolution for example, the water is stored within the matrix until a dilute solution of the substance is obtained (Palzer 2010).

The hygrosensivity describes how the physico-chemical properties of hydrophilic food materials vary with changes in water content. In the case of crystalline products, properties such as viscosity vary very little with the water content compared to changes noted for amorphous products.

Generally at the glass transition temperature, two main types of physical properties are changed: the rheological properties and thermodynamic properties (enthalpy, heat capacity and expansion coefficient). When exceeding the glass transition (from glassy to rubbery), the material becomes more and more ductile, and therefore, the viscosity decreases (Roos 1995a). As a result, different techniques have been developed based on these properties to measure the glass transition temperature such as differential scanning calorimetry (measures a change in specific heat), and dynamic mechanical analysis (measures a change in mechanical properties) (Roos 1995b). However, it is worth noting that the resulting measured glass transition is dependent on the technique used and the temperature/time gradient used.

The glass transition temperature is dependent on the molecular weight of the material and the water content. Gordon and Taylor describe the relationship between glass transition and composition with the following equation (Gordon and Taylor 1952):

$$T_g = \frac{x_1 T_{g1} + K x_2 T_{g2}}{x_1 + K x_2} \qquad \text{Eq. 2-7}$$

where T_g, T_{g1}, and T_{g2} are the glass transition temperatures of the binary mixture (˚C), component 1, and component 2, respectively, x_1 and x_2 are the molar fractions or weight fractions of components 1 and 2, respectively, and K is the arithmetic average of a series of K values that are obtained by solving the equation for a series of binary systems at different ratios of components 1 and 2.

This equation can be used to relate the influence of water content of the powder on the glass transition temperature. From Equation (2-7) it can be deduced that the glass transition temperature will decrease with increasing powder water content.

During the dissolution process the product will encounter the glass transition and the material will pass from the glassy to rubbery state where, as described earlier, molecular mobility and free volume is increased influencing the diffusion of the solvent penetrating the tablet.

2.4 Production of food tablets

Tablets are produced from the compression of different ingredients found in a powder form. Different compression techniques can be used to produce such a tablet. In the food industry, the preferred process is direct compression as it is a fast and economic process. The raw formulation is compressed directly from the powder mixture, thus no granulation step is carried out prior to the tabletting.

The tabletting process can be divided into four different steps:

- filling of the powder in the die

- compression (deformation and breakage of particles)

- decompression (elastic re-expansion of the tablet)

- tablet ejection

Most food tablets contain amorphous substances that deform visco-elastically when a stress is applied (Palzer 2007). The final property of the tablet will thus depend on the pressure load, the dwelling time (the time the pressure is applied), and the mechanical properties of the material. In addition, each of these parameters is a function of temperature and moisture content of the powder. It was observed that an increase in moisture and temperature will lead to more plastic deformation (Palzer 2007). Malamataris and Karidas (1994) investigated the influence of moisture content on the strength of HPMC (hydroxypropyl methylcellulose) tablets and noticed that the tablet tensile strength increases when the moisture content increases and reaches a maximum before decreasing at high moisture contents.

During the compression, the density of the tablet increases. The distance between single particles decreases and the contact area increases. In addition, particles may deform and break. The most important intermolecular force which holds the particles together are Van der Waal forces (Pitt and Sinka 2007). These forces are a function of the number of contact points between the particles which occur during compression. Additionally, interlocking of primary particles may occur and increase the strength of the tablet. Moreover, at the contact points amorphous materials might sinter which is the result of a temperature increase due to particle friction and presence of water due to capillary condensation (Palzer 2007). The presence of sinter bridges would greatly increase the adhesion forces between the particles as due to the presence of solid bonds.

2.5 Conclusions

The literature reviews on experimental techniques used to study both the dissolution and the disintegration revealed that most of the techniques employed provide very little information on the mechanisms behind the two processes. Most of the techniques simply follow the concentration of certain constituents but do not provide full explanations of the phenomenon implied. In addition, dissolution and disintegration have been studied separately whereas they should be considered together as they are happening simultaneously and affecting each other. Considering these problems it was thus necessary to develop a new approach which would present the ability to follow both the dissolution and disintegration process. Moreover, the distinction of disintegration from dissolution is necessary to gain knowledge; as this is still a not very well understood process.

One of the most promising techniques which has shown an increasing interest among scientists in the past decade is image analysis. One of the advantages of image analysis is the ability to follow the dissolution of tablets with time and being able to keep record of a sequence of events happening during the dissolution process and have a visual proof. It allows an accurate measurement of the tablet dimensions with a non-invasive technique without disturbing the process of dissolution (Manuel and Konstantinos 2009).

Many authors have used imaging analysis techniques to follow the dissolution of tablets (Bettini, Colombo et al. 1994). Lately, Chirico et al. (2007) investigated the erosion and swelling fronts in swelling hydroxypropyl methylcellulose (HPMC) tablets. In their work, the tablet is placed between two Plexiglass slabs

and the light intensity (grey scale) passing through the tablet is recorded as a function of the tablet radius. The dry core is white as it does not let light pass through its structure, whereas the swelling part is represented by a darker halo. However, image analysis was not used to follow the combination of dissolution and disintegration.

In addition, the use of an image analysis technique can allow the direct measurement of the size distribution of particles during dissolution. Even though, such data were experienced to be difficult to gather by other authors. It was reported by Zhao and Augsburger (2006) that they have made several unsuccessful attempts to obtain direct measurements of the size distribution of particles during disintegration. Methods such as optical microscopy, laser scattering and sieving were tried in the case of a non-dissolving matrix. They put forward that particle sifting or hardening were experienced.

CHAPTER 3 – MATERIALS AND METHODS

3.1 Introduction

This chapter introduces the different materials which were used in this work as well as the different techniques which are commonly referred to in all chapters. In the first part, maltodextrin which is the main ingredient used in this work is defined and followed by only general information about disintegrants as a specific chapter is later dedicated to disintegrants (Chapter 5). In the second part, the different methods used to produce tablets, measure their dissolution time t_{90} and tensile strength are described.

3.2 Materials

3.2.1 Maltodextrin as a food model product

Maltodextrins are mixtures of poly and oligosaccharides. They are generated from starch by enzymatic or acidic hydrolysis. They are described by their dextrose equivalent number (DE). The DE number is a measure of the amount of reducing sugar, related to glucose, of a carbohydrate. The more advance the hydrolysis, the higher the DE number and the shorter is the carbohydrate chain length. Generally, maltodextrins have a DE number lower than 20. Above this number the term glucose syrup is more commonly used (Rong, Sillick et al. 2009).

Amorphous spray dried maltodextrin IT21 (Glucidex® 21 – DE21) was purchased from Roquette (France). It is the main material that is used in this work. It is a white, hygroscopic spray-dried powder. It is mainly used in the food industry as a thicknening agent. It can be found in products such as instant coffee, instant soups and bouillon cubes. Maltodextrin IT 21 was chosen as it can be considered as a food model powder. The understanding of the dissolution behaviour of maltodextrin can be extrapolated to the dissolution behaviour of other amorphous food powders.

For this study, maltodextrin powder was equilibrated prior to tablet production at a water activity of a_w=0.3. Indeed, for an amorphous material behaving visco-elastically such as maltodextrin, the water content of the powder will influence largely the compression behaviour of the powder (Palzer 2005). Figure 3-1 shows the cumulative size distribution of maltodextrin IT21.

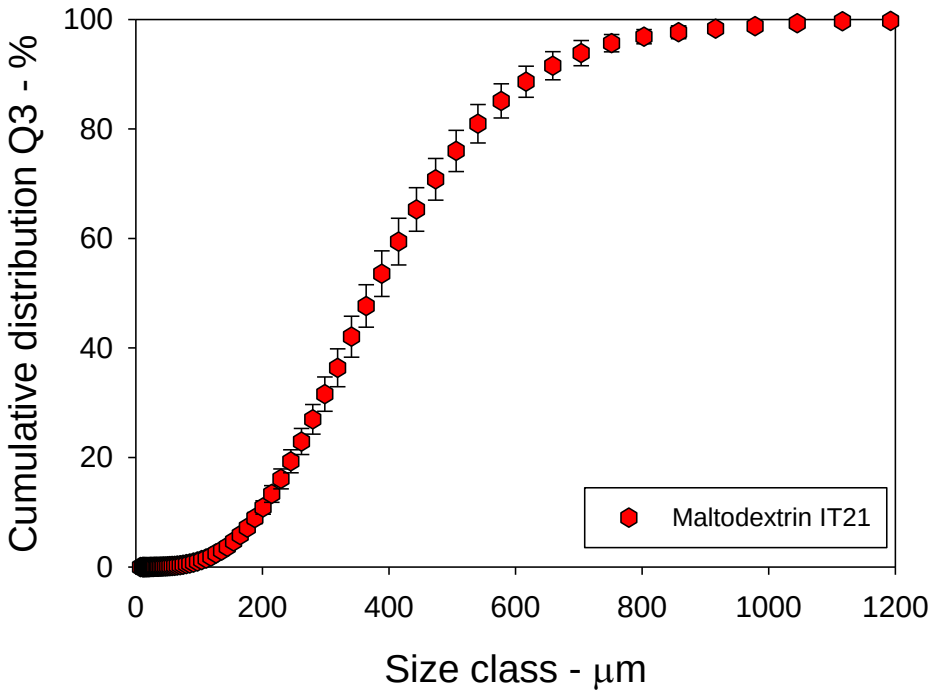

Figure 3-1: Cumulative size distribution of maltodextrin IT21

3.2.2 Disintegrants and food fibres

Disintegrants are ingredients with the ability to induce tablet disintegration. They are mainly used in the pharmaceutical industry, thus most of the disintegrants are pharmaceutical grade. However, such products have not all been approved for use in the food industry. Additionally, the trend towards natural ingredients in the food industry hinders the possible use of ingredients whose chemical name drives a "chemical" reputation to the food product in which they could be used. As a result, it seemed necessary to search for ingredients which show the same properties and advantages as the original and well established disintegrants but which would be obtained from a natural source such as plants. In this study, one established disintegrant used in the pharmaceutical industry called Vivasol is used

as a reference. In addition, other ingredients have been tested for their possible disintegration capabilities. More details about these ingredients can be found in Chapter 5 which is dedicated to the disintegrants used in this study.

3.3 Methods

3.3.1 Tablet production

Cylindrical tablets of maltodextins or mixes of maltodextrin/disintegrants were produced with a single punch tablet machine (Figure 3-2, MiniTab T, Kg-Pharma, Germany). The diameter of the tablets is fixed to 12 mm. The tablet machine allows the filled depth and the upper punch displacement to be controlled. The force developed during the compression of the powder is recorded but cannot be controlled. A value for the maximum upper and lower punch force can be obtained. The technical characteristics of the tablet machine are given in Table 3-1.

Table 3-1: Tablet machine technical characteristics

Instruments characteritics	**Technical information**
Maximum compression force	30 kN
Maximum fill depth	18 mm
Production capacity	15 to 60 tablets per minute
Maximum upper punch displacement	13 mm

The compression speed was set to 10 mm/s and the consolidation time was measured to be equal to 80ms from the force time curves. The upper punch forces were measured and vary for each formulation and displacement – fill depth combinations. The tablets porosities were measured post compression as described later in this Chapter. Several combinations of filled depth / upper punch displacement have been performed to obtain a complete map of the different settings to be used in order to obtain a desired porosity. As it will be explained later, it was required to produce tablets of a same porosity but different thicknesses. Such work required the development of a thickness - porosity map which is presented in Figure 3-3; each set of colours correspond to a similar upper punch displacement setting D, it corresponds to an arbitrary setting present on the tablet machine which is set manually. Each point, in Figure 3-3, from a same set of colour corresponds to an increment in fill depth of 0.2 mm. From this map, it is possible to know the tabletting settings to be used to obtain a desired set of tablets with a same porosity but different thicknesses. As it will be explained in Chapter 4, six sets of porosities were studied with a minimum of four thicknesses per porosity. Such a tool is only specific to the powder of maltodextrin IT 21 equilibrated at a water activity a_w=0.3.

Figure 3-2: Tablet machine, MiniTab T, Kg Pharma, Germany

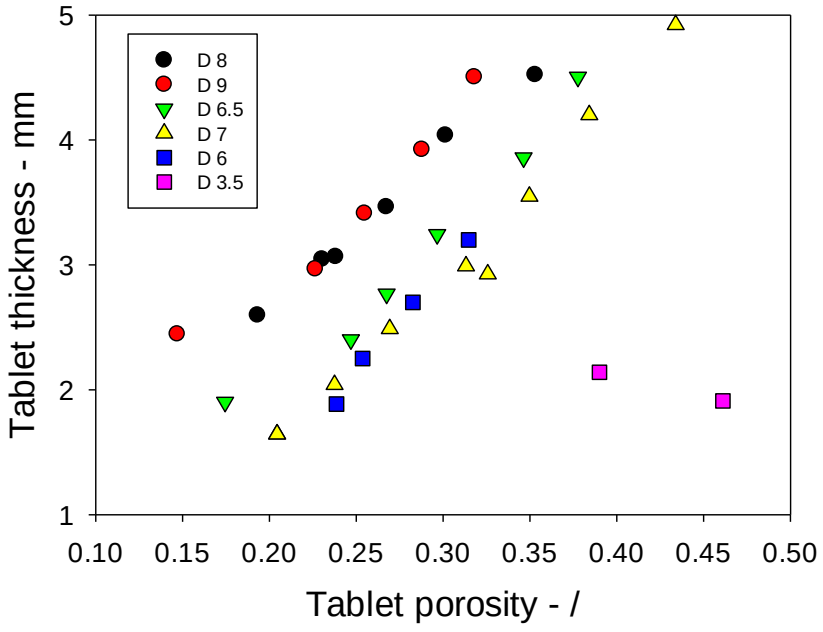

Figure 3-3: Tablet porosity – thickness map developed to select the tabletting settings (displacement D) required.

Alternative tablet designs are introduced later in this work. The following section aims at explaining how these tablets were produced. The aim of these new design was to allow the disintegrant to be placed at desired location within the tablet to study the possible channelling of water within the tablet.

The new designs included the production of (Table 3-2):

A triple layered tablets where a disintegrant layer is placed in between two layers of maltodextrins.

A cross design where the disintegrant is placed in a middle layer similar to the design above but additionally place across the tablet as shown in Tablet 3-2.

In order to achieve this, the mass of the different parts were weighted carefully to ensure the constant concentration of disintegrants. For the triple layer tablet, the mass of maltodextrin at the bottom of the tablet was first introduce manually in the tablet machine dye and evenly distributed on the whole surface. Afterwards, with the same process the disintegrants layer was added and finally the top layer of disintegrants was added before the compression was carried out. The desired mass were calculated from the volume of the tablet before compression and the powder densities. In the case of the cross design, the disintegrant and maltodextrin were kept apart at the bottom and top with the help of metal frames who were built specifically for this study as shown in Table 3-2.

Table 3-2: Different tablet design for the introduction of carrot fibres within tablets of maltodextrin IT21. The location of the disintegrant particles is pictured in orange in the tablets.

Triple layer design	Cross design
	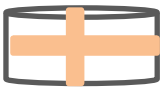
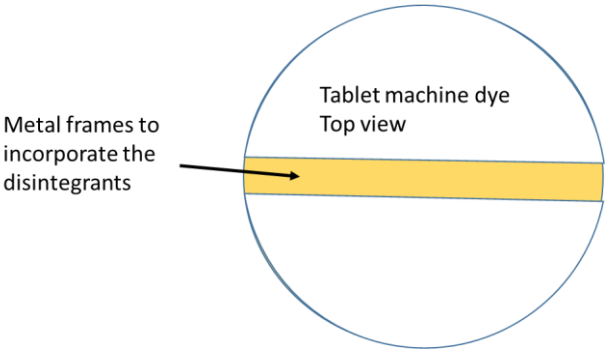	

3.3.2 Dissolution time t_{90}

The tablet dissolution time was measured by means of electrical conductivity in 40 ml of distilled water (Figure 3-4). Electrical conductivity has been largely used by other authors to study the dissolution of tablets (Marabi, Mayor et al. 2008). It has the benefit of providing the researcher a fast and easy technique to determine the dissolution time of a solid which conducts electricity. The electrical conductivity meter (Jenway 4510, UK) is connected to a PC where the change in conductivity upon dissolution is recorded on an Excel file. The conductivity probe has a constant of k=0.1 which, allows very small conductivities to be

measured. The water temperature and agitation by a magnetic stirrer was varied for the different experiments as it will be explained in Chapter 4. Temperature equilibrium was achieved before introducing the tablet in water. The tablet was placed in a mini basket to maintain its position constant from measurement to measurement. The time at which 90% of the tablet is dissolved t_{90} is used to compare the dissolution time of the different tablets. The average of 5 repetitions is presented as well as the standard deviation. An example of the dissolution curve obtained is shown in Figure 3-5. 100% dissolution is defined as when the maximum conductivity is reached described by a plateau on the dissolution curve.

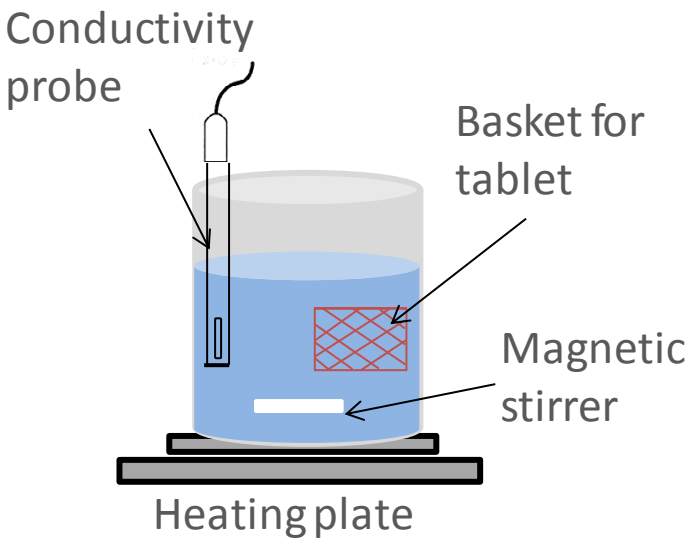

Figure 3-4: Dissolution time measurement set-up

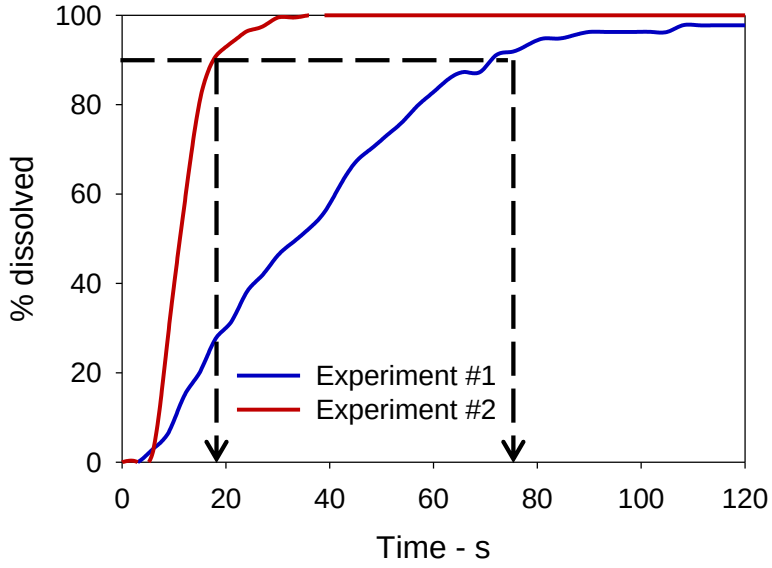

Figure 3-5: Determination of t_{90} from electrical conductivity curves

3.3.3 Measurement of the tablet tensile strength

The tablet tensile strength was measured by compressing the tablet diametrically with a material tester Zwick Roell Z0.5 shown in Figure 3-6 (Ulm, Germany). A load cell with a maximum force measurement of 500N with an accuracy of 0.001N was used. Ten repetitions were carried out. The following equation (Eq. 3-1) was used to calculate the tensile strength σ_t from the measured maximum breaking force F:

$$\sigma_t = 2\frac{F}{\pi H D_t} \qquad \text{Eq. 3-1}$$

where H is the tablet thickness and Dt is the tablet diameter. The tablet thickness and diameter were measured with the aid of a micro-precision calliper.

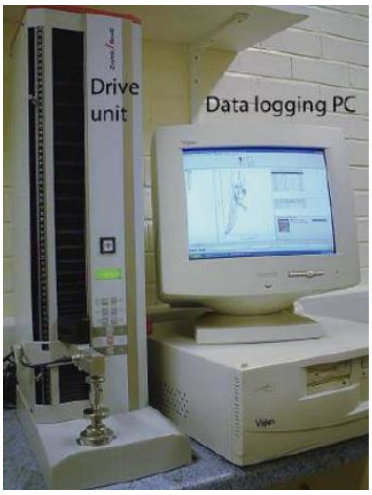

Figure 3-6: Compression tester Zwick Roell Z0.5

3.3.4 Determination of the tablet porosity

The porosity of each tablet was deducted from the tablet apparent density ρ_a and its true density ρ_t through the following equations:

$$\emptyset = \left(1 - \frac{\rho_a}{\rho_t}\right) \times 100 \qquad \text{Eq. 3-2}$$

The tablets apparent density ρ_a is determined from:

$$\rho_a = 4\left(\frac{m_t}{\pi H D_t^2}\right) \qquad \text{Eq. 3-3}$$

where m_t is the tablet mass

The tablet true density is determined from the true densities of the tablet constituents by:

$$\rho_t = \left(\sum_i \frac{\varphi_i}{\rho_{t,i}} \right)^{-1} \quad \text{Eq. 3-4}$$

where φi is the mass fraction of ith component in the tablet and ρt,i is its true density

The apparent density was obtained from the mass and volume of the tablets. The mass was measured on a high precision balance. The tablet dimensions, thickness and diameter, were measured with a micro precision slide calliper. The powder true densities were obtained from a gas displacement technique with an AccuPyc 1330 Pycmometer (Micromeritics, USA).

3.3.5 Particle size measurement

The size of the particles prior to tabletting was measured by image analysis with the QicPic apparatus (Sympatec, Germany) as shown in Figure 3-7, equipped with a vibratory feeder at the top of the instrument. The QicPic uses a high speed camera (up to 450 frames per second) combined with a very short exposure time to provide clear images of particles whose size and shape are further analysed by the WINDOX software. The image analysis equipment is suitable for measurement of particles in the range 1 µm to 30 mm. The size distributions are number based but can be converted to volume based distributions. In general, the total size distribution is presented, but for comparison purposes the $d_{50,3}$ (volume based median value) is favoured.

Figure 3-7: QicPic apparatus (taken from the Sympatec website)

3.3.6 Powder water activity

As mentioned in section 3.2.1 (Maltodextrin as a food model product), the water activity of the powder prior to tabletting needs to be controlled. The powders were then equilibrated at the desired water activity in a climatic chamber (RH=30%, 25°C). The powder activity was then checked with HygroLab 2 (Rotronic, UK) water activity cells. Powders are placed in cells and the relative humidity in the headspace is measured as a function of time; the relative humidity at equilibrium corresponds to the water activity in the powder.

3.3.7 Scanning Electron Microscope (S.E.M) images

S.E.M images of maltodextrin IT21 and of the different disintegrants investigated in this work were taken with an InspectF FEI microscope (FEI Company, The Netherlands), as shown in Figure 3-8. The apparatus was operated at 10kV under low vacuum conditions and the samples were sputtered with gold. The magnifications used are always specified on the images.

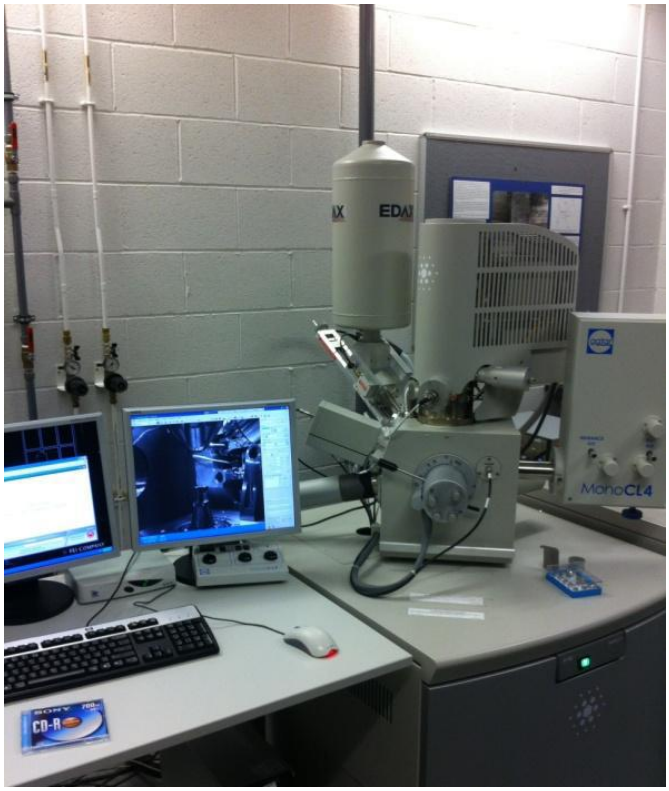

Figure 3-8. Image of the Scanning Electron Microscope

3.3.8 Sorption isotherms

The sorption isotherms of the different powders were built using a dynamic vapour sorption instrument SPS11 (Projekt Messtechnik, Germany). Samples were maintained at a controlled relative humidity (RH) and temperature in a chamber and were sequentially weighed with a high precision balance. The relative humidity was increased by 10% every 5h until 90% RH was reached and decreased to 10%. The sorption isotherms indicate the water content when the powder has equilibrated, i.e. a plateau was reached at each stage confirming the equilibration within the 5 hours. Figure 3.9 shows the equilibration of vivasol at the different relative humidities and as a function of time.

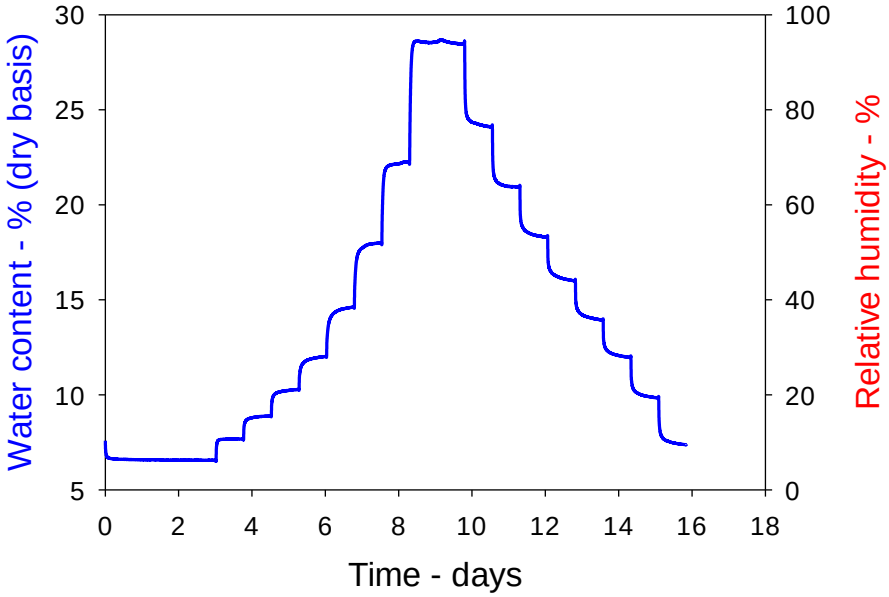

Figure 3-9 Equilibration of vivasol in a dynamic vapour sorption instrument SPS11 at different relative humidities and a function of time at 25°C

3.4 Conclusions

This chapter introduced the different materials and methods used to investigate the dissolution of maltodextrin tablets. Chapter 5 will further present and describe the different disintegrants investigated in this work. Chapter 7 will present a novel method which was designed specifically for this study, allowing a deeper understanding of the relationship between dissolution and disintegration for the overall reconstitution of a tablet.

CHAPTER 4 - DISSOLUTION BEHAVIOR OF MALTODEXTRIN TABLETS

4.1 Introduction

Chapter 2 describes the work which was researched in the past in the field of tablet and powder dissolution. The following introduction summarises our conclusions from the literature review and explains why the following work was carried out.

The dissolution of tablets has been widely studied in the pharmaceutical industry (Mikac, Demsar et al. 2007). Several theories based on the Fick's laws of diffusion and several empirical models such as Peppa's model have been developed to try to explain the dissolution process (Costa and Sousa Lobo 2001). However, these models focus mainly on the release of the active ingredients and not on the overall tablet reconstitution which is of interest in the food industry.

Few publications address the dissolution of food powders in general and of food tablets in particular (Marabi, Mayor et al. 2008).

Dissolution and disintegration are processes which are associated in the overall tablet reconstitution of food tablets. However, in order for dissolution and disintegration to occur, the solvent must be able to penetrate the tablet. The liquid will disrupt the inter particle bonds and lead to the breakage of the tablet. A fast disintegration will increase the surface area available for dissolution to occur. The tablet porosity is the main parameter influencing the liquid penetration (Hogekamp and Schubert 2003; Forny, Marabi et al. 2011). Brielles et al. (Brielles, Chantraine et al. 2007) showed that for industrial disinfectant tablets the porosity limits the liquid penetration within the tablets. As a result, depending on the porosity, three different disintegration regimes from low to fast were observed in their work. The different regimes varied from scare particles liberation at the surface of the tablet to complete destruction of the tablet structure. Even if understanding the change in dissolution behaviour is important for the complete reconstitution of the tablet, few papers highlight the link between dissolution and disintegration of tablets in relation to their porosity.

To conclude, the understanding of food tablet dissolution and disintegration is limited. Even though the aim of this PhD work is to investigate the possible introduction of disintegrant in food tablets, it is first necessary to study the dissolution and disintegration of tablets excluding any disintegrants. This chapter aims at answering the following questions:

- What are the main parameters influencing food tablets dissolution and disintegration?
- Can we control and predict what will happen to a food tablet when placed in water?

In the first part, the dissolution times of a food model product, maltodextrin, is investigated experimentally to understand the influence of the porosity, the water temperature and stirring speed. This is of great important for dissolution of food products (Opota, Maillols et al. 1997). Each parameter, porosity, temperature and stirring speed, is studied for several tablet surface areas. In the second part, a theoretical description of the tablet dissolution is developed and compared with the experimental results.

4.2 Experimental study

The material used in this chapter is maltodextrin which is introduced in Chapter 3. The determination of the tablet dissolution times, tablet tensile strength and porosity were obtained according to the methods presented in Chapter 3.

4.2.1 Influence of the tablet porosity: erosion or disintegration

In the literature, the dissolution time of tablets is mainly investigated as a function of the tablet strength, as pointed out in Chapter 2. However, water penetration in the tablet is mainly dependent on the tablet porosity. Tablet porosity and tensile strength can be linked together, as shown later in this chapter, but in a nonlinear way. Thus, it seems more adequate to study the dissolution time of tablets as a function of the tablet porosity. However, it is possible to produce two different tablets with a same porosity but with a different surface area, or thickness in our case as the diameter is fixed. By analysing the dissolution time of tablets of several porosities and surface area (thickness in this case), it is possible to understand how these two parameters influence the dissolution time.

Sets of tablets with a common porosity but different initial thickness were produced according to the methods described in Chapter 2.

In Figure 4-1, the tablet dissolution times are presented as a function of the tablet thickness for all the different porosities studied from 0.19 to 0.43. Examples of the complete dissolution profiles are shown in Appendix A-1. Due to limitation in compression force, it was not possible experimentally to produce tablets with a large thickness and a small porosity. As expected, a tablet with a higher porosity will dissolve faster, for a constant surface area (thickness in this case).

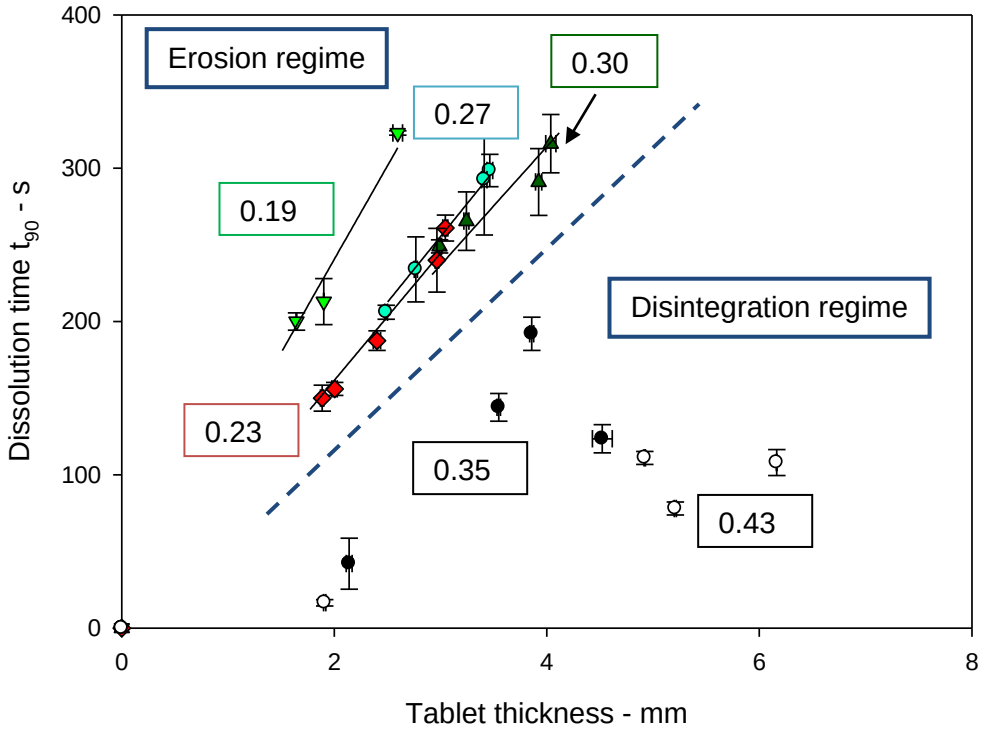

Figure 4-1: Evolution of the dissolution time t_{90} as a function of the tablet thickness for different porosities. Five repetitions were carried out and the error bars represent the standard deviation in dissolution time and thickness. Experimental conditions: 50°C and 300 rpm

For the porosities of 0.19, 0.23, 0.27 and 0.30, a linear fit can be obtained between the dissolution time and the tablet thickness (or tablet surface area). For porosities of 0.35 and 0.43, no linear relationship is observed.

It should be noted that the slope of the linear correlation is different for the four porosities studied. The slopes β of the four linear correlations were calculated and plotted against the tablet porosity as shown in Figure 4-2. It is interesting to note that a linear approximation between the slope β and the tablet porosity can be made. A higher slope β, at low porosity, indicates that the tablet thickness (or

surface area) is more important in the dissolution of tablets at low porosities compared to higher porosities.

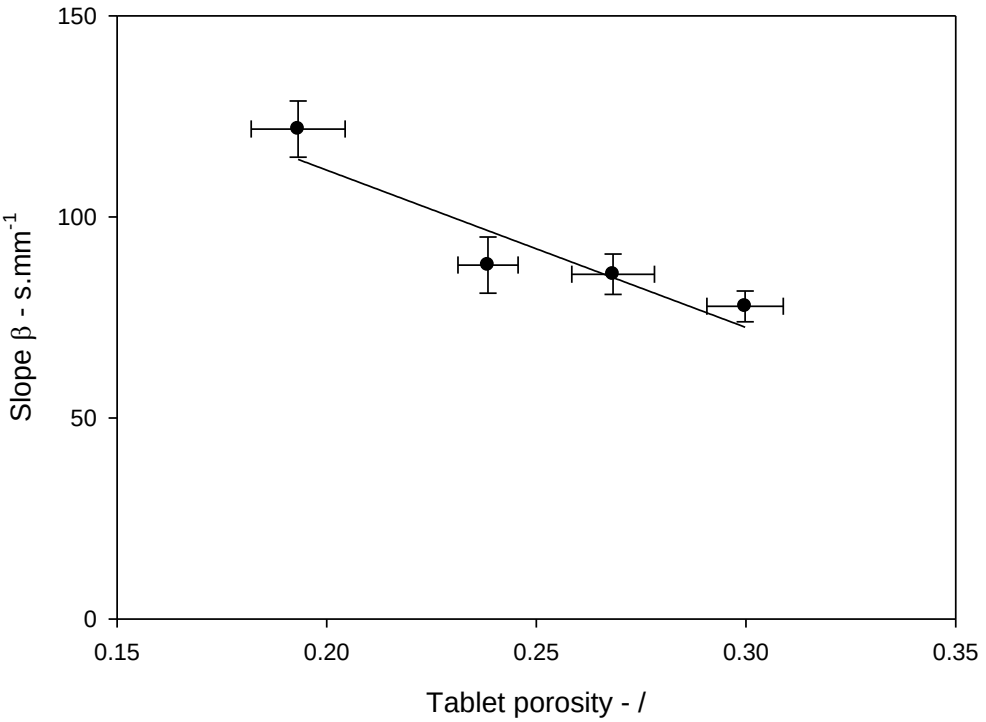

Figure 4-2: Variation of the slope β as a function of porosity

The difference in dissolution behaviour between the low and high porosity tablets was observed visually. In the first case, low porosity tablets, the cylindrical shape of the tablet was kept during its dissolution. A decrease in the diameter and thickness is observed but the structure of the tablet does not break. In the second case, high porosity tablets, the tablet structure is broken, liberating large fragments of solids. From this observation the following explanations are put forward:

- At low porosities, the two processes, disintegration and dissolution, only occur at the surface of the tablet. Physically, the tablet does not disintegrate, only erosion occurs at its surface. Particles are liberated from the surface and are released in the solvent. In addition, dissolution happens at the surface of the tablets. Single molecules are detached from the tablet. This type of dissolution behaviour can be described as the erosion regime.
- At high porosities, tablet disintegrates quickly in contact with water. The tablet structure is broken down very quickly. This results in a larger solid surface area in contact with water, leading to a faster dissolution. This type of behaviour can be described as the disintegration regime.

Such separation between the erosion and disintegration regimes was pointed out by Brielles et al. (Brielles, Chantraine et al. 2007; Brielles, Chantraine et al. 2008) for a crystalline system. The authors describe in total three different regimes, including an intermediary regime where the tablet first dissolves according to an erosion process and then quickly disintegrates. The transition between erosion and disintegration regimes is at porosities between 0.30 and 0.35 in this case, which is higher than the values obtain by Brielles et al. (2007). The authors obtained transitions at porosities of 0.10 and 0.20 for tablets of a chlorine provider for the detergent industry (Brielles, Chantraine et al. 2007). However, the systems studied were different; a crystalline system was investigated in their case while an amorphous polymer is used in this study. Thus different dissolution properties can be expected. It is interesting to note that, to the best of the author's knowledge, such behaviour was never pointed out for an amorphous powder.

It can be argued that the variation in dissolution time for different tablet thicknesses observed in Figure 4-1 could be due to a variation in tablet strength, despite an identical porosity. Consequently, the tablets tensile strengths were determined (Eq. 3-1). Figure 4-3 shows the evolution of the tensile strength for the different tablet thicknesses (same as in Figure 4-1) at the five porosities studied. It can be seen that for each porosities, the change in thickness does not affect the tablets' tensile strength. This is true for all porosities except for the low porosity value of 0.19 where the difference in tensile strength is more pronounced. It could be due to the fact that for these low porosities sintering was observed on the tablets' surface which is in contact with the die wall during the tabletting process. Indeed, the tablets which have to travel longer along the die wall before ejection are prone to undergo a higher stress level due to the friction with the die wall. This could result in favourable conditions, i.e. temperature increase, for sintering to occur. It could lead to a difference in interparticle bonding mechanisms and affect the tablet strength. Further work is needed to confirm this idea; however it is not the purpose of this study.

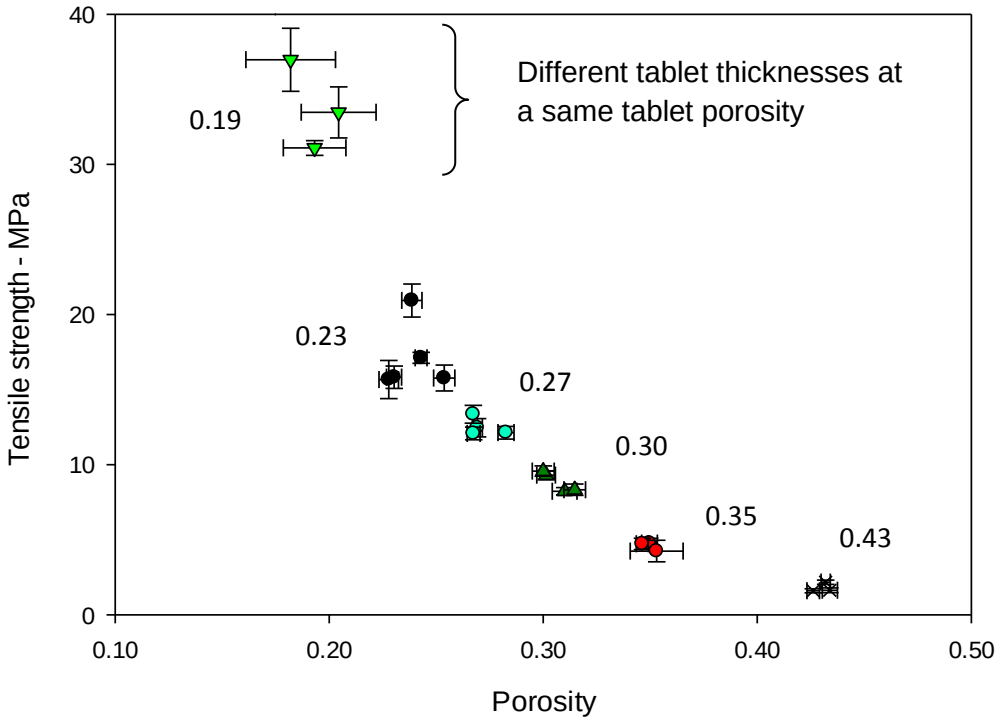

Figure 4-3: Tablet tensile strength for the different thicknesses at the five porosities studied (noted on the figure frfom0.19 to 0.43). The data is fitted with the Ryshkewitch-Duckworth equation (Eq. 4-1)

The evolution of the tablet tensile strength with the porosity has been well studied and the Ryshkewitch-Duckworth equation can be used to fit the data as follows (Wu, Best et al. 2005; Ryshkewitch, 1953) :

$$\sigma_t = \bar{\sigma} e^{-k_b \varepsilon} \qquad \text{Eq. 4-1}$$

Where ε is the tablet porosity, k_b is a constant representing the bonding capacity and $\bar{\sigma}$ is the tensile strength of the material at zero porosity.

According to Wu et al., (2005) the Ryshkewitch-Duckworth equation is suitable for describing the variation in tensile strength for a wide range of porous materials. A value of 12 was found for k_b and $\bar{\sigma}$ was determined to be equal to 325 MPa after fitting Eq. 4-1 to the experimental values. The value of k_b is is agreement with the finding of other authors. Patel and Bansal (2011) found similar value of 12.66 for k_b in case of the compression of microcrystalline cellulose. Michrafy et al., (2007) reported values of 20.15 for lactose and 5.95 for microcrystalline cellulose. According to Steendam et al., (2001) a higher value of k corresponds to a stronger bonding of the primary particles.

4.2.2 Influence of the dissolution water temperature

Important findings on the difference between erosion and disintegration regimes were obtained from Figure 4-1 due to the fact that the porosity and initial tablet surface area were investigated together. The same framework is kept to study the influence of the dissolution temperature.

In Figure 4-4, the evolution of the dissolution time of tablets of porosity 0.27 at different thicknesses as a function of the temperature of water is shown. Examples of the complete dissolution profiles are shown in Appendix A-2. The value of 0.27 was chosen as it corresponds to the value of 0.25 which is the average porosity for tablets of interest in the food industry (Forny 2010). It can be seen that the temperature plays a large influence on the dissolution time and the higher the temperature the shorter the dissolution time. Such findings were to be expected as many other studies have concluded the same (Marabi, Mayor et al. 2008). However, it is interesting to notice that a linear correlation is obtained

between the dissolution time and the initial tablet thickness (surface area) for all four temperatures investigated. Also, it should be noted that for high temperature, such as 70°C in this study, the initial tablet thickness has less impact on the dissolution time. To the best knowledge of the author, such correlation was not shown before.

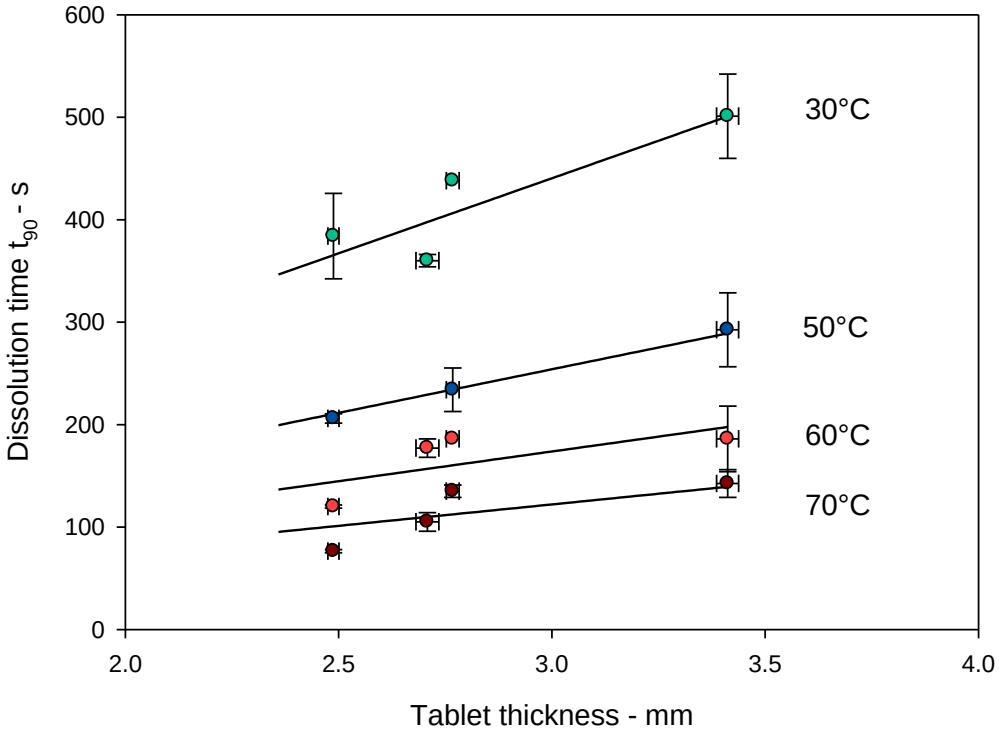

Figure 4-4: Evolution of the dissolution time for different tablet thicknesses of porosity 0.27 as a function of water temperature. The results express the average of 5 repetitions and the error bars represents the standard deviation.

Experimental conditions: porosity of 0.27 and 300 rpm

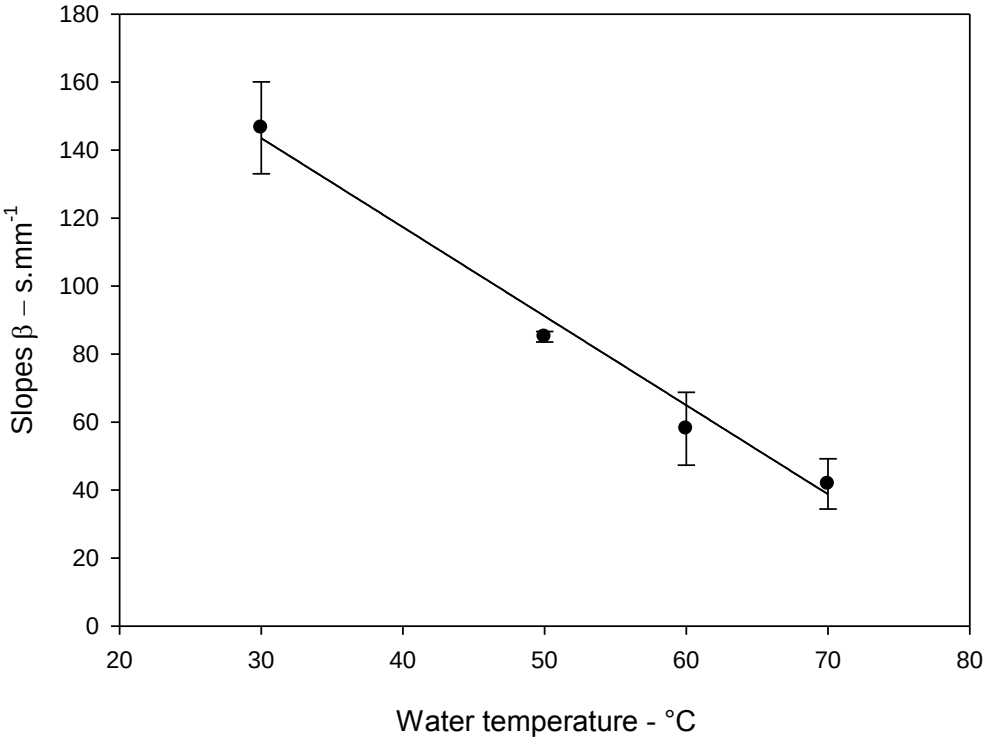

Figure 4-5: Evolution of the slopes β as a function of the temperature

It can be seen that the slopes β of the linear correlations obtained in Figure 4-5 are also evolving linearly with the temperature of water used for the dissolution of tablets of maltodextrin IT 21.

4.2.3 Influence of the stirring speed

The influence of the stirring speed is as well investigated according to the same framework, dissolution time versus initial tablet thickness for different stirring speed.

In Figure 4-6, the evolution of the dissolution time of tablets of porosity 0.27 with different thicknesses as a function of the stirring speed is shown. Examples of the complete dissolution profiles are shown in Appendix A-3. It can be seen in Figure 4-6 that the faster the stirring speed, the less influence the tablet thickness has on the dissolution time.

A linear correlation can be found between the dissolution time and the tablet thickness for all five stirring speeds studied. The slope β of the correlation is also linearly linked to the stirring speed as shown in Figure 4-7.

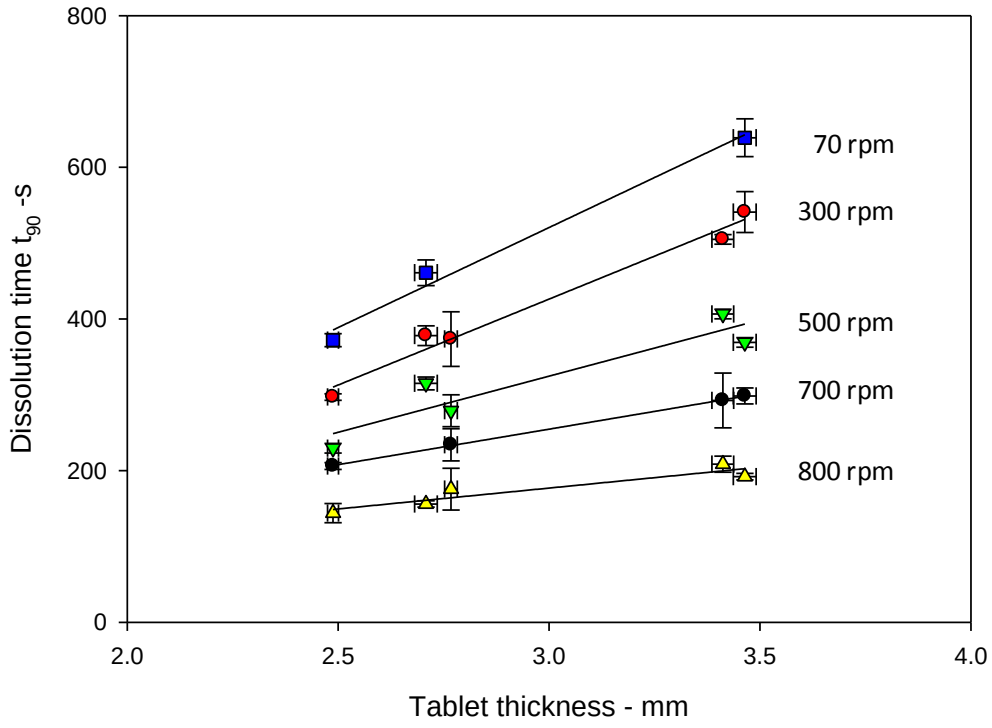

Figure 4-6: Evolution of the dissolution time t_{90} as a function of the initial tablet thickness for different rotation speed. The results express the average of 5 repetitions and the error bars represents the standard deviation. Experimental conditions: porosity of 0.27 and 50°C

The influence of the agitation rate on dissolution has been previously studied. In general, a power law is found to relate the dissolution rate and the stirring speed (Dokoumetzidis and Macheras 2006). However, to the best knowledge of the author, no correlation between the stirring speed, the dissolution time and the tablet thickness were ever published, hence the difficulty to compare these results.

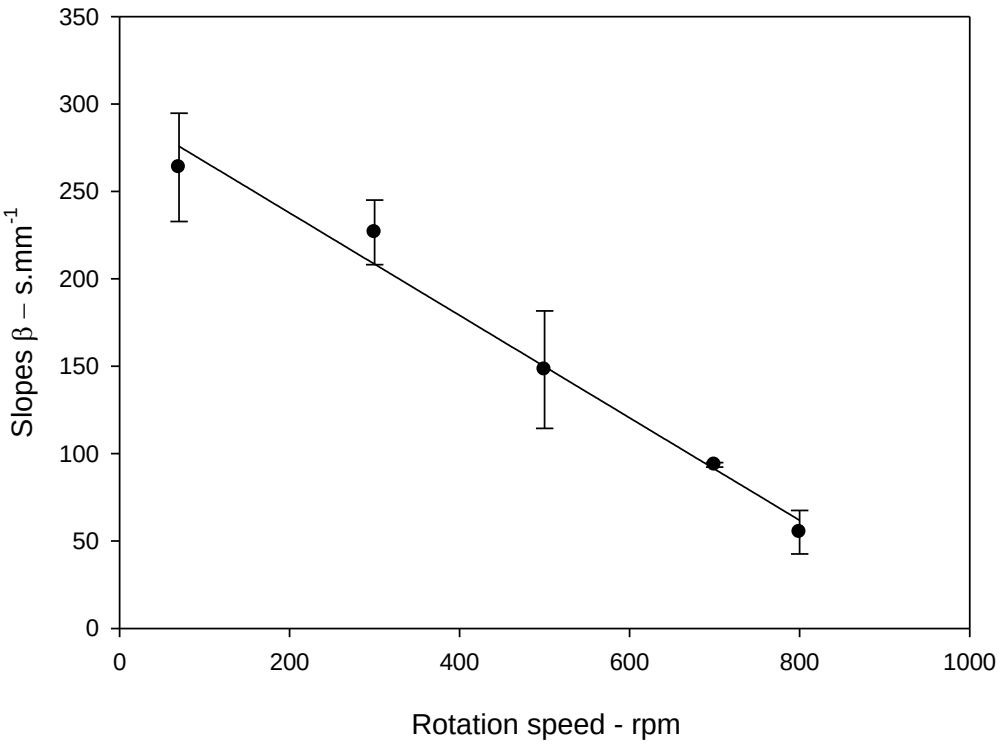

Figure 4-7: Evolution of the slopes β as a function of the rotation speed

4.3 Mathematical description of the influence of the tablet porosity and water temperature

The following sets of equations described in this paragraph were developed to understand the linear correlations obtained in Figure 4-2 and 4-5. Such an understanding will help answer the following questions:

- Is the erosion regime hypothesis valid?
- How is the temperature influencing the dissolution time?

It is assumed the tablets are made of an assembly of particles with their number density is n and volume v. The number flux of particles leaving the surface of the tablet is defined is J. The particles are defined here as either dissolved molecules of maltodextrin or solid particles detached from the surface of the tablet due to disintegration. The solid-liquid interface of the largest surface area of the tablet will move due to the release of the particles in the opposite direction with a velocity u_i as precised on Figure 4-8. It is thus assumed that the particles are only released from the largest surface area of the tablet which is much larger than the area of the solid-liquid interface on the cylindrical sides of the tablet.

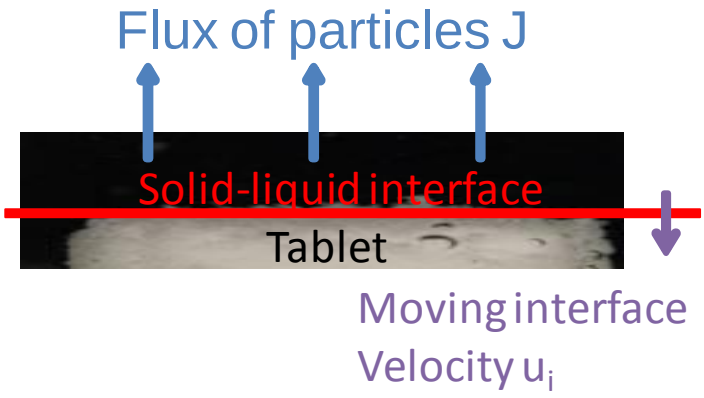

Figure 4-8: Particle flux at the moving solid-liquid interface (tablet surface)

The definition of the flux gives:

$$J = -u_i n \qquad \text{Eq. 4-2}$$

In addition, the number density of particles n can be defined as,

$$n = \frac{1-\varepsilon}{v} \qquad \text{Eq. 4-3}$$

where ε is the tablet porosity and v is the volume of one particle.

The velocity of the moving interface can then be expressed as a function of Eq 4-2 to give:

$$u_i = -\frac{Jv}{1-\varepsilon} \qquad \text{Eq. 4-4}$$

By considering that the tablet diameter D is much larger than the tablet thickness, and the variation of tablet volume with time $\frac{dV}{dt}$ is a function of the flux of particles and the following can be written:

$$(1-\varepsilon)\frac{dV}{dt} = -Jv\frac{\pi}{4}D_t^2 \qquad \text{Eq. 4-5}$$

If it is assumed that the flux of particles leaving the surface of the tablet and that the variation of volume of the tablet with time are constant, then Eq. 4-5 can be developed to give:

$$V = V_0 - Jv\frac{\pi}{4}D_t^2\frac{t}{1-\varepsilon} \qquad \text{Eq. 4-6}$$

At time t = t_{90}, the volume of the tablet will be equal to 10 % of the initial volume and thus:

$$t_{90} = \frac{0.9V_0(1-\varepsilon)}{Jv\frac{\pi}{4}D_t^2} \qquad \text{Eq. 4-7}$$

The initial tablet volume V_0 can be expressed as:

$$V_0 = \frac{\pi}{4}D_0^2H \qquad \text{Eq. 4-8}$$

As a result, Eq. 4-7 can be rearranged to the following after including Eq. 4-8 and with $D_0=D_t$:

$$t_{90} = \frac{0.9H(1-\varepsilon)}{Jv} \qquad \text{Eq. 4-9}$$

Eq. 4-9 states that t_{90} should be directly related to the initial tablet thickness H and the tablet porosity ε. In addition, the slope β can be defined as:

$$\beta = \frac{0.9(1-\varepsilon)}{Jv} \qquad \text{Eq. 4-10}$$

Eq. 4-10 explains the relationship between the porosity ε and β. Indeed, when the porosity increases the value of β decreases accordingly.

The flux expressed in Eq. 4-2 can be also be defined by the following equation based on the Noyes and Whitney equation (Dokoumetzidis and Macheras 2006).

$$vJ = \frac{1}{\rho} k_c (C_s - C) \qquad \text{Eq. 4-11}$$

Where C is the instantaneous concentration of solute in solvent, C_s is the saturation concentration, ρ is the particle density and k_c is the mass transfer coefficient.

It can be assumed that in this work, C_s is much larger than *C*, i.e. the final concentration of dissolved maltodextrin is low compared to the saturation concentration. As a result, the following can be written:

$$vJ = \frac{1}{\rho} k_c C_s \qquad \text{Eq. 4-12}$$

Finally β and t_{90} can be defined as follows by including Eq. 4-13 into Eq. 4-10 and Eq. 4-11:

$$\beta = \frac{0.9\rho(1-\varepsilon)}{k_c C_s} \qquad \text{Eq. 4-13}$$

And

$$t_{90} = \frac{0.9H\rho(1-\varepsilon)}{k_c C_s} \qquad \text{Eq. 4-14}$$

Eq. 4-13 and Eq. 4-14 gives the relationship between the dissolution time t_{90}, the porosity ε, tablet thickness H and the solubility C_s which depends on the temperature.

According to Eq. 4-13 and Eq. 4-14, a linear correlation between β and $(1-\varepsilon)/C_s$ and between t_{90} and $(1-\varepsilon)H/C_s$ should be found. Figure 4-9 and 4-10 shows that these two correlations are valid in our system.

In order to plot Figure 4-9 and 4-10, the saturation concentration C_s values were obtained by measuring the maximum amount of maltodextrin which can be dissolved in a known volume of water at the different temperatures as shown in Table 4-1.

Table 4-1: Solubility values as a function of the temperature

Temperature (°C)	**Solubility ($kg.kg^{-1}$)**
30	0.9
50	1.5
60	2
70	2.5

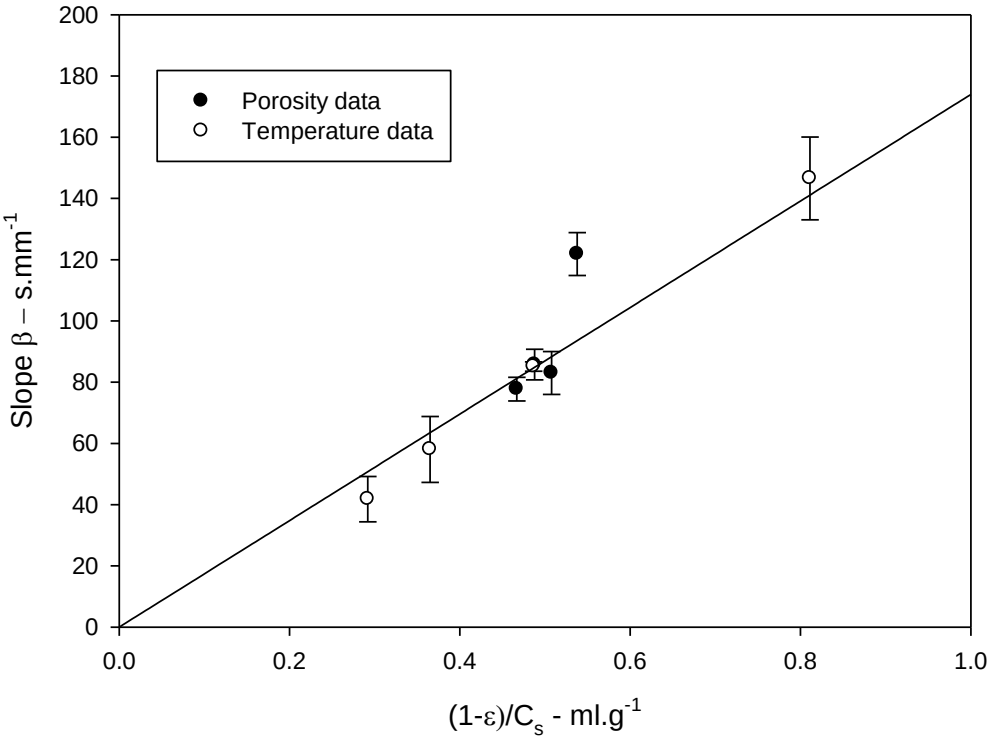

Figure 4-9: Plot of the slope β against (1-ε)/C_s following Eq. 4-14

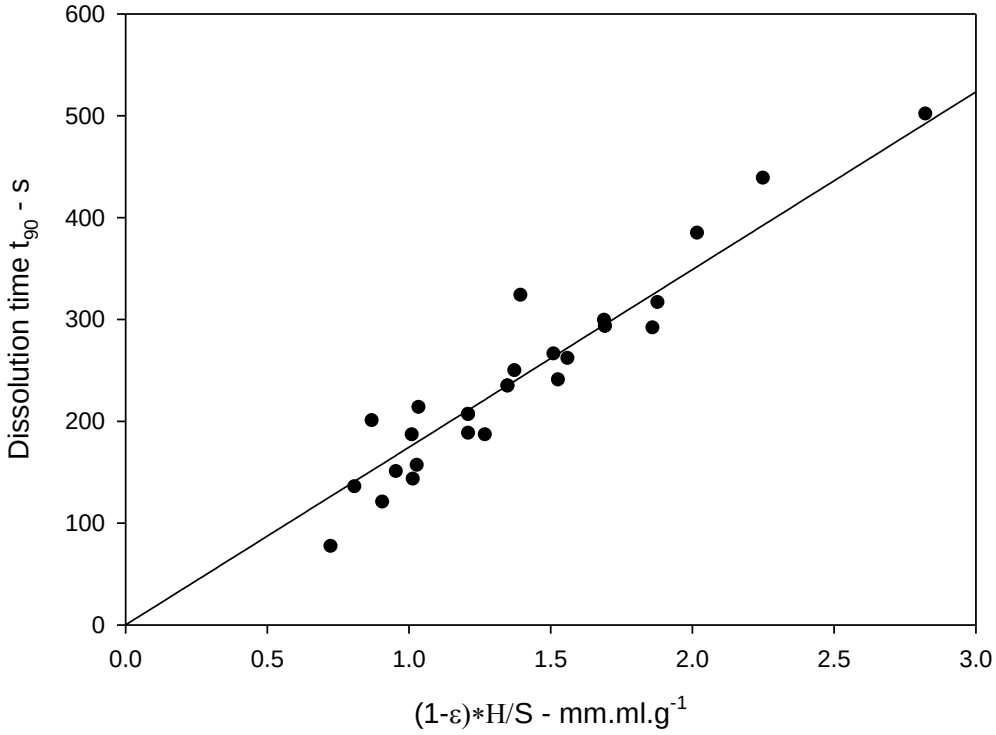

Figure 4-10: Plot of the dissolution time t_{90} against (1-ε)H/C_s following Eq. 4-15 from porosity and temperature data.

The results presented in Figure 4-9 and 4-10 show that the hypothesis of the erosion regime for the low porosities is correct. Moreover, it shows that the temperature influences the dissolution time through the driving force for dissolution, which is a function of the temperature dependent saturation concentration C_s.

4.4 External mass transfer coefficient: Sherwood vs Reynolds numbers

The mass transfer coefficient k_c defined in equation 4-14 represents the mass transfer of particles from the surface of the tablet to the bulk solution. The fluid velocity (stirring speed) around the tablet will affect the mass transfer of particles. It is interesting to understand how the mass transfer coefficient develops when the fluid velocity is modified. In addition, it gives an insight on the relationship between the external mass transfer and the dissolution behaviour.

The mass transfer coefficient k_c can be deducted from equation 4-13 and Figure 4-9 from which the value of the slope of the linear correlation between β and (1-ε)/Cs can be obtained.

$$k_c = \frac{0.9\rho(1-\varepsilon)}{\beta C_s} \qquad \text{Eq. 4-15}$$

A mass transfer coefficient can be calculated for each stirring speed, i.e. each value of β, from Figure 4-7. The mass transfer coefficient can then be transformed into a dimensionless number; the Sherwood number (Sugano 2008).

It is defined as:

$$Sh = \frac{k_c D}{\mathcal{D}} \qquad \text{Eq. 4-16}$$

Where $\mathcal{D}$ is the diffusion coefficient.

The Sherwood number can be related to the Reynolds number which describes the flow conditions. The Reynolds number for a stirred vessel is described as follows:

$$Re = \frac{\rho_f N D_a^2}{\mu} \qquad \text{Eq. 4-17}$$

Where N is the rotational speed, D_a the diameter of the agitator, ρ_f the density of water and μ is the dynamic viscosity of water.

Figure 4-11 shows the evolution of the Sherwood number as a function of the Reynolds number. The five Reynolds number plotted correspond to the five different rotation speed studied earlier in this Chapter. It can be seen that for Reynolds numbers below 22 000, the Sherwood number tends to increase. However, this increase is only slight. For Reynolds values larger than 22 000, however, a much more abrupt increase can be noticed. It can be seen that on Figure 4-11, two different lines are drawn on the plot. It should be mentioned that these two lines are not fitted to the data points; their purpose is solely to highlight the trend of the results.

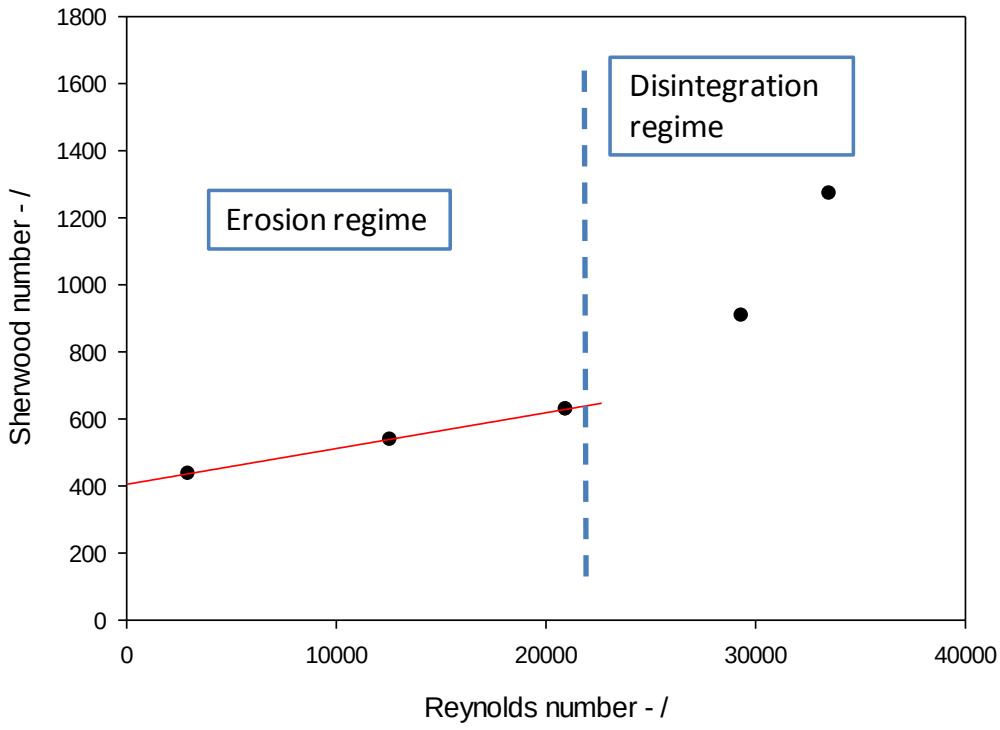

Figure 4-11: Influence of the rotation speed on the mass transfer coefficient: Sherwood vs Reynolds numbers.

The following paragraphs aim at giving a possible physical explanation to the results plotted in Figure 4-11. At low flow, the tablet dissolution and disintegration is mainly dominated by the formation of particles at the surface of the tablet. The particles are generated by erosion of solids at the surface of the tablet or by the formation of solute during the dissolution at the solid-liquid interface. The tablet reconstitution behaves accordingly to the erosion regime shown in section ***4***.2.1 (Influence of the tablet porosity: erosion or disintegration). The stirring speed is moderately influencing the mass transfer coefficient.

However, when the Reynolds number is higher than 22 000, the mass transfer increases sharply with the stirring speed. In this part of the curve, the external mass transfer dominates the dissolution and disintegration kinetics. The particles are removed from the surface at a rate which is limited by the flow of water around the tablet. The fluid flow will increase the tablet breakage and the disintegration regime is obtained. From Figure 4-11, it can be deduced that a critical Reynolds number exists between the erosion and disintegration regime. It also means that the change between erosion regime and disintegration regime based on the tablet porosity will be a function of the Reynolds number of the dissolution fluid. The difference between the erosion and disintegration regime can be noticed visually. The same behaviour occurs as noticed with tablets of different porosities.

The most accepted theory to understand dissolution kinetics states that a boundary layer is present at the surface of the tablet. This boundary layer, also called the diffusion limited boundary layer determines the kinetics for the dissolution in case of an externally limited type of dissolution (Dokoumetzidis and Macheras 2006). The thickness of such a boundary layer h_l is commonly admitted to be linked to the Sherwood number. Such a correlation can be written as:

$$h_l = \frac{D}{Sh} \qquad \text{Eq. 4-18}$$

It can be deducted from equation 4-18 that increasing the Sherwood number (stirring speed in this case) will decrease the thickness of the diffusion controlled boundary layer around the tablet, thus increasing the mass transfer coefficient. This correlation may potentially be true for a Reynolds number below 22 000 in this work. However, above such value the flow around the tablet is responsible for its disintegration.

4.5 Conclusions

In this work, it was shown that the dissolution of tablets of maltodextrin IT 21, an amorphous powder, behaves accordingly to two different regimes, erosion and disintegration, depending on the tablet porosity. In addition, in the erosion regime, it was shown that the dissolution time is linearly related to the initial tablet thickness for a given porosity. The slopes of these linear correlations are also linearly dependent on the tablet porosity.

The mathematical expressions developed in this thesis explain the linear relationship between the slope β and both the tablet porosity and water temperature. The decrease in dissolution time with an increase in water temperature can be explained by an increase in solubility.

The results presented in this chapter show that the external mass transfer of particles from the surface of the tablet to the bulk solution is the limiting factor for the dissolution process. The mathematical expressions, which were developed based on the Noyes and Whitney equation, show that the main parameters influencing the dissolution rate are the temperature of water and the stirring speed. Temperature increases the driving force for mass transfer from the surface of the

tablet to the solution. As this mass transfer is the limiting factor in the dissolution process, the dissolution time can be greatly impacted by the temperature.

The stirring speed reduces the thickness of the diffusion layer at the surface of the solid in the erosion regime. It is also shown that the disintegration regime can be reached by increasing the stirring speed. A critical Reynolds number was defined as the point where the Reynolds number is large enough that the flow induces tablet disintegration.

To further the work developed in this Chapter, it would be interesting to investigate how the stirring speed affects the transition from erosion to disintegration regime based on tablet porosities. In practice, it means developing the same type of work as in Figure 4-1 for different stirring speeds.

CHAPTER 5 - DISINTEGRANTS CHARACTERISATIONS

5.1 Introduction

This chapter presents the selection process for choosing the 5 different types of disintegrants used in this study. In addition, each disintegrant is characterised in term of powder properties (size distribution, density, morphology) and potential disintegrant mechanisms.

This study deals with the possible introduction of disintegrants in food products, and therefore, their food grade must be guaranted. In addition, the recent negative view of consumers for E-numbers ingredients (chemical reputation) pushes towards using ingredients which are derived from natural products such as plants.

5.2 Selection of food grade disintegrants

Typical disintegrants used in the pharmaceutical industry are based on the fact that some polymer carbohydrates such as cellulose swell in contact with water. For example, croscarmellose sodium which is widely used in the pharmaceutical industry is a derivative of cellulose. However, the name of this ingredient would not look appealing to consumers in the ingredient list at the back of a food product packaging. The idea was thus to find ingredients which contain cellulose or derivatives of cellulose but which are obtained from natural sources such as plants. Cellulose is the structural component of the primary cell of green plants. Numerous plants such as carrot or tomatoes are used in the food industry, especially their fibers which are directly obtained from the product itself or the waste generated (peel) during product processing. Ingredients such as carrot fibres are obtained from the carrot itself (BolthouseFarms 2002). Carrots are milled down into fine particles and the soluble part (sugar, colour...) of the particle is washed away in water. The resulting insoluble material is then dehydrated to produce particles which are milled down to a desired size. The final dried particles contain a majority of fibers (92%) and some other products such as proteins and minerals. The fibres obtained from carrots are composed of cellulose, hemicellulose and lignin which all are insoluble long-chain carbohydrates.

The use of an ingredient such as carrot fibres combines the positive effect of the cellulose for the disintegrant specifications and the natural source acclaimed by consumers. A choice of four other plant fibres was decided for this study, in order to obtain a wide range of food fibres. In addition to carrot fibres, two types of

citrus fibres and tomato fibres were selected. The two types of citrus fibres have the advantage of having the same composition but are available under two different size distributions. As a result, an additional study of the effect of the size distribution of the disintegrants can be performed. In addition, carrot, tomato and citrus particles all have a different total content of fibres which may affect their possible disintegrant ability. Finally, another type of ingredient, croscarmellose sodium (Vivasol, JRS Pharma, Germany) which was mentioned earlier, is also investigated. Such product is widely used in the pharamceutical industry, it is thus interesting to compare possible disintegrants to a reknowned one.

Figure 5.1 sums up the thoughts behind the choice of the five disintegrants selected for this study. Table 5.1 summarizes the content of the different fibres and their origin.

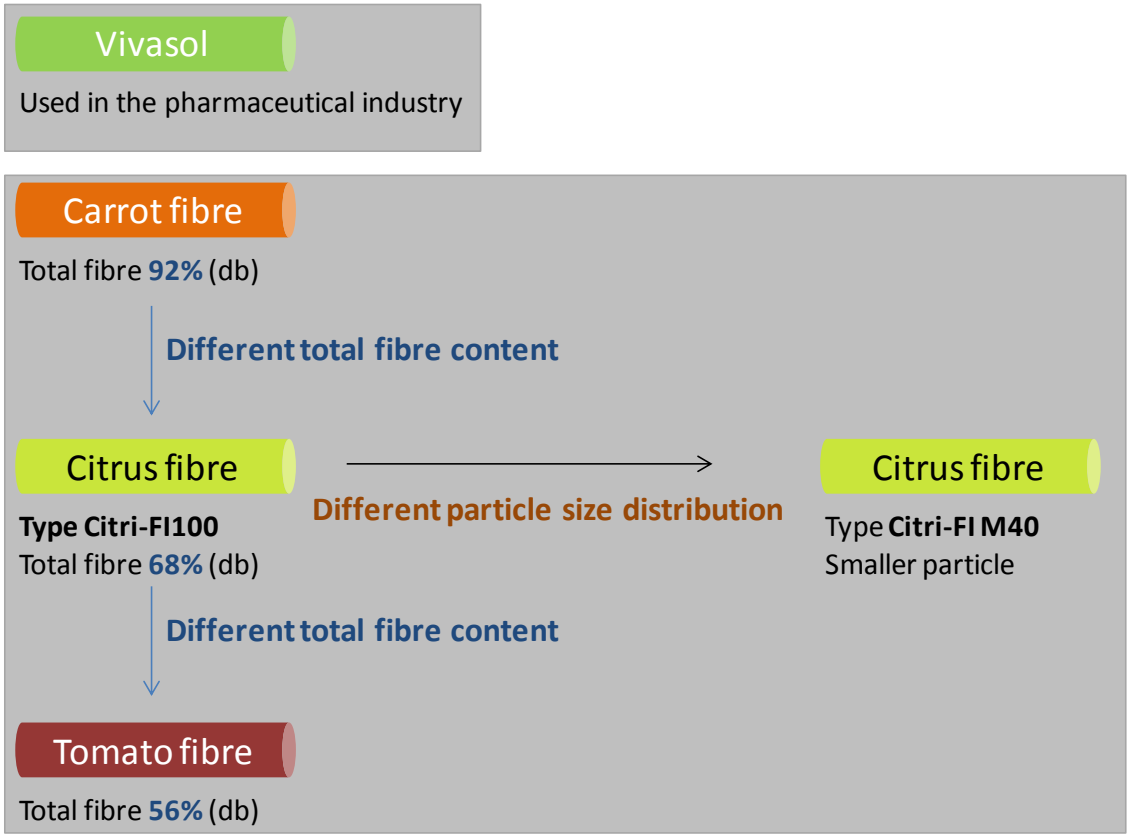

Figure 5-1: Summary of the five disintegrants used in this study. Vivasol is used as reference ingredient and the fibres were chosen for their different concentrations of fibre content or particle size distributions. The fibre contents are expressed on a dry basis (db)

Table 5-1: Characteristics of the different disintegrants

	Carrot fibres - Hydrobind	**Citrus fibres - Citri-Fi 100**	**Citrus fibres – Citri-Fi M40**	**Vivasol – Croscarmellose sodium**	**Tomato Fibres**
Color	Creamy white	Light yellow	Light yellow	White	Red - pink
Total fibre content (db)	**92 %**	**78 %**	**78 %**	**/**	**56%**
Insoluble fibre content (db)	78 %	40 %	40 %	/	46%
Sugars (db)	0.1 %	8.4 %	8.4 %	/	26%
Protein (db)	3 %	9.3 %	9.3 %	/	13.4%
Fat (db)	0.4 %	1.3 %	1.3 %	/	0.6%
Ash (db)	4.5 %	3 %	3 %	/	4%
Origin	Whole carrot	Dried orange pulp	Dried orange pulp	Chemically derived from cellulose	Tomato by products : skin and seeds
Producer	Wm. Bolthouse Farms, U.S.A	Fiberstar Inc, U.S.A	Fiberstar Inc, U.S.A	JRS Pharma, Germany	CONESA, Spain

The nutritional contents of the fibers were obtained from the manufacturers. It should be noted that these products are derived from a natural source and their nutritional content may vary. No nutritional information about Vivasol is included in Table 5-1 as Vivasol is chemically derived from pure cellulose.

It should be noted that in this work the five types of ingredients are refered to as disintegrants even though the different fibres are not described as disintegrants by the different suppliers and the FDA.

5.3 Disintegrants characterisation

Each of the fibres chosen in this study are already used in the food industry for different purposes. Carrot fibres for example, can be used as a texturisers in bakery products, where they are known to improve the softness of the products. They can also be used as binders in meat products. The functions of these ingredients is mainly based on their ability to absorb and retain water. The manufaturer of carrot fibres, Bolthouse farms (USA), claim that carrot fibres can absorb 10 times their weigth in water. However, their possible use as a disintegrant has never been presented, and their hypothetical mechanism of action is not known.

In this part of Chapter 5, the disintegrants are characterised for two purposes:

- in terms of particles properties such as size, shape and density. These properties will have an impact on the processing of the tablets.

- in terms of water absorption and single particle swelling to asses their mechanisms of action.

5.3.1 Particle size distribution

The cumulative size distributions of the different disintegrants were determined with the QicPic appartus as described in Chapter 3 and the results are presented in Figure 5-2.

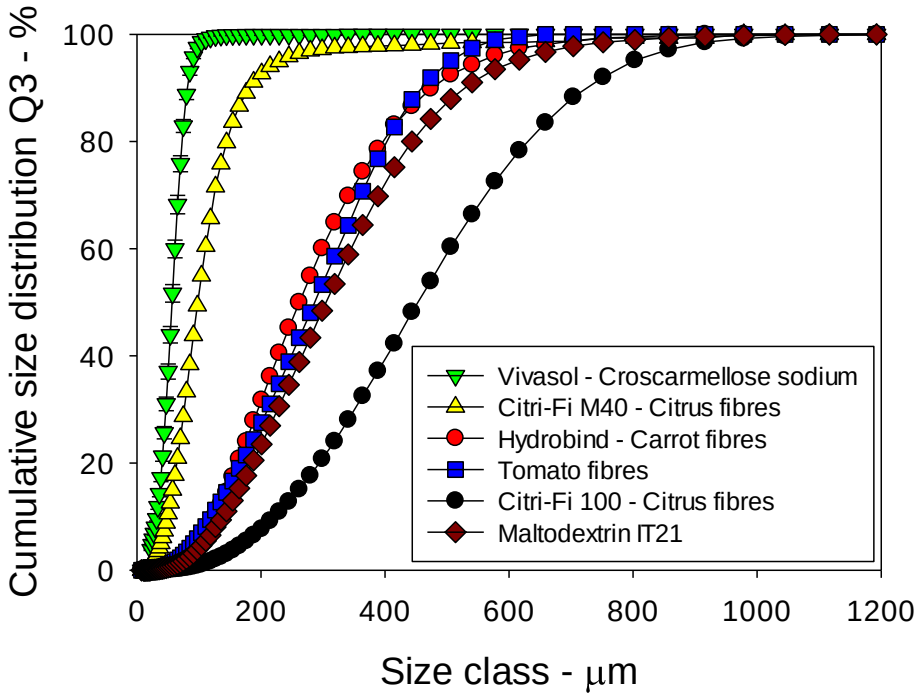

Figure 5-2: Cumulative size distributions of the different disintegrants chosen for this study compared to maltodextrin IT21. The results are based on 3 measurements and the error bars show the standard deviation

In Table 5-2, the median values $d_{50,3}$ for the cumulative distributions are indicated to ease the comparison between the different ingredients. It can be seen that a large range of sizes will be used. It can also be noticed that all the disintegrants with the exception of Citri-Fi 100, have a smaller median size than maltodextrin.

As pointed out by Koynov et al (2013), the compression of a mix of two components can be affected in the case where two different sizes are compressed together. The mix of a small quantity of smaller particles withing the bulk of larger particles can lead to changes in the tablet properties, such as porosity and tablet tensile strenght. This is mainly due to the fact that smaller particles can rearrange themselves in the void in between larger particles, thereby reducing the porosity. However, such small particles can lead to the opposite effect in the case where they are not mobile during the compression of the powder. Indeed, if the small particles simply recover the surface of larger particles, they can hinder the possible interparticles bonding of two large particles.

Table 5-2: Median diameter of the particles size distribution of the different disintegrants, compared with maltodextrin.

Ingredients	**Maltodextrin**	**Vivasol**	**Citrus fibre M40**	**Carrot fibre**	**Tomato fibre**	**Citrus Fibre 100**
$d_{50,3}$ - µm	298 (±9)	57 (±5)	100 (±4)	261 (±14)	279 (±16)	443 (±14)

5.3.2 Single particle swelling

As pointed out in Chapter 2, the main mechanism for disintegrants to cause tablet disintegration is the swelling of the individual particles in contact with water.

The different particles were placed under a digital microscope on top of which a high resolution SLR camera was placed. A single droplet of water was brought into contact with the particle and high resolution images were taken at regular intervals. Figure 5-3 shows the set-up used for the capture of the images.

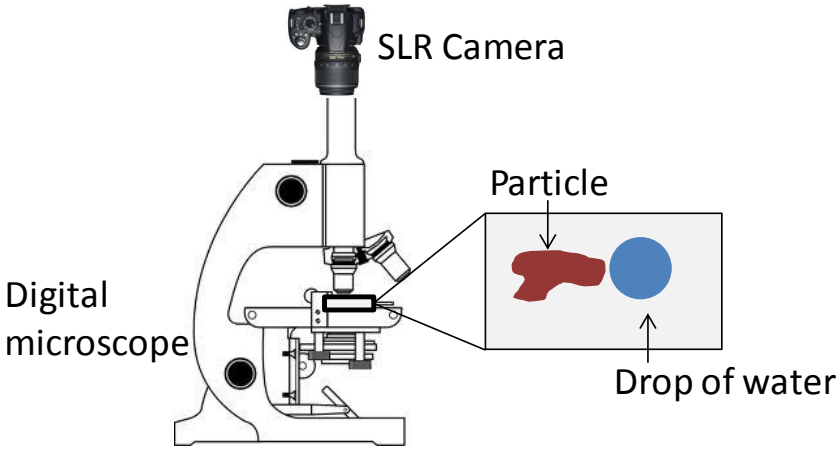

Figure 5-3: Set-up used to capture images of the swelling of individual particles

An example of a set of images obtained is presented in Figure 5-4. It shows the swelling and unfolding of a particle of carrot fibre after a drop of water (0.05 mL out of a needle and syringe) was brought in contact with it. The time scale between each image is 0.1s. It is clear from Figure 5-4 that there is an increase in particle volume after the addition of water. It is also interesting to note that the particle seems to unfold as water allows the release of the stress which was brought to the particle during processing.

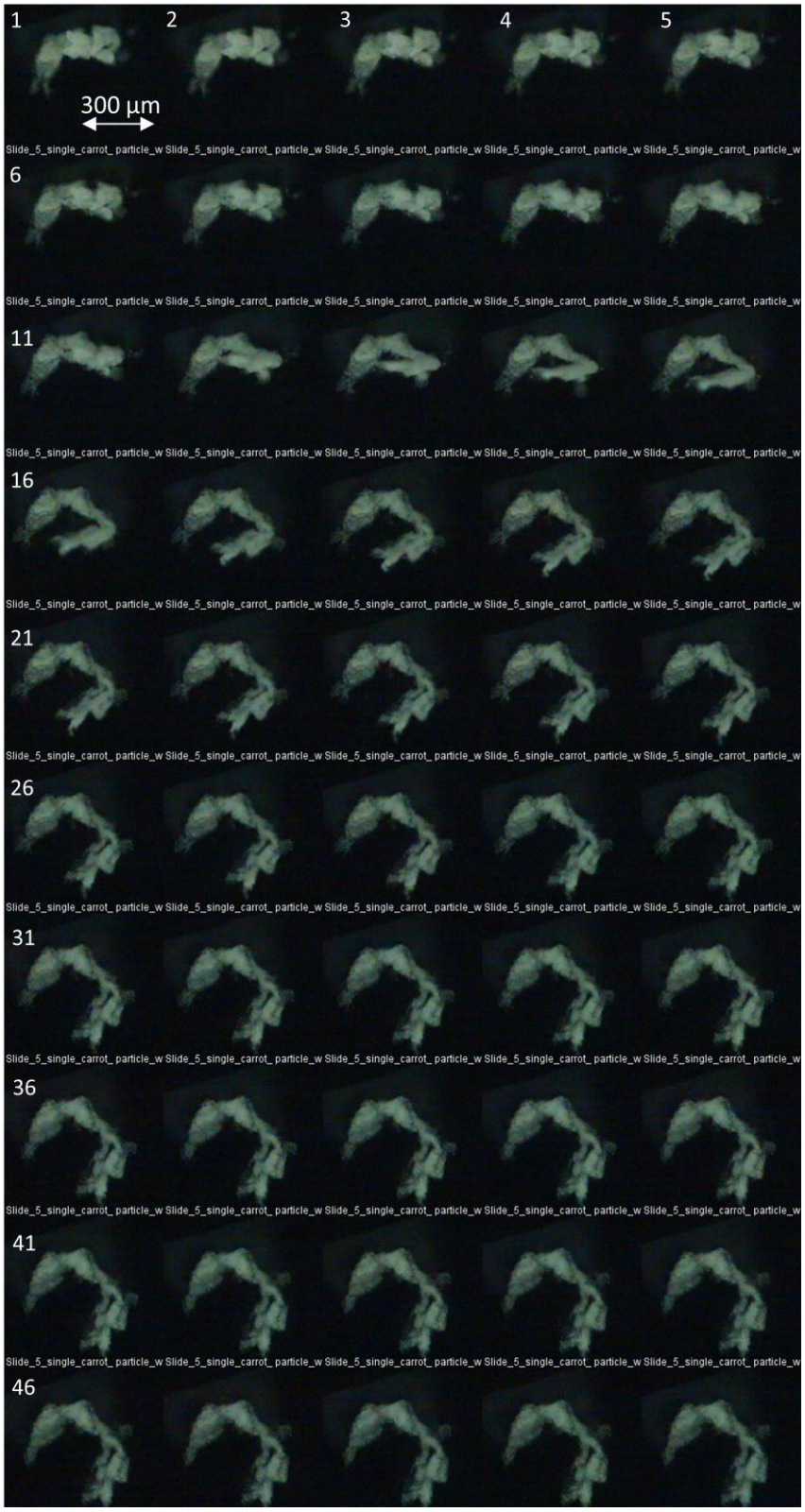

Figure 5-4: Example of a stack of images obtained during the swelling of a single particle of carrot fibre after addition of a droplet of 0.05mL at 25°C. The sequence of images can be read from left to right and then down.

The same experiment was carried out on different particles of carrot fibre; similar stack of images was obtained as in Figure 5-4. However, to obtain a more quantifiable answer to how much swelling actually occurs, the boundaries of the particle were selected and followed with time. Such work was carried out with the image analysis software Image J (National Institutes of Health, U.S.A). Once the boundaries of the particles were selected, a few images were selected and superposed to show the swelling of the particles as shown in Figure 5-5. The actual images obtained with the set-up presented in Figure 5-2 are shown at the top of Figure 5-5. The drop was added at t=0s. The bottom image show the boundaries of the particle at the different stages of the swelling. It can be seen that all boundaries seem to be increasing. The swelling appears to be fast as the maximum volume was reached in under 1 second.

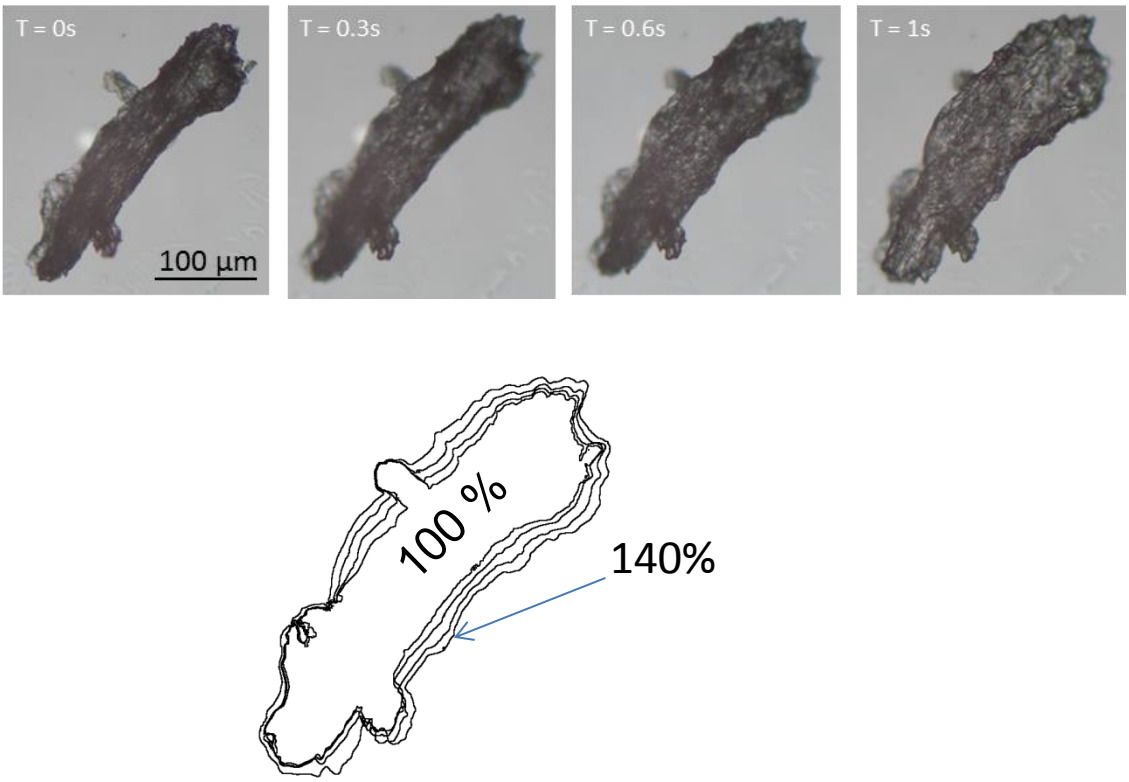

Figure 5-5: Swelling of a single particle of carrot fibre. Actual images (top) and boundaries with time

Similar work was performed for the particles of tomato fibres and citrus fibre (Citri-Fi 100). The small particles of vivasol and CitriFi M40 proved to be difficult to handle and the addition of water always lead to the wipe out of the particle across the glass slide. As a result, only images for tomato and Citri-Fi 100 were obtained. Figure 5-6 shows an example for each type of fibres.

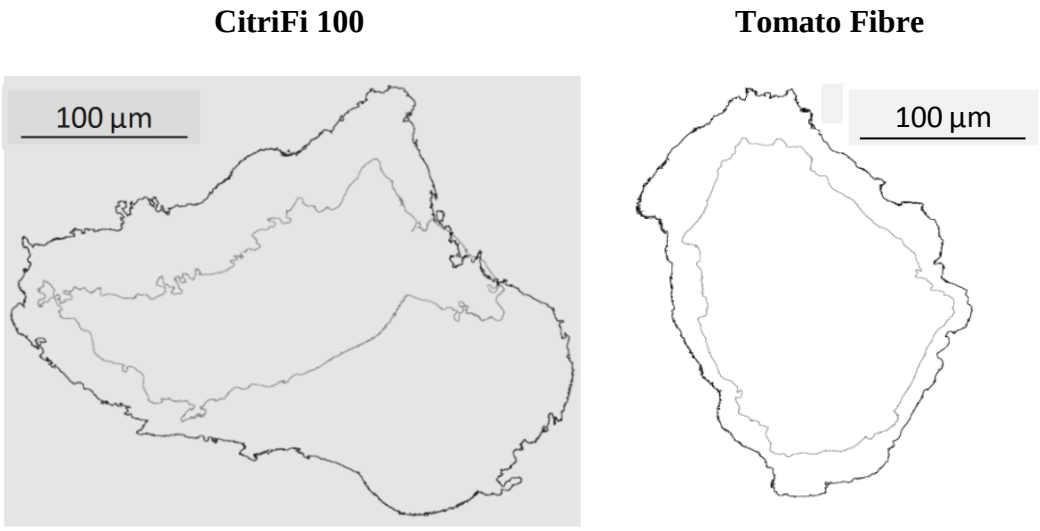

Figure 5-6: Single particle swelling of CitriFi 100 and Tomato Fibre

Even though it can be shown that the particles of the different disintegrants do swell in contact with water, it is not possible to get quantitative data to about how much swelling is actually obtained with this technique. First of all, the deposition of the water droplet on the particle is very subjective and difficult to replicate. In addition, to obtain reliable data, numerous particles should be studied. And finnally, only 2D image of the swelling of a 3D particle are obtained; obviously, the real behaviour in contact with water cannot be completely understood here.

However, it is shown that the particles do swell in contact with water which was the aim of theses experiments. The work presented in the next Chapter will investigate whether this swelling does induce tablet disintegration.

5.3.3 Hygrocapacity

The hygrocapacity describes the ability of a powder to attract and retain water molecules from the environement. It is described by the sorption isotherm which links the water content and the water activity of a product. The sorption isotherm can give information about which disintegrants attract more water and how fast. Indeed, a fast absorption of a large quantity of water can favor a quick penetration of water within the tablet.

The sorption isotherms of the individual powders are presented in Figure 5-7. For all powders a hysterisis can be noticed between the sorption and desorption of water. Several reasons can be formulated to explain this difference. Kachrimanis et al (2006) summarised the hysterisis phenomena to be due to two possible effects: the ink bottle effect and swelling. The ink bottle effect, which happens with small pore entrance and large volume beyond the entrance, is typically used to explain hysteresis at relative humidities higher than 75%, whilst at lower water activities swelling would be the reason. In addition, it can be thought that a possible collapse of the microstructure, a change in supramolecular structure (crystallisation) or structural relaxations can lead to such a hysteresis.

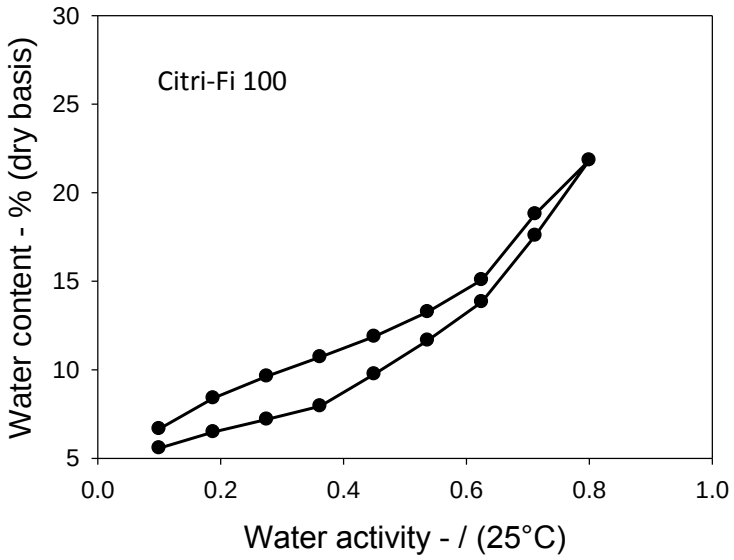
Citri-Fi 100
Water content - % (dry basis)
Water activity - / (25°C)
30
25
20
15
10
5
0.0
0.2
0.4
0.6
0.8
1.0

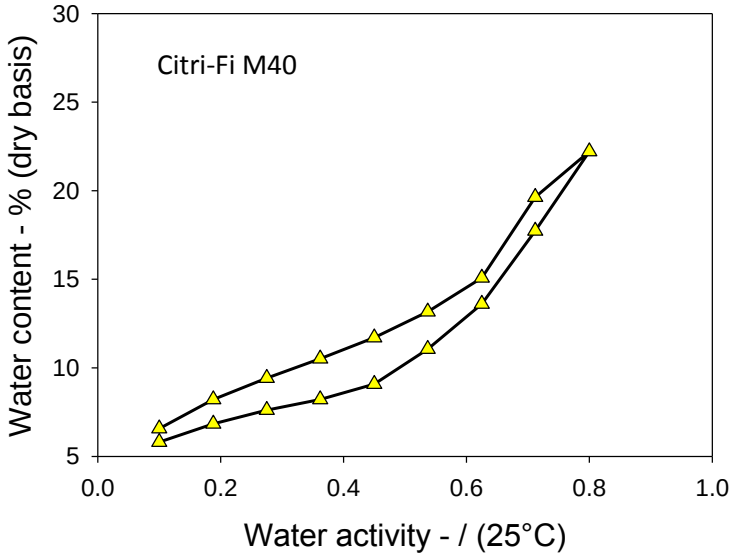
Citri-Fi M40
Water content - % (dry basis)
Water activity - / (25°C)
30
25
20
15
10
5
0.0
0.2
0.4
0.6
0.8
1.0

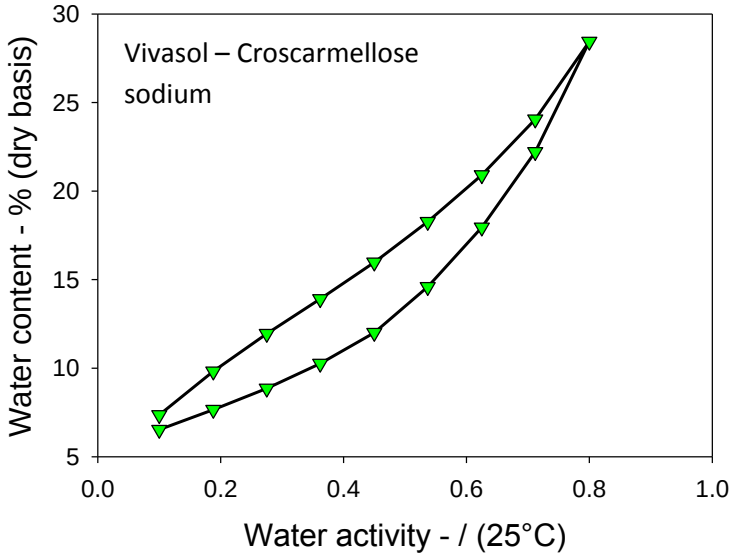
Vivasol – Croscarmellose sodium
Water content - % (dry basis)
Water activity - / (25°C)
30
25
20
15
10
5
0.0
0.2
0.4
0.6
0.8
1.0

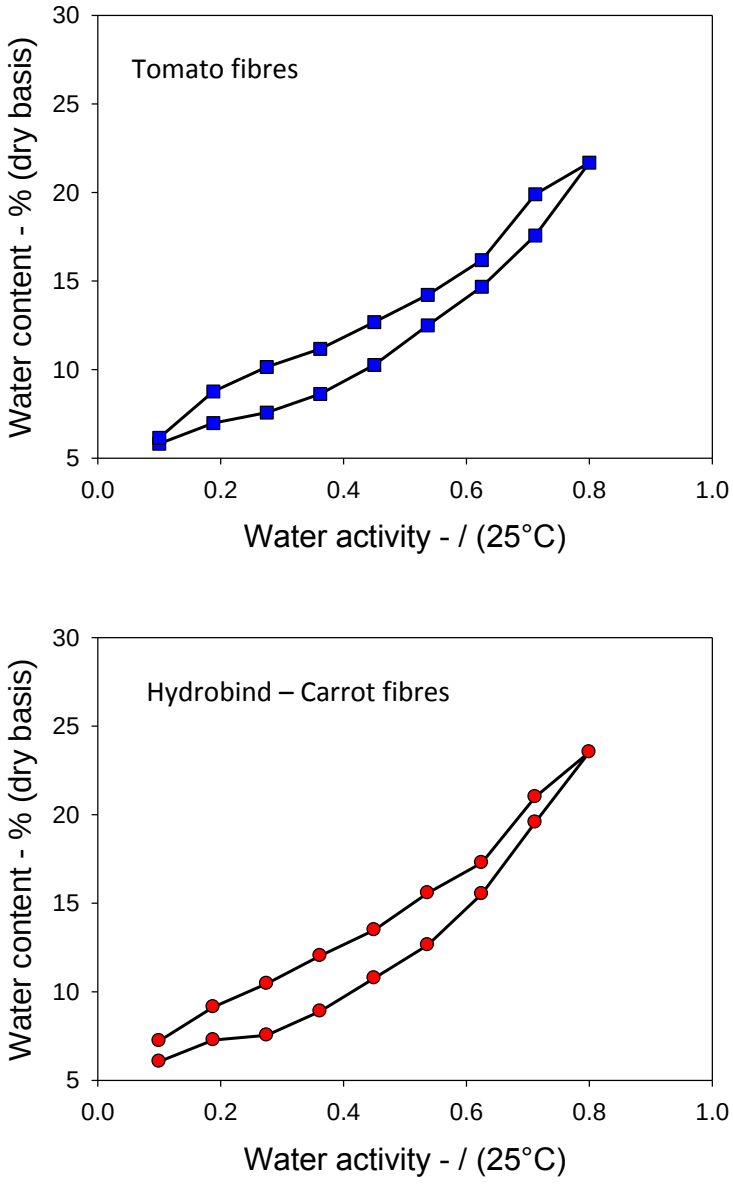

Figure 5-7: Sorption isotherms of citrus fibres Citri-Fi 100, citrus fibres Citri-Fi M40, Vivasol, Tomato fibres and Carrot fibres

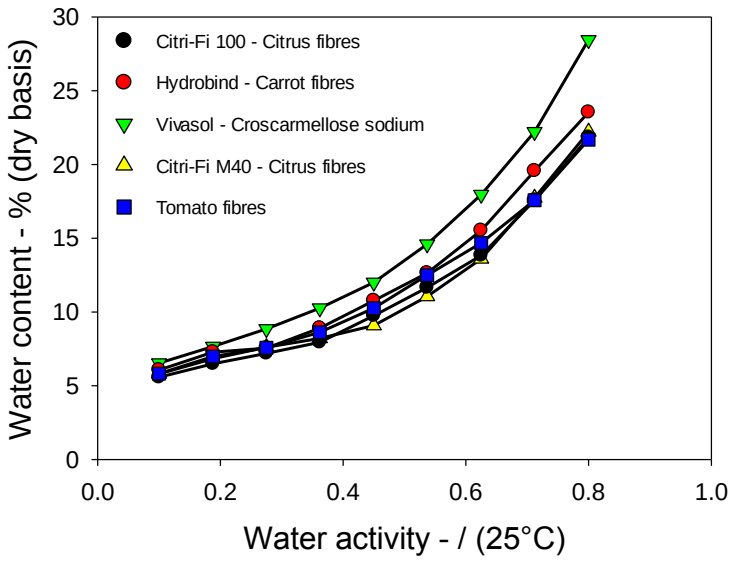

Figure 5-8: Comparison of the absorption curves of the different disintegrants

Figure 5-8 shows the difference in water content of the different powders during the absorption process. Only the absorption phase is shown to ease the comparison. It is interesting to see that all fibres contain less water at any awater activity than Vivasol which is a commercial disintegrant. The absorptions curves of the other disintegrants show little difference with, perhaps, carrot fiber able to absorb a larger quantity of water than the other three fibers. Vivasol, or croscarmellose sodium, is a crosslinked derivative of cellulose. Cross linking provides the non-dissolving capacity to the molecules by hindering the chain separation and polymer diffusion into the solvent (Mesnier, Althaus et al. 2013). However, the swelling of croscarmellose sodium is made possible due to the bonding of water in between the polymer chains (Schott 1992). The carboxyl groups which can be seen on the chemical structure of croscarmellose sodium (Figure 5-9) offer more sites for water to bond with the molecule. This increases its affinity with water over a typical cellulose molecule. During the sorption of

water, bonds are created and the system passes to the rubbery state. However, when desorbing water, the outer layer endures a phase transition back to the glassy state. In the glassy state, the diffusion rate of water is slower (Gianfrancesco, Vuataz et al. 2012). Thus more time would be needed to reach the same equilibrium level as during sorption. It leads to the fact that less water is removed for a same water activity as shown in Figure 5-7.

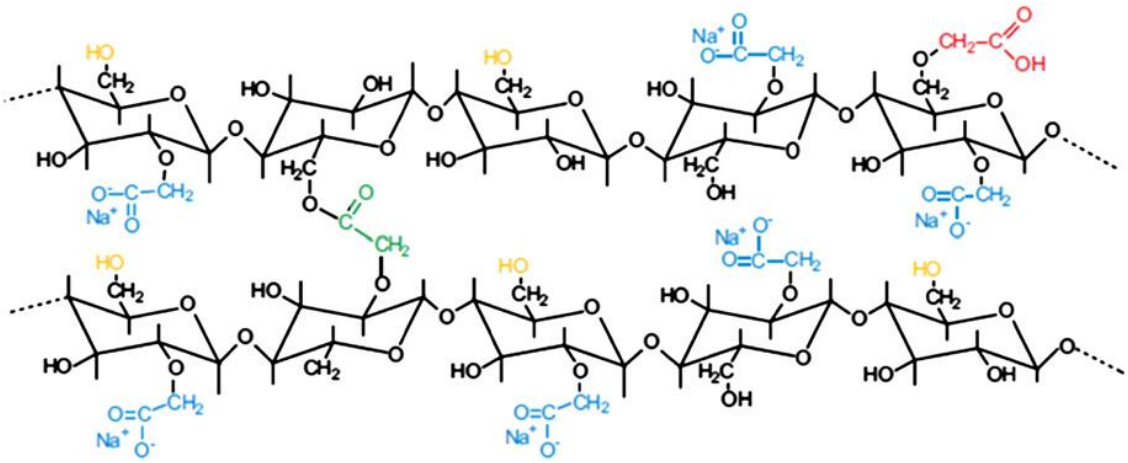

Figure 5-9: Chemical structure of croscarmellose sodium (JRS Pharma, Germany)

The difference in water content between the different disintegrants may be due to the difference in total fibre contant in the powders. Vivasol, which is a pure product, does not contain traces of fat, ashes and other compounds that may prevent water sorption. However, overall, it can be conluded that all powders can sorb large quantities of water and fairly quickly. It was seen on the individual particle swelling that maximum swelling was reached in less that a couple of seconds. This is a positive result for their potential use as disintegrants.

5.3.4 Scanning Electron Microscope images

Scanning Electron Microscope (SEM) images of the different powders were taken using the protocol described in Chapter 3. The SEM images show that the different fibres have a long needle-type shape. Examples of each powder are presented in Figure 5-10. Such a shape can prove to be difficult to compress, as the shape may prevent the mobility of the particle during the compression; especially during the first stage where particle rearrangement occur (Pitt and Sinka 2007).

Croscarmellose sodium - Vivasol

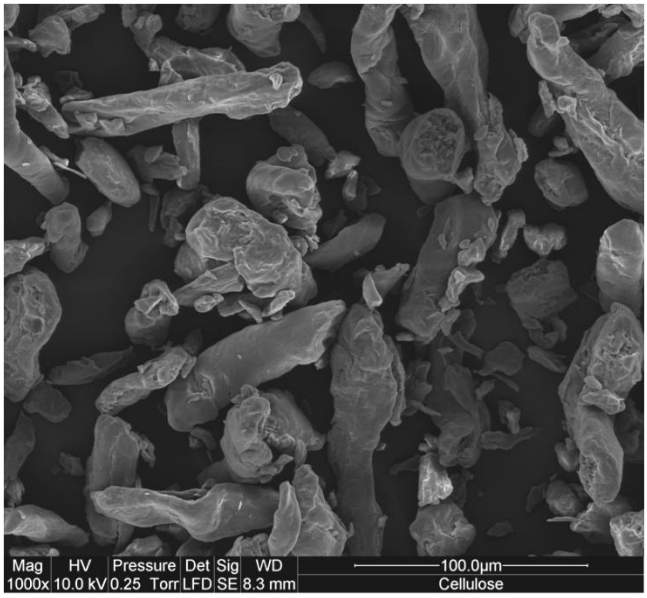

Hydrobind - carrot fibres

Citi-Fi 100

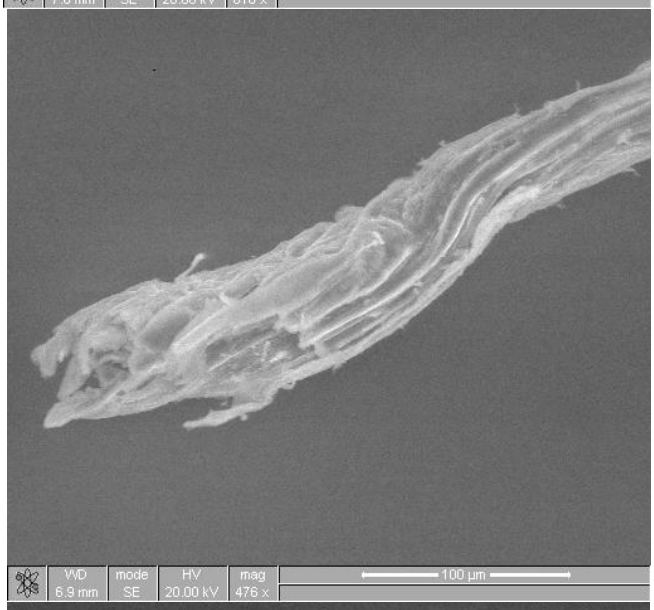

Citri-Fi M40

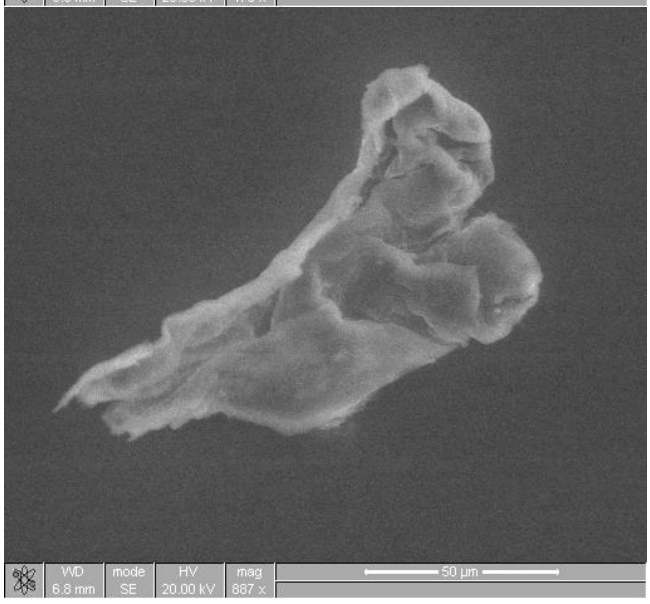

Tomato fibres

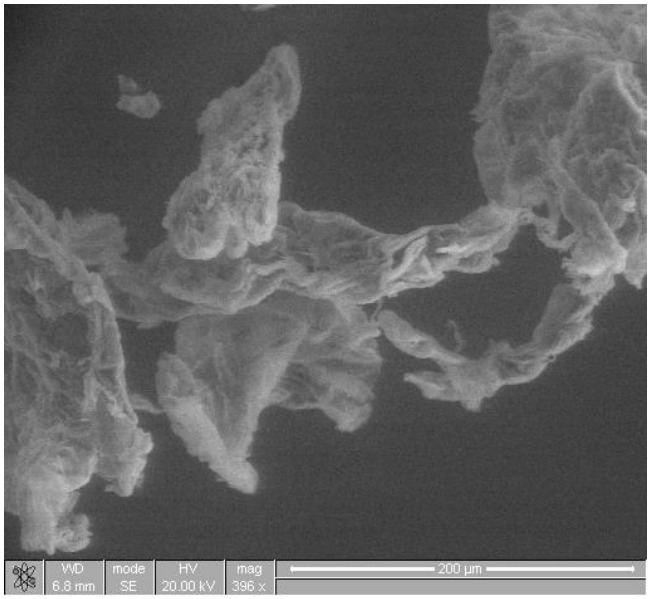

Figure 5-10:S.E.M. images of the different types of disintegrants used in this work

Vivasol has certainly been the most studied of all powders. Several papers present SEM images of vivasol. Thibert and Hancock (1996) have looked at the change in morphology of croscarmellose sodium particle equilibrated at different relative humidities in an environmental SEM. They showed that at high relative humidities (80%), the particles present extensive swelling and twisting. It is interesting to note that, in their study, when the relative humidity was reduced down to 40%, the particles did not regain their original shape. This fact was linked by the authors to the observed hysterisis on the sorption isotherm. The hysterisis was observed in this work as well (Figure 5.7). The fact that the shape of the particles is not regained also indicates that the disintegrants should be kept at low relative humidities as exposure to moisture might change their swelling and thus the disintegrant properties.

5.4 Conclusions and Outlook

This chapter, dedicated to the process thinking for the choice of disintegrants and their charaterisation, introduced 5 types of powders. Four types of natural fibres were chosen for their potential as a disintegrant which was measured in terms of single particle swelling and water sorption capabilities and compared to a commercially used disintegrants in the pharmaceutical industry.

The different disintegrants were then mixed with maltodextrin IT 21 powder and tablets were made using two different tabletting settings. The settings (upper punch maximum displacement and powder fill depth) are the ones corresponding to the setting used to produce tablets of maltodextrin IT 21 at porosity 0.27 and 0.35. These two porosities were chosen as it was shown previously in Chapter 4 that their dissolution behaves accordingly to two different type of regime: erosion and dissolution. In addition, the value of 0.27 was chosen as it corresponds to the value of 0.25 which is the average porosity for tablets of interest in the food industry (Forny 2010). The aim was to study the effect of the incorporation of disintegrants in tablets of maltodextrin IT 21 and observe their effect on both types of regimes

CHAPTER 6 - ADDITION OF DISINTEGRANTS IN MALTODEXTRIN TABLETS

6.1 Introduction

Chapter 4 was dedicated to the study of the dissolution of pure maltodextrin tablets. In Chapter 5, the disintegrants used in this work were introduced and characterised. In this Chapter, maltodextrin and disintegrants are finally mixed together. The dissolution of tablets containing a mix of maltodextrin and disintegrants is thus investigated.

The five different types of dinstegrants are mixed with maltodextrin prior to tabletting. In addition to the type of disintegrants, different concentrations are also investigated. This chapter aims at answering the following questions:

- What is the influence of the use of disintegrants and their concentration on the dissolution times? Will they be of benefit?
- Can disintegrants decrease the dissolution time of tablets dissolving accordingly to either the erosion or the disintegration regimes, which were highlighted in Chapter 4?

Futhermore, this chapter will present possible solutions to deal with the dissolution time – tablet strength trade off. This trade off, which is well known to powder technologists is tackled with a simple but effective use of the spatial distribution of the disintegrants within the tablet.

6.2 Disintegration regime

According to Chapter 4, the dissolution of tablets of maltodextrin can be categorised into two types: erosion and disintegration. It was shown that in the disintegration regime, tablets would disintegrate quickly because of the fast liquid penetration within the pores. This fast liquid penetration would be very useful when disintegrants are present within the tablet. Indeed, the liquid can trigger fast swelling of the disintegrant particles which would strongly increase the tablet disintegration and allow a fast dissolution.The mechanical setting used to produce a tablet of porosity equal to 0.35, thus dissolving according to the disntegration regime, were chosen as a reference. The value of 0.35 was chosen as it is at the low limit of porosity for the disintegration regime. Higher values of porosities have already a very fast dissolution, thus it is not necessary to include disintegrants. Mixes of maltodextrin and different concentrations of disintegrants (1, 2, 5, 10, 20% in weights) were compressed to these same settings. The dissolution time of these tablets are compared in Figure 6-1.

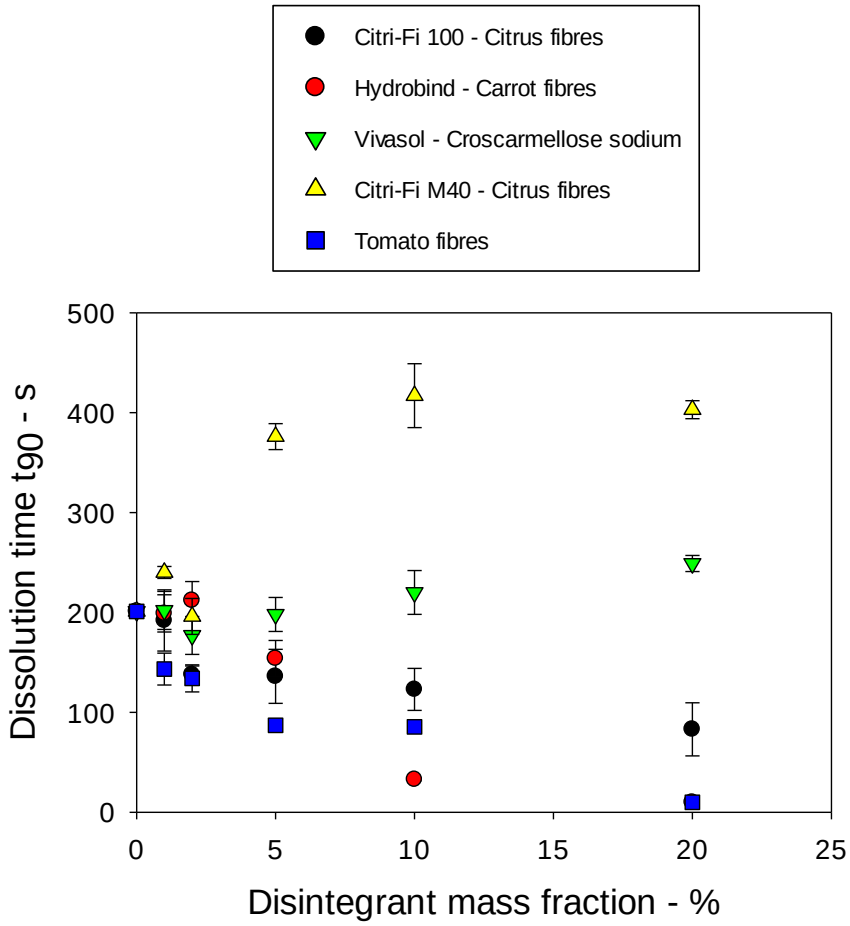

Figure 6-1: Dissolution time of tablets of maltodextrin containing different mass fractions (1, 2, 5, 10, 20%) of disintegrant: disintegration regime. The point at 0% disintegrant is the dissolution time of maltodextrin IT21 (0.35 porosity) without any disintegrant. Experimental conditions: 50°C and 300 rpm

The first point to notice is the fact that not all disintegrants induce a reduction in dissolution time when present in the tablets. It seems that the most effective disintegrants are carrot fibres, tomato fibres and Citri-Fi100. Citri-Fi 100 seems to be more effective at low concentrations (1 to 5%) than carrot fibres, even if the difference in dissolution time is very small. However, the incorporation of carrot fibres at concentrations of 10 or 20% (same point as 20% of tomato fibres)

induces a very short dissolution time. The dissolution time is decreased by 85 and 95 % for these two concentrations when carrot fibres are included in the tablets.

Vivasol is a disintegrant which is commonly used in the pharmaceutical industry and is used here as a reference. The incorporation of vivasol in maltodextrin tablets does not seem to be effective, even though a slight decrease in dissolution time is noticed at 2% concentration. It appears that the dissolution time is actually increased for a concentration greater than 5%. Such a result is in agreement with previous studies carried out with vivasol on different systems. Ferrero et al., (1997) observed an increase in disintegration time at concentrations of 10%. The main reason put forward is the creation of a gel layer surrounding the tablets at high concentrations which prevents water penetration within the tablet. Such a gelly structure may prevent the liquid to access the solid tablet and slow down the dissolution. It is interesting to notice that such a gel is not present when fibres are used. It is one of their advantages.

It is interesting to observe that the incorporation of the two types of citrus fibres results in very different dissolution times, as it shows the influence of the disintegrants particle size on the dissolution time. The main difference between the two types of powder is their particle size distribution. As it was observed in Chapter 5, Citri-Fi 100 has a significaty higher particle size (Figure 5-2). The size of the powder should influence the tabletting step, thereby having an effect on particle rearragement and tablet porosity. In Figure 6-2, images of the powders show that the particles also have different shapes which may also influence the tabletting properties. Further insight about the difference in dissolution times is given later in this section when comparing tablets tensile strengths.

Citri-Fi 100 Citri-Fi M40

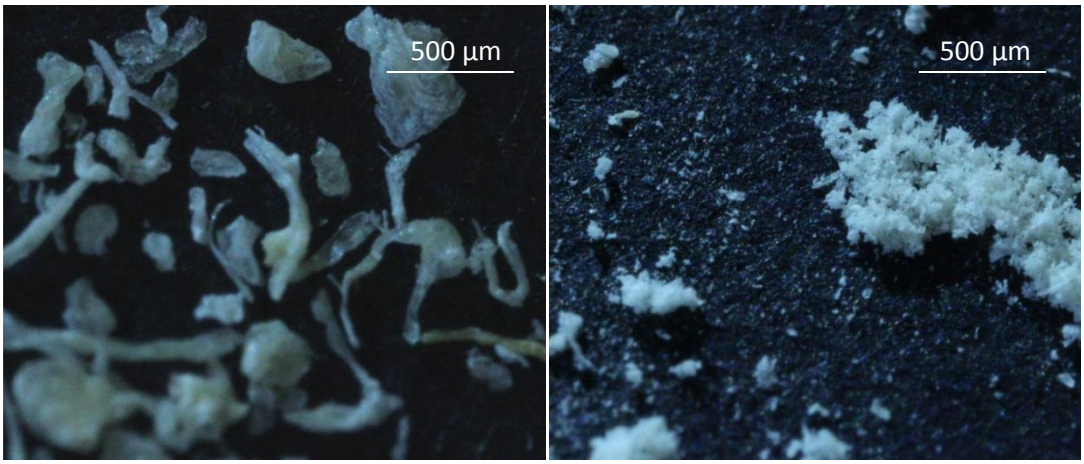

Figure 6-2: Difference in size and chape of the two types of citrus fibres; Citri-FI 100 and Citri-Fi M40

The three disintegrants which seem to perform the best are carrot fibres, Citri-Fi 100 and tomato fibres. Their dissolution time is reproduced more clearly in Figure 6-3. Out of all three disintegrants, tomato fibres seem to be the most efficient for all concentration, except for 10% where carrot fibres perform the best. At concentrations of 20 %, the results obtained with carrot fibres are similar to the ones obtained with tomato fibres.

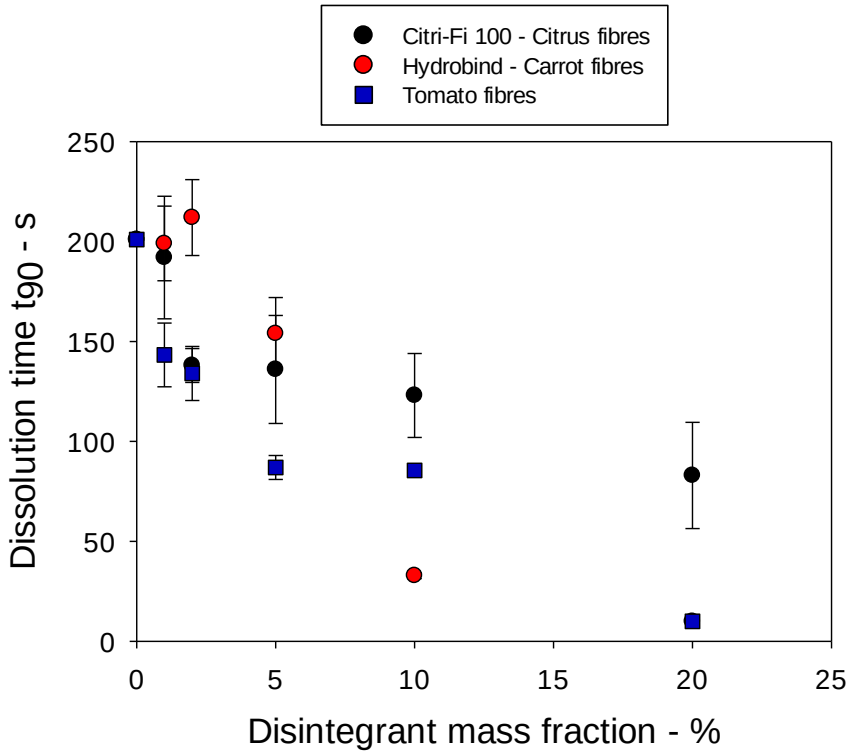

Figure 6-3: The three disintegrants that show a decrease in dissolution time

The effect of the incorporation of disintegrants was also measured on the tablet tensile strength as presented in Figure 6-4.

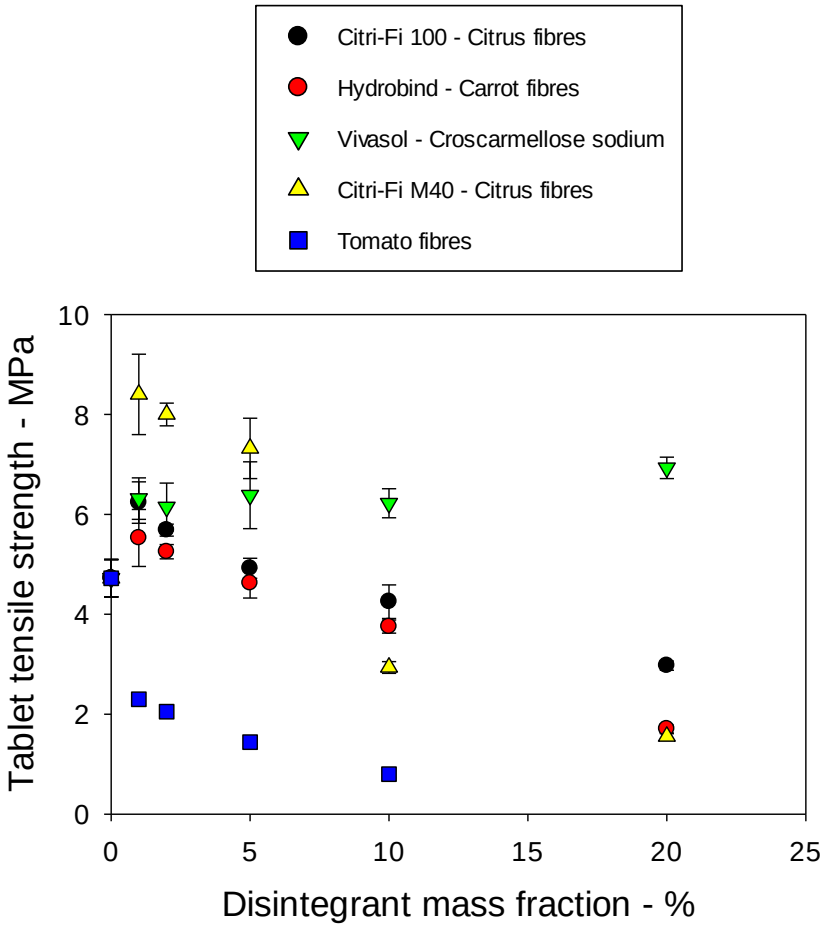

Figure 6-4: Tensile strength of tablets of maltodextrin containing different mass fractions (1, 2, 5, 10, 20%) of disintegrants: disintegration regime. The point at 0% disintegrant represent the tensile strength of maltodextrin IT21 (0.35 porosity) without any disintegrant.

The tensile strength of tablets containing carrot fibres, tomato fibres and Citri-Fi 100 is decreasing with higher disintegrant concentrations. This could be the result of weaker inter-particle bonding or an increase in tablet porosity due to the presence of fibres.

It is interesting to notice that tablets containing Vivasol show an increase in tensile strength compared to the tensile strength of pure maltodextrin tablet.

Vivasol particles ($d_{50,3}$ = 55 µm) are much smaller than maltodextrin particles ($d_{50,3}$ = 350 µm). The reason behind this increase in tensile strength may be that the small particles of vivasol fill the gaps between the particles of maltodextrin resulting in a decrease in the porosity and thus stronger tablets. The same phenomena was observed by Koynov et al (2013) for a mix of microcrystalline cellulose and several micronized actives ingredients. They concluded that a second rearrangement steps occurs when a mix of two particles with a large difference in size is compressed. This appears to be the case for Vivasol.

In the case of the addition of Citri-Fi M40, a sharp increase in tablet tensile strength is noticed for low concentrations of 1, 2 and 5% compared to the tensile strength of pure maltodextrin IT21. A similar mechanism to the addition of vivasol could explain such an effect. However, for larger concentrations of disintegrant, 10 and 20%, the tensile strength is actually reduced. It was noticed that when Citri-FI M40 was mixed with maltodextrin IT 21, prior to tabletting, it appeared that the small particles of Citri-Fi M40 were covering the particles of maltodextrin. Such a phenomenon could be compared to a coating by the smaller disintegrant particles, similar to the action of lubricant (Chouk 2010). This may probably result in a decrease of the bonding capacity between maltodextrin particles producing weaker tablets.

The difference in tensile strength noticed between the two types of citrus fibres is also another reason for the different in dissolution time highlighted in Figure 6-1. It has been shown previously that an increase in tablet tensile strength results in a longer tablet dissolution time (Gabbott 2007). In addition, it cannot be excluded that the disintegrant capabilities of citrus fibres may be affected by the size of the particles introduced in maltodextrin tablets. Indeed, it was reported that in some

cases the larger particles of a disintegrant perform better than the smaller ones (Bele and Derle 2011).

Figure 6-5 highlights the tensile strength of the three disintegrants which seem to improve the dissolution time. Even though the incorporation of tomato fibres results in a dramatic decrease in dissolution time, in compensation, the tensile strength is largely reduced as well. The tensile strength of tablets containing 20% of tomato fibres could not even be measured due to its extremely low strength. The low tablet strength would be an issue for transport capabilities.

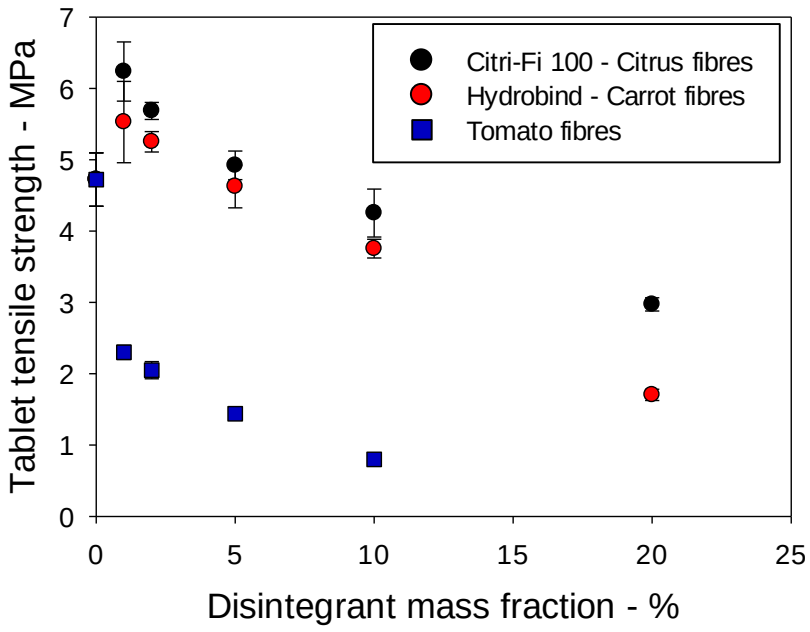

Figure 6-5: Tensile strength of tablets containing the three disintegrants that show a decrease in dissolution time in Figure 6-2.

From Figure 6-5, it can be concluded that tomato fibres are not suitable for use as disintegrants, mainly because they cause a non desirable dramatic reduction in tablet strength. As a result, it will not be considered further in this section.

The reduction in tensile strength may be due to a change in tablet porosity resulting from the introduction of disintegrants. Figure 6-6 shows the porosity for all tablets investigated. The porosities were obtained through the method presented in Chapter 3. The values of the true densities required to calculate the porosities are shown in Table 6-1. The method used is described in Chapter 3.

Table 6-1: True densities of the different disintegrants.

Disintegrants	**True density ($g.cm^{-3}$)**
Citri-Fi M40 – Citrus fibres	1.5047
Carrot fibres	1.5695
Citri-FI 100 – Citrus fibres	1.5057
Vivasol	1.5940

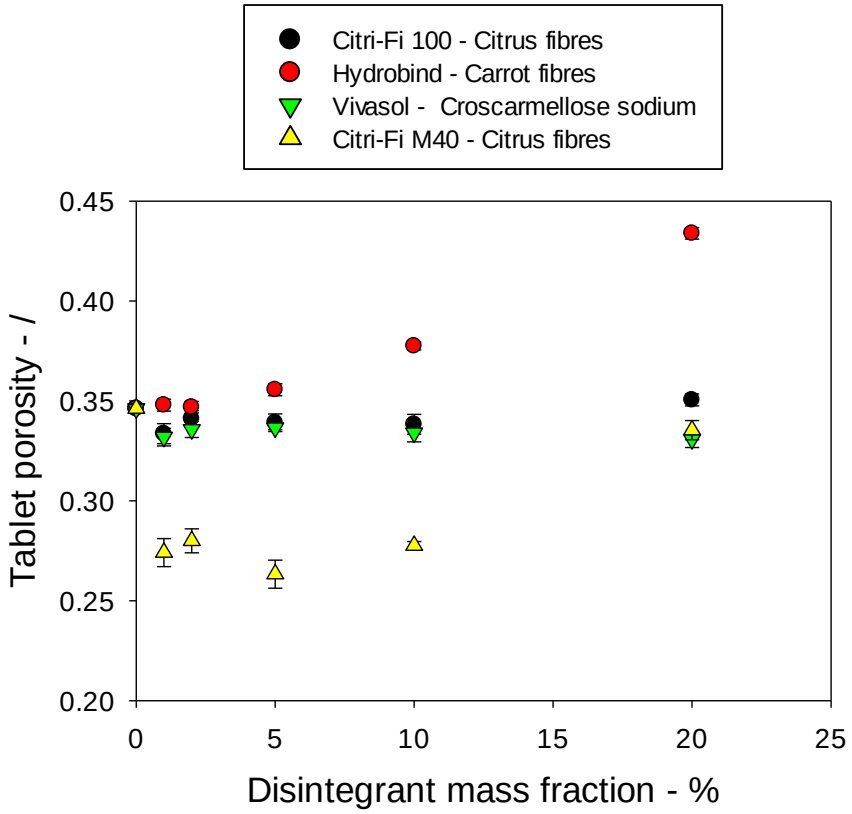

Figure 6-6: Porosities of tablets of maltodextrin containing different mass fractions (1, 2, 5, 10, 20%) of disintegrants: disintegration regime. The point at 0% disintegrant represent the tablet porosity of maltodextrin IT21 tablet without any disintegrant

It is interesting to note that the incorporation of vivasol and Citri-Fi 100 does not alter the porosity of the tablets significantly. However, in the case where Citri-Fi M40 is included in the tablets, a large decrease in tablet porosity can be seen. This result links very well with the increase in tensile strength and the longer dissolution time observed in Figures 6-4 and 6-1. The hypothesis put forward here is that the small particles fill the gaps between the particles of maltodextrin resulting in a decrease in the porosity and thus stronger tablets.

On the contrary, an increase in tablet porosity is observed with the incorporation of carrot fibres in comparison with tablets of pure maltodextrin IT21. This increase in porosity might play a role in the shorter dissolution time measured in Figure 6-1. The increase in porosity can be explained by the elastic behaviour of carrot fibres. As it can be seen in Figure 6-7, an increase in expansion post compression is noticed when carrot fibres are included in the tablets. After compression, the size of the tablets tend to increase due to the release of part of the stress accumulated during compression, this phenomena is called post-compression expansion (Hardy, Cook et al. 2006). It is obtained from the difference in thickness measured during tablet production (minimal punch separation) and the thickness 24 hours after production according to the following equation:

$$Elastic\ re-expansion\ (\%) = \frac{h_{24} - h_c}{h_c} \qquad \text{Eq. 6-1}$$

Where h_{24} is the tablet thickness after 24 hours and h_c, is the tablet thickness at minimum punch separation.

Maltodextrin tablets present on their own such behaviour as pointed out by Palzer (2009). A similar value of 29 % re-expansion was measured by Palzer (2009), for the same water activity a_w=0.3. However, the introduction of carrot fibres amplifies the elastic response. The energy stored during the compression of the particles is restored through the elastic re-expansion which increases the size of

the tablets post compression and thus the porosity. Such behaviour was not observed for the other types of disintegrants.

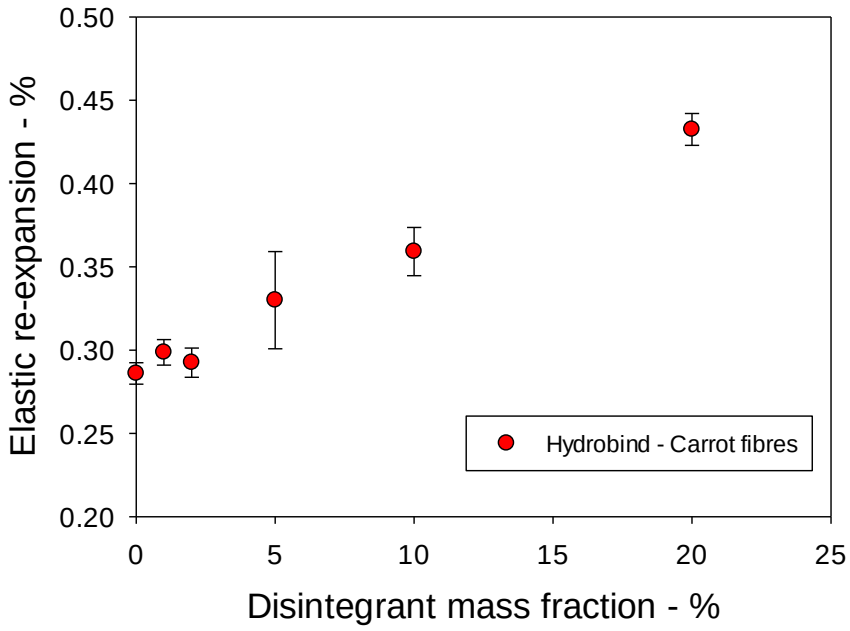

Figure 6-7: Elastic re-expansion observed when carrot fibres are present in the tablets of maltodextrin at different mass fractions

6.3 Erosion regime

It was seen in section 6.2 that the incorporation of disintegrants in a tablet of maltodextrin, normally behaving according to the disintegration regime, does improve the dissolution time. However, such an improvement is associated with a non desirable reduction in tensile strength. This section aims at investigating the introduction of disintegrants in a tablet of lower porosity: 0.27. At this porosity, the dissolution behaves according to the erosion regime. In this regime, dissolution occurs at the surface of the tablet and liquid penetration is limited. If

the liquid penetration is limited, the swelling of the disintegrants might be less probable.

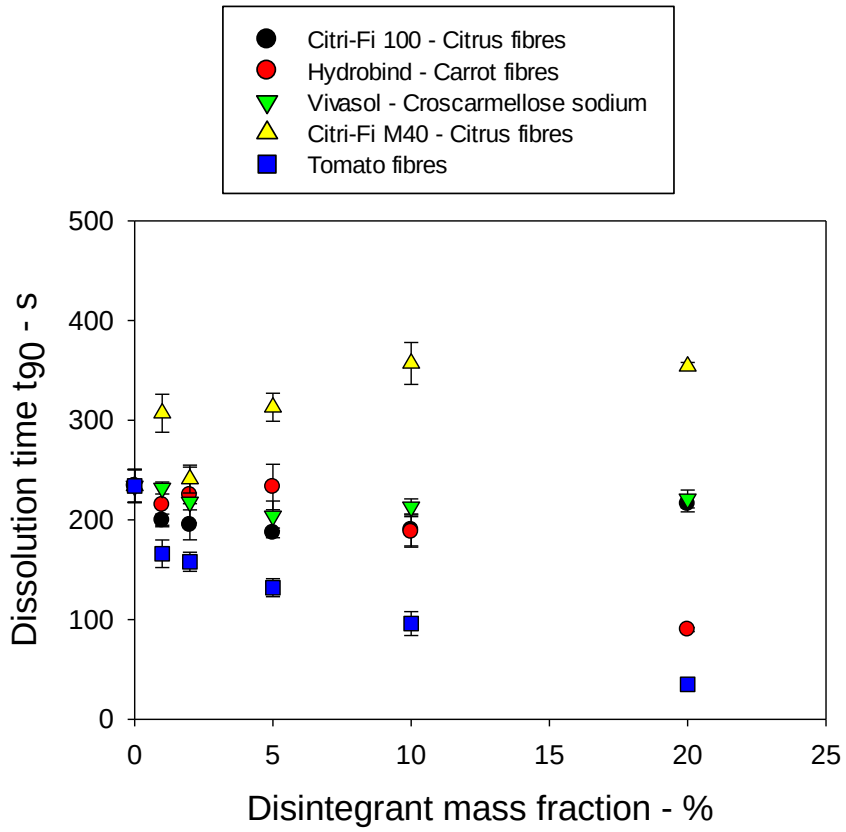

Figure 6-8: Dissolution time of tablets of maltodextrin containing different mass fractions (1, 2, 5, 10, 20%) of disintegrants – erosion regime. The point at 0% disintegrant is the dissolution time of maltodextrin IT21 (0.27 porosity) without any disintegrant. Experimental conditions: 50°C and 300 rpm

In Figure 6-8, the dissolution times of tablets of maltodextrin containing different concentrations of disintegrant are presented and compared to the dissolution time of tablets made of pure maltodextrin at a porosity of 0.27. Similar trends to Figure 6-1 can be found, except that the incorporation of disintegrants does not reduce the dissolution time as significantly. In the case of carrot fibres, which was the

best disintegrant in section 6-2, the dissolution time of tablets containing 10% of the disintegrant, is reduced by 84% in Figure 6-1 and by only 20% in Figure 6-8. This difference could mainly be due to two factors. Firstly it could be due to the fact that the tablets have a smaller porosity to the ones presented in Figure 6-1. Indeed, the same tabletting settings used to produce tablets of pure maltodextrin at a porosity of 0.27 were used to produce the tablets containing disintegrants presented in Figure 6-8. In addition, a different dissolution type regime is expected at this porosity. If the tablets still dissolve accordingly to the erosion regime in the presence of disintegrants, it might be expected that the access to water by the disintegrants is more limited than in the disintegration regime. The determination of the type of dissolution regime for these tablets would be useful to understand the action of the disintegrants. Indeed, the incorporation of the disintegrants aims at shifting from an erosion to a disintegration regime to shorten the dissolution times of food tablets. It will be discussed later in this chapter how the study of the dissolution regime is being investigated in the next chapters.

The tablet tensile strengths were also measured for tablets introduced in Figure 6-8. The results are presented in Figure 6-9. Similar trends to as Figure 6-4 can be seen and the same interpretation can be expressed.

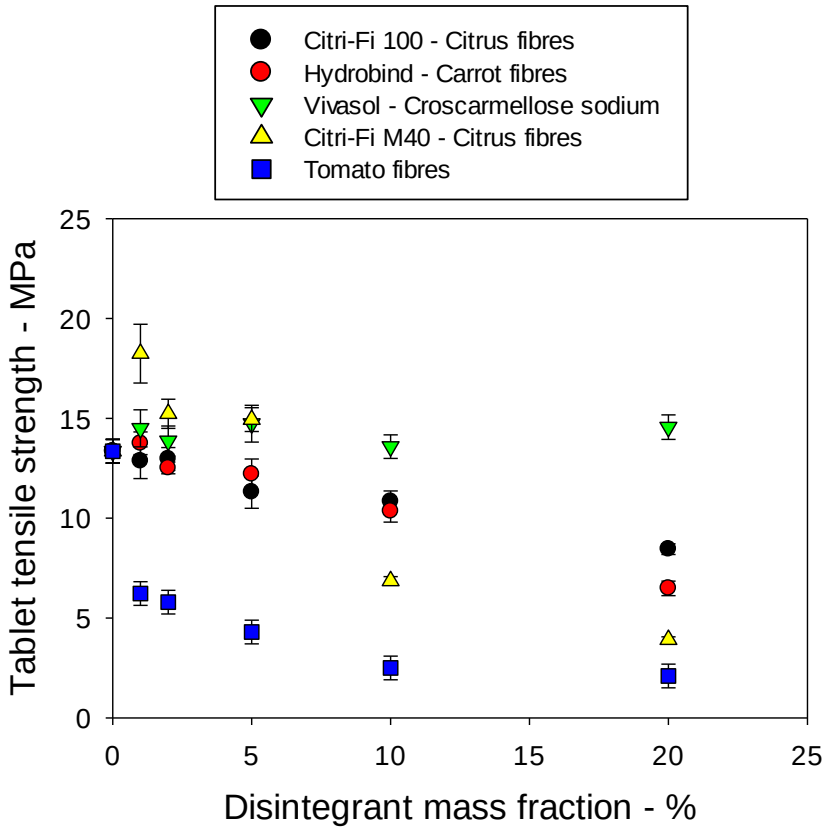

Figure 6-9: Tensile strength of tablets of maltodextrin containing different mass fractions (1, 2, 5, 10, 20%) of disintegrant

6.4 Disintegrants' spatial distribution in tablets

Figure 6-10 shows the trade-off between the tablet tensile strength and dissolution time obtained when, in this case, carrot fibres are introduced within tablets of maltodextrin IT21. Only carrot fibres are further studies in this section as they showed to be the best disintegrants previously. It can be seen that the greater the concentration of disintegrant, the shorter is the dissolution time. However, the tensile strength is also reduced which may be prove to be problematic when considering the handling capabilities of the tablets. The reduction in tensile strength upon incorporation of disintegrants was also shown by several authors such as Lundqvist et al., (1997) and Adebayo et al (2008). In both cases, the

difference in strength was explained by a change in elastic and plastic responses of the mixes during compression.

In order to reduce the dissolution time of maltodextrin IT21 tablets only the concentrations of 10 and 20% are effective. However, including these very large concentrations into a tablet would largely impact the gustative properties.

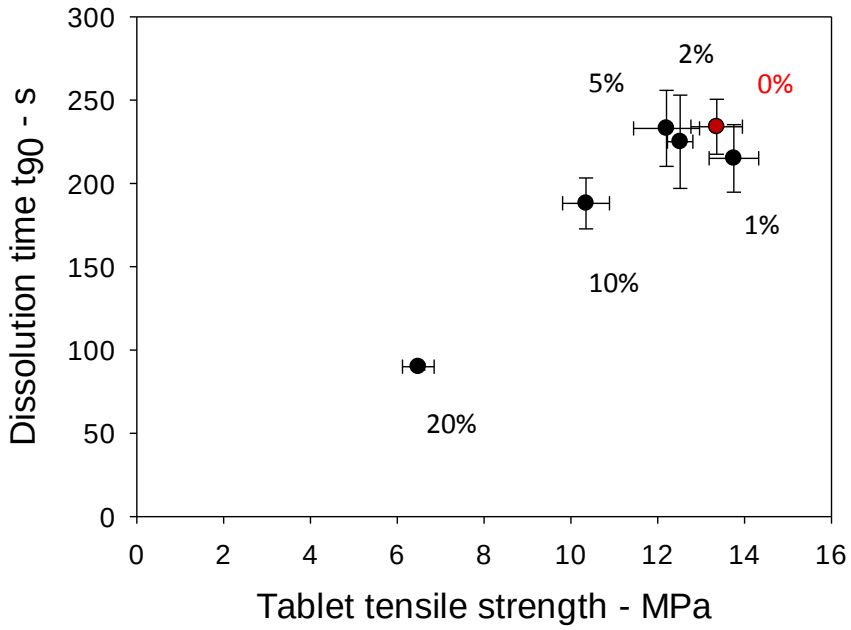

Figure 6-10: Evolution of the tablet tensile strength and dissolution time of tablets of maltodextrin IT 21 when different concentrations (w/w) of carrot fibres are introduced in maltodextrin tablets. The point at 0% disintegrant corresponds to a tablet at 0.27 porosity

Disintegrants act mainly by swelling and wicking as highlighted in Chapter 2. However, in order for swelling to occur and lead to the breakage of the tablet into smaller pieces, water needs to reach the disintegrant particles. The liquid penetration of water in different tablets was then studied as shown in Figure 6-11 and 6-12. The tablet is placed longitudinally above water, dyed in red for a better

visual inspection, and brought in contact with the liquid. It can be seen that the liquid penetrates very quickly, in less than 5s, through the pores to wet the whole tablet of pure maltodextrin IT21. However, when different concentrations of carrot fibres are introduced, the final liquid penetration length is reduced dramatically. In the presence of 10% carrot fibres, liquid penetration ceases after a third of the tablet thickness (figure 6-12). As a result, it appears that the swelling capacity of the disintegrant particles is not fully used to its potential as most of the disintegrants are not in contact with water.

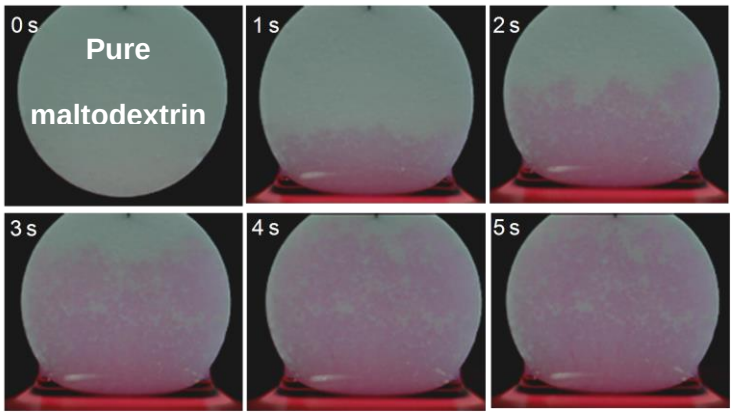

Figure 6-11: Liquid penetration as a function of time in a tablet of maltodextrin IT21

However, it could be noticed that disintegration would occur at the bottom part of the tablet where the disintegrants are reached by the liquid (Figure 6-12). Porosity is the main factor influencing liquid penetration within a tablet when wetting is favourable (Forny, Marabi et al. 2010).The porosities of the different tablets show that introducing carrot fibres tends to slightly increase the tablet porosity, as seen in Figure 6-13 (from 0.27 for pure maltodextrin tablets to 0.34 when the tablet

contained 20% of disintegrant), which should lead to improved liquid penetration. The fact that the opposite is noticed is a problem for the disintegrant's action and could be due to the closing of the pores due to the swelling of the disintegrants and that most of the water is retained by the disintegrants.

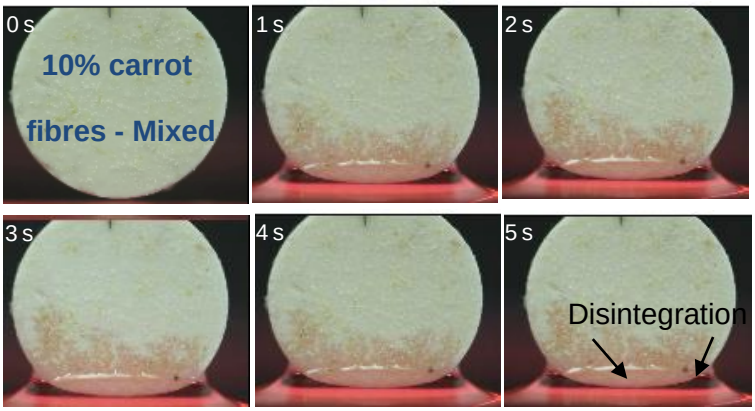

Figure 6-12: Liquid penetration as a function of time in a tablet of maltodextrin IT21 containing 10% (w/w) of carrot fibres

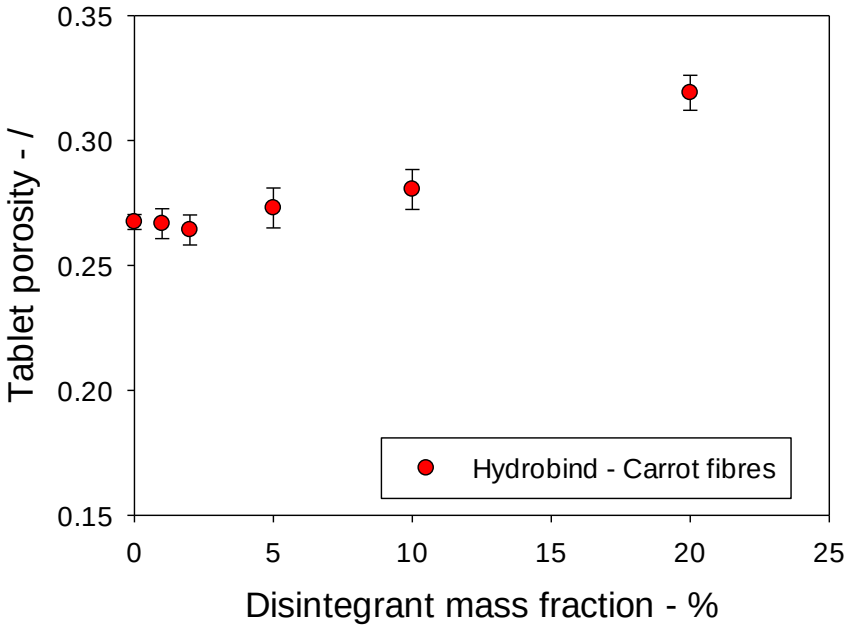

Figure 6-13: Porosity change upon incorporation of different concentrations of carrot fibres in maltodextrin tablets

For improved tablet disintegration and dissolution, the liquid needs to reach the disintegrants in the tablet quickly and in all directions at the same time. In order to combine both fast liquid penetration and tablet disintegration, a creative design of the tablet was sought to be able to influence this. Two different tablet designs were created as explained in Table 3-2. The disintegrants can be introduced at specific locations within the tablet to take advantage of their swelling capacity. Figure 6-14 shows the liquid penetration in a tablet where the disintegrants were incorporated according to the cross design. It can be seen that the liquid penetrates very rapidly within the tablet and can reach the disintegrant particles quickly to induce their swelling. After 5 seconds, the tablet starts to break up.

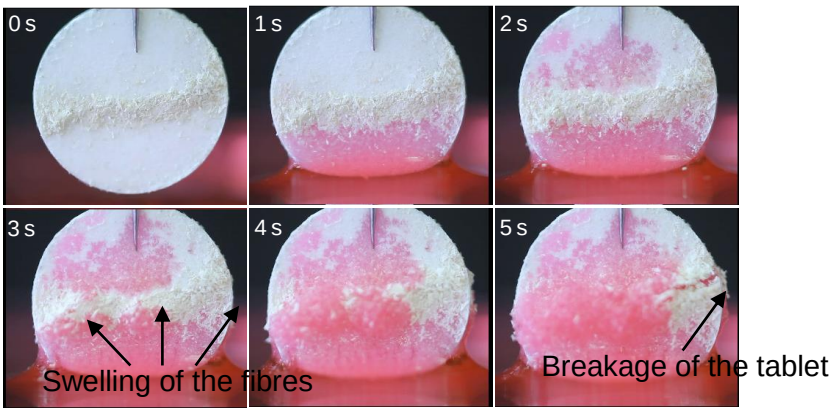

Figure 6-14: Liquid penetration as a function of time in a tablet of maltodextrin IT21 containing 10% (w/w) of carrot fibres at a specific location within the tablet: cross design.

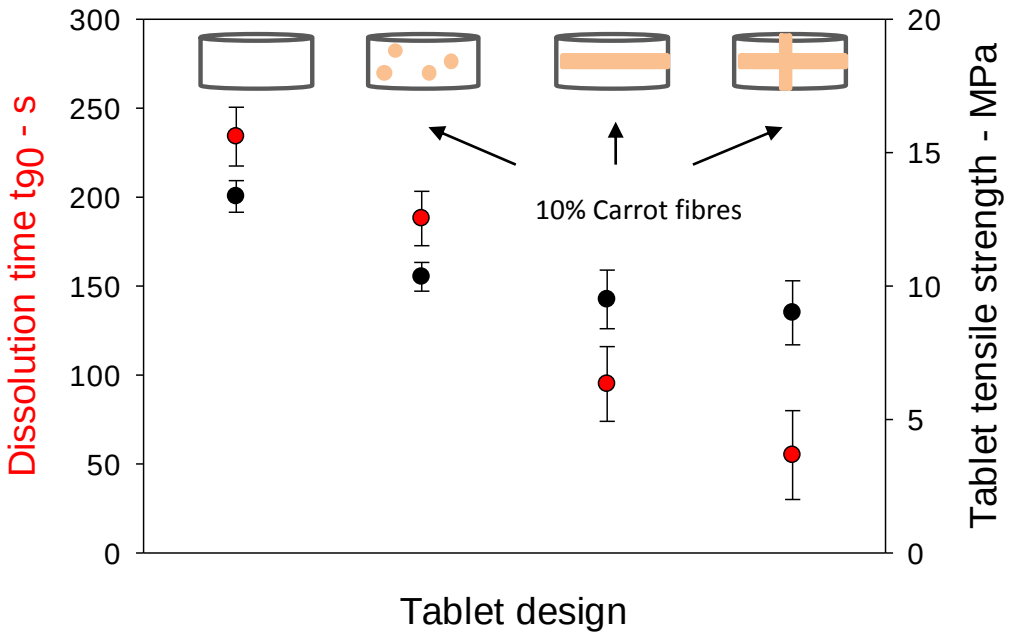

Figure 6-15: Dissolution time, t_{90}, and tensile strength of the four different types of tablets

Figure 6-15 shows the dissolution times and tensile strength of the different tablet configurations. It can be seen that the two new designs present much shorter dissolution times (reduced by 80%). The tensile strength is also reduced with the new configurations but to values similar to the normal configuration; mixed disintegrant.

Obviously, such designs would be difficult to achieve on a production line, but it is interesting to notice that water could be channelled inside the tablet to reach more easily the disintegrants and improve dramatically the dissolution of tablets.

6.5 Conclusions

To summarize the findings of this chapter , the following can be put forward:

- Vivasol, which is the reference disintegrant in this study does not influence the dissolution time in a positive way. A longer dissolution time was even noticed at high concentrations of 10 and 20%. Such results were explained by the formation of a viscous layer surrounding the tablet by the swelling of the disintegrants which slows down the access of water to the tablet.
- The size of the particles is of importance as it can be noticed in the large difference in dissolution time between the two types of citrus fibres: Citri-Fi 100 and Citri-FI M40.
- Carrot fibres and Citri-Fi 100 are the most promising disintegrants; however a real difference is only noticed at high concentrations of 10 and 20%. Such concentrations are not acceptable; a product formulation cannot be modified by such a large concentration of a new ingredient without impacting the gustative qualities of the product.
- The addition of disintegrants also conveys a decrease in tablet tensile strength.
- Natural sources of disintegrant can be found, however, more work on their selection is needed to accentuate their potential as disintegrants.
- The spatial distribution of disintegrants within the tablet can be engineered to better channel the water penetration within the tablet. This can ensure that water reaches all disintegrant particles. Examples showed that a dramatic reduction in dissolution time can be obtained.

It cannot be concluded that the incorporation of disintegrants does indeed reduce the dissolution time of tablets. The shorter dissolution times could result from a weakening of the tablets. There is no proof that disintegrants actually induce the tablet disintegration, especially in the erosion regime. The following chapter will show that it is possible to obtain data on the dissolution and disintegration of tablets in a novel way.

CHAPTER 7 - A NOVEL METHOD TO STUDY TABLET DISSOLUTION AND DISINTEGRATION

7.1 Introduction

The literature review highlighted the fact that experimental techniques used to study disintegration provide very little information on the mechanisms behind the process. In addition, dissolution and disintegration have been mainly studied separately whereas they should be considered together as they are happening simultaneously and affecting each other.

One of the most intrinsic characteristics of the disintegration process is the breaking up of the tablet into pieces, which does not always correspond to the size of the primary particles which have been compressed. The size and number of these fragments will determine the dissolution speed in the case of a surface limited dissolution process. Moreover, the number and size of the fragments will be dependent on several parameters such as tablet strength, porosity, disintegrant

type and concentration. However, such data were experienced to be difficult to gather by other authors. It was reported by Zhao and Augsburger (2006) that they had made several unsuccessful attempts to obtain direct measurements of the size distribution of particles during disintegration. Methods such as optical microscopy, laser scattering and sieving were tried in the case of a non dissolving matrix.

As a result, it is important to gain more knowledge about the disintegration process in relation to the dissolution process. In order to achieve such knowledge, a novel technique or method had to be developed. This chapter introduces the two components of such a novel method. First, the flow cell design from which high resolution images of the tablet undergoing dissolution and disintegration are taken. Second, the image analysis code which was written specifically for this method.

Finally, the method calibration and image analysis code validation are presented.

7.2 Why is it a novel method and what are the deliverables?

The aim of the technique to be designed is to allow the instantaneous determination of the size and number of particles being released due to disintegration or erosion at the surface of the tablet. In addition, the evolution of the tablet's diameter and thickness are measured with time. The delivery of such data presents a new method to study of dissolution and disintegration of tablets.

In the pharmaceutical industry several methods have been used to follow the disintegration of tablets. In most papers, authors have used an image analysis system where they are able to follow the tablet dimensions with time. Frenning et

al. (2005) have been able to determine the projected surface area and perimeters of pellets with a light microscope. Efentakis and Stamoylis (2009) investigated the swelling of tablets made of polymeric materials under a microscope. However, the tablet axial and radial changes in size were always measured manually. A similar study had previously been carried out by Moussa and Cartilier (1996). However, all these studies do not allow several data to be captured and studied simultaneously. Firstly, the accurate automatic determination of the tablet dimensions, thickness and diameter, have not been made possible as only manual determination was carried out. Secondly, no authors have been able to link the evolution of the tablet dimensions with the size distribution of the particles released from tablet disintegration.

Wilson et al. (2012) have been able to obtain the size distribution of particles released from the disintegration of a tablet. However, in their system, the particles produced after disintegration are entrained by a pump to a conventional size measurement equipment, QicPic. It means that only a non dissolving material can be used for this measurement as the size of the particles would be different after dissolution. In addition, the fact that the size of the particles are not measured immediately after release means that only a sample of the particles are entrained to the QicPic and analysed. As a result, it is difficult to obtain reliable information about the evolution of the particle size with time. Finally, they do not provide any information about the actual tablet change in size.

The following aims at showing that the new method introduced in this chapter brings several advantages in comparison to the systems used by other authors. The major benefits are as follow:

- Ability to work with dissolving materials as the particle sizes are measured immediately after release when limited dissolution has occurred.
- Ability to obtain the size of all particles produced during the disintegration and not only a sample, representative or not, of the particles released by tablet disintegration.
- Ability to obtain the tablet dimensions, especially the thickness and diameter and not only a projected surface area.
- Ability to link the results with time.
- Ability to have a visual proof of the tablet and particles from the images.

The novelty of this method lie in the fact that all the above mentioned data are available from one technique, allowing the complete dissolution and disintegration processes to be analysed as a whole.

7.3 Flow cell design

A flow cell was designed and built specifically for this study, as shown in Figure 7-1. The design of the flow cell is based on the well established flow through cell or USP 4 apparatus, which is one the standard dissolution apparatus used in the pharmaceutical industry (Kakhi 2009). The flow cell is constituted of a cylindrical shaped vessel containing a mesh on which the tablet rests during dissolution. A flat imaging window was built on two opposite sides as shown in

Figure 7.1 by polishing the round surface. In front of the imaging window a camera is placed and captures images of both the tablet and the particles detached during the tablet dissolution and disintegration. The water is introduced from the bottom of the vessel and exits through the upper part. The water flow rate and temperature can be controlled as described in the following paragraph. Water is directed from the bottom of the tablet to the top to ensure that all the particles released flow upwards so they only get measured once. The lower part is filled with 1mm glass beads to allow a uniform flow to be created around the tablet, similar to the USP 4 apparatus (Kakhi 2009).

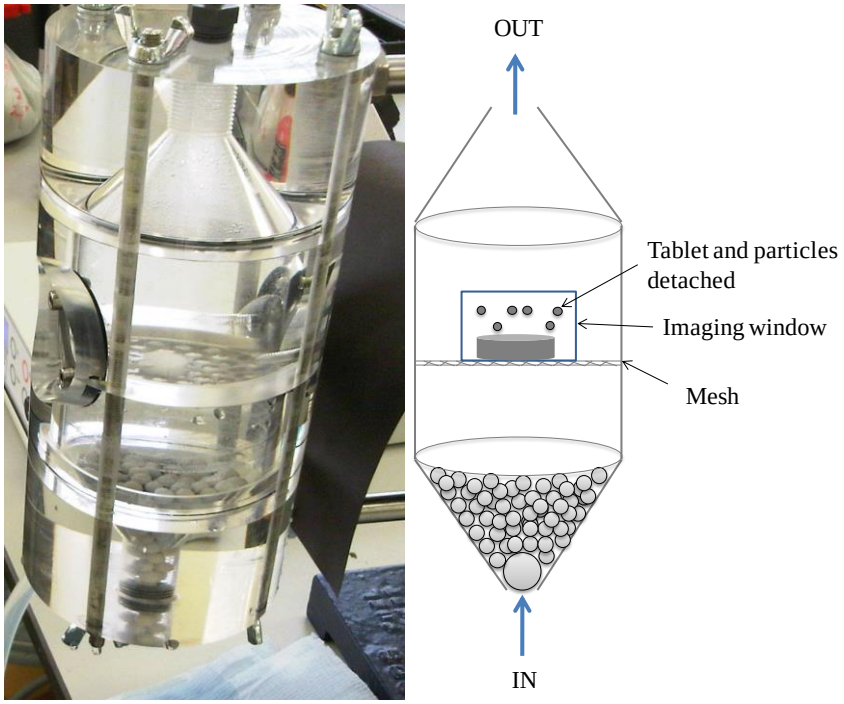

Figure 7-1: Left: Picture of the actual flow cell. Right: Schematic of the flow cell and tablet

In this section, the design of the overall system including water reservoir, pump and controls is described. A heated water reservoir (A on Figure 7.2) (20 – 70 °C) contains the water which is pumped (B on figure 7.2) to the bottom of the flow cell (C). The water flow rate can be regulated from the control box which was specially developed within the department of Chemical and Biological Engineering (D on Figure 7.2). The flow rate was set at 15 $cm^3.s^{-1}$. The flow cell is placed under controlled lighting conditions and different beams of light are directed to the tablet to ensure constant illumination conditions (E on Figure 7.2). This is important for two different reasons. Firstly, the camera settings such as ISO number and shutter speed were set for a specific lighting condition. Change in the light may prevent part of the tablet or particles to be seen on the images. Secondly, it is also important for the image analysis code that all pictures should have the same definition or clarity as it will be explained in section 7.4. The specific type of macro lens used in this work was chosen carefully as it allows a large depth of filed, which is wider than the width of the flow cell. This to ensure that all particles are in focus when the image is taken. Additionally, very little difference was noticed between the sizes of particle if measured close to the camera of further away. The high resolution camera (F) is placed in front of the imaging window on top of a X-Y-Z micro precision stage (G). The micro-precision stage is useful to ensure that the camera working distance stays the same from experiment to experiment. A change in working distance can influence the ratio µm to pixels and affect the final results. In this case, the working distance is of 10 cm. Finally, the water exits from the upper part of the flow cell to a water reservoir (H). The exiting water is not mixed with the incoming water

as non-dissolved particles could be reintroduced in the flow cell which would alter the results.

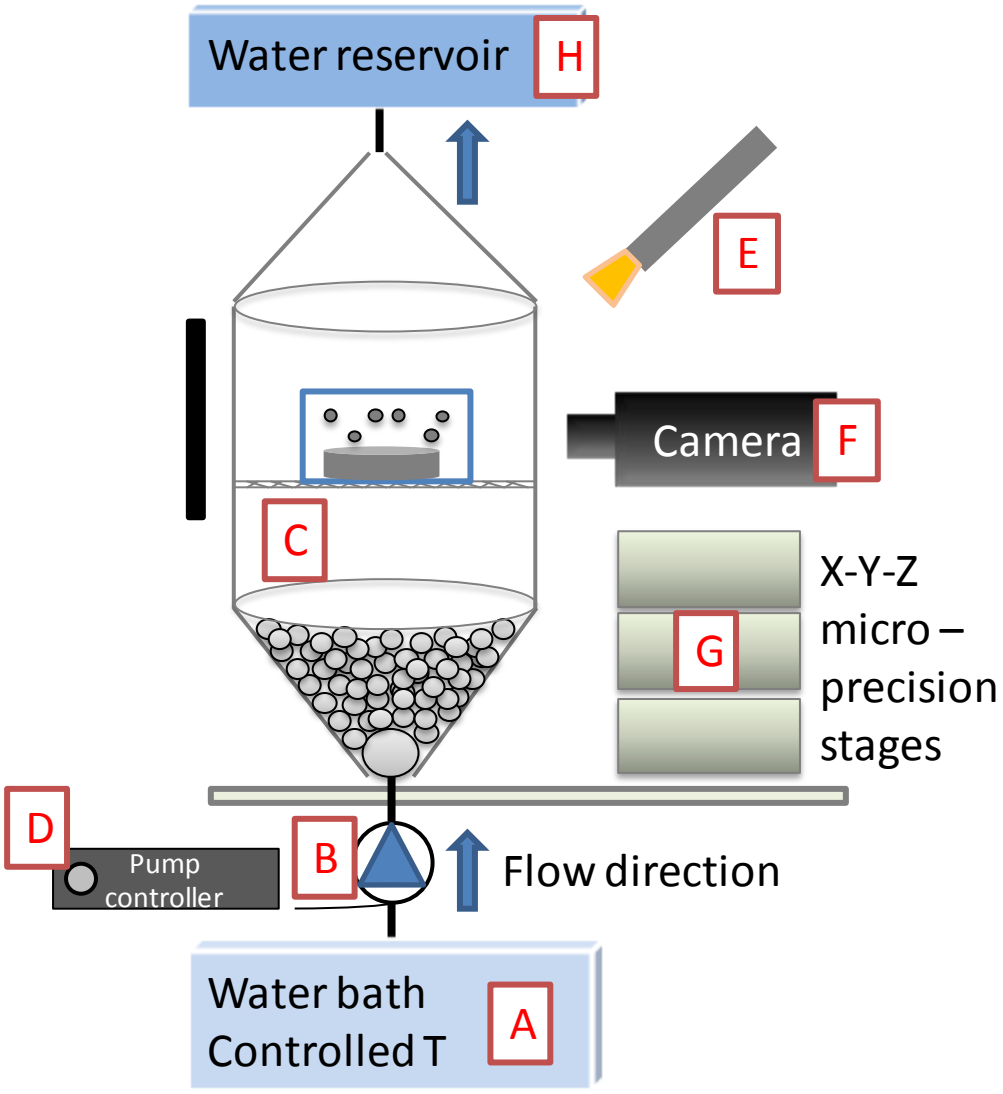

Figure 7-2: Schematic of the overall system

In Table 7-1 the characteristics of the different parts of the system presented in Figure 7-2 are given.

Table 7-1: Instruments characteristics

Instruments	Characteristics
Water Pump	Micro pump, RS (UK), 2.80 l/m, 6 mm tubing, 12V
Camera	Canon (Japan) EOS 1D Mark IV
Lens	Canon (Japan) MP-E 65 mm f/2.8
Water bath	Clifton (UK) water bath, 8L, 20 to 70°C
Light source	Zeiss (Germany) 1800 LCD

7.4 Image analysis

A program based on the Matlab image toolbox (R2009b, Mathworks inc., USA) was written to follow the tablet size reduction and the size distributions of the particles released from the tablet as a function of time. A full analysis of 3000 images (typical quantity of pictures per dissolution test) can take up to 20 hours to be completed on a PC with 8GB of RAM and a processor tuned at 3.40GHz. A copy of the code is given in Appendix B. The procedure developed in the code is summarized in Figure 7-3. More information on each step is given in the next following sections.

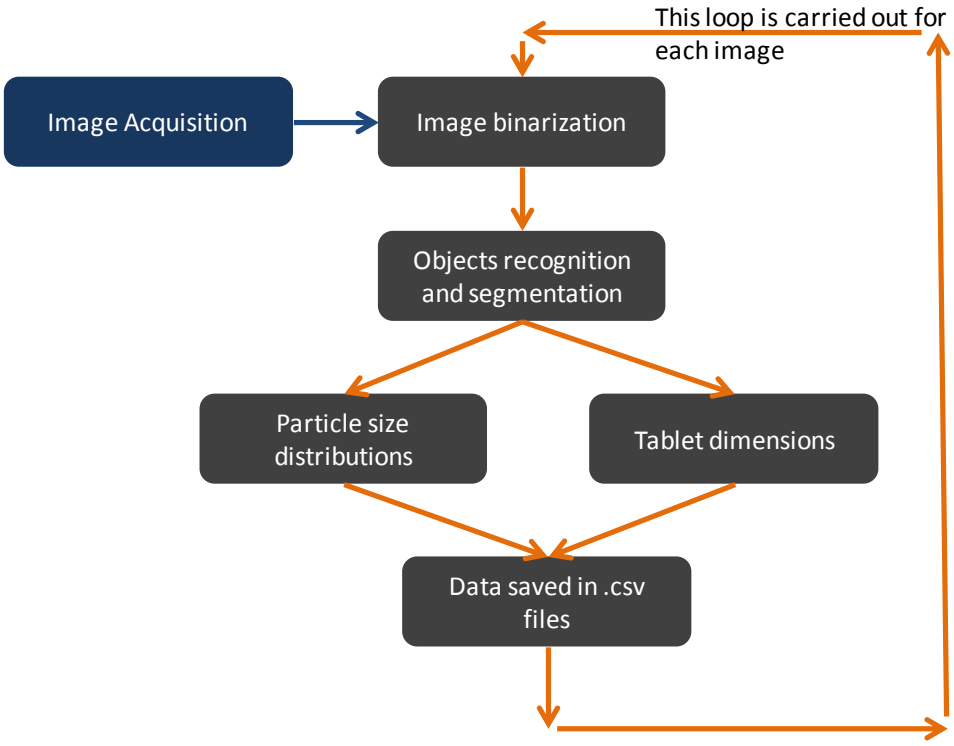

Figure 7-3: Image analysis procedure

Image acquisition

The optical system is able to take images of 16 Mpixel at a rate of 10 images per second. The set of images are saved as a colour JPEG image. The resolution is equal to 1.25 µm/pixel. A typical experiment produces approximately 3000 images to be analysed. As the particles are moving in the flow cell after disintegration, it was important to use a high shutter speed to obtain a sharp image with well-defined objects contours; 1/100 second was used in this case. In order to reduce the noise of the image, the lowest ISO number should be used. Beams of light were used to allow the use of low ISO numbers. These beams of light were focussed directly on the tablet and particles to increase the difference in greyscale on the image. Indeed, the greyscale is used to differentiate the objects from the background in the next step. Figure 7-4 shows an example of a

typical image which is obtained. It should be mentioned that this picture was chosen for a demonstrative purpose. Images may contain many more particles but for clarity this image was picked.

Figure 7-4: Typical colour image generated using the flow cell during tablet dissolution in water

Each image is then saved on a PC where the image analysis is carried out. The code reads the images as a stack but the analysis is carried out through a loop that works on a single image at a time. The results of each single image are saved in a .csv file where the data are appended on the same file.

Binarization

The colour images obtained are then transformed into a 8bit greyscale image for the binarization to be performed. Binarization is the most common technique to separate objects of interest from the background in an image. A grey threshold value is chosen; all pixels with a grey intensity below this threshold value are set to 0, leaving the objects a value of 1. An example of a binary image is shown in Figure 7-5. The large difference in pixel value between the tablets and particles

which are illuminated during the experiment and the dark background make the manual choice of the threshold value based on the grey pixels values distribution easy and accurate.

Figure 7-5: Binary image obtained from Figure 7-4 after thresholding (white - tablet and particles, black - background)

Objects recognition and segmentation

From the binary image, single objects can be separated from each other. One object is recognized as a connection of pixels with a value of 1 as it can be seen in Figure 7-6. Figure 7-7 shows the result of the objects' segmentation on a typical image. The largest object, in term of number of pixels, is set to be the tablet. From this part, the particles and the tablet are treated separately.

1 1 1 1 1 0 0 0 0 0 0 0 0 0 0 1 1 1
0 0 1 1 1 0 0 0 0 0 0 0 0 0 0 1 1 1
0 1 1 1 0 0 0 0 0 0 0 0 0 0 0 1 1 1
0 0 0 1 0 0 0 0 0 0 0 0 0 0 0 0 0 0

Figure 7-6: Image segmentation: each object is recognized as a sequence of pixels with value=1. When two sequences are not linked together, they are considered as two different objects

Figure 7-7: Object segmentation example: each object was attributed a different colour on the image

Particle size distribution

The size of each object is determined in pixels. Knowing the conversion of µm to pixel, the area in mm^2 of all objects can be obtained.

In addition, the perimeter of each object is determined and compared to the object area to obtain the object circularity. Bubbles which are formed from the gas entrapped in the tablet matrix should not be considered as particles. Bubbles are disregarded by excluding all objects whose circularity exceeds 0.95.

The most convenient way to describe the particle size of 3D particles captured as a 2D image by a single number is the circle equivalent diameter. It is the diameter of a circle with the same area as the 2D image of the particle. Obviously, the shape of the particle will influence the circle equivalent diameter. However, a larger object will always have a larger circle equivalent number. The same principle is used by the main particle size measurement technique based on image analysis. The procedure is summarised in Figure 7-8.

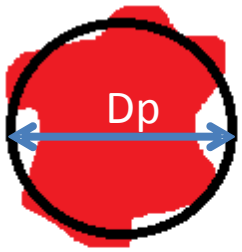

Figure 7-8: A circle equivalent Dp is obtained from a circle with the same area as the red particle

The size of each particle is saved in an Excel file (Appendix C). Each line in the file contains the sizes of all particles extracted from one image. Each file contains as many lines as there are images. This file will be subsequently reorganised into size distributions with the help of a code written in Fortran90 (Appendix D) run under Linux. The use of this code allows a fast organisation of the data as a function of the desired bin size and time. The particle size distribution can be presented on a number or volume basis based on the assumption that particles are spherical.

Tablet dimensions

It can be seen in Figure 7-4, the tablet surface is not smooth and flat. As a result, is it not accurate to calculate the diameter and thickness from a single line across the tablet. An average of the coordinates of the pixels at the top and bottom part should be calculated to obtain an accurate determination of the tablets' thickness and similar procedure should be carried out to obtain the tablet diameter. However, the obtainment of such averages requires establishing a fair determination of the starts and ends of the top, bottom, left and right sides of the tablet. As a result a strategy had to be developed; such a strategy is explained as follow:

1. Determination of the tablet boundary. This step is carried out by looking at the transition from a background pixel (value of 0) to an object pixel with value 1. Each of the pixel lines and columns of the image are scanned and when such a transition is found, the pixel coordinates are saved in a different file. The coordinates of all saved pixels allow the reconstruction of the tablet boundaries (Figure 7-9).

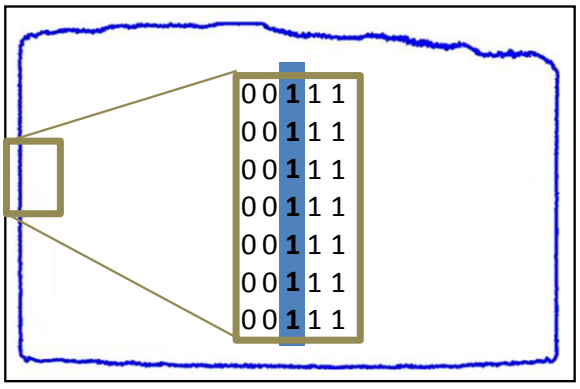

Figure 7-9: Tablet boundaries defined by the transition from a pixel value of 0 to 1

2. In the second step, the tablet is separated into four parts: top, bottom, left, right. The average pixels coordinates are calculated for the four parts. The difference between the average coordinates of the left and right part gives the tablet diameter. The thickness, for example, is obtained from the difference in average coordinates of the top ($\overline{Y2}$) and bottom ($\overline{Y1}$)) parts as shown in Figure 7-10.

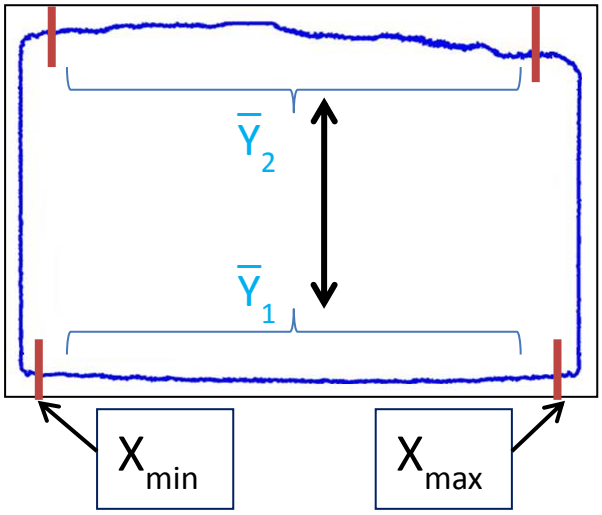

Figure 7-10: Tablet side limits determination

3. However, an accurate determination of the limits of each of the four parts needs to be used. Figure 7-10 shows the limit Xmin and Xmax of the bottom part. The coordinates of the limits of the four sides are determined at the inflexion of the frequency curves of the number of pixels along the X and Y axis. An example of the determination of the tablet diameter is given in the next four points:
    - ✓ The first step requires the tablet to be separated into two parts; left and right (Figure 7-11). This is done by separating the pixel

coordinates on the X-axis lower and larger than 2248, which is the coordinate corresponding of the middle of the image.

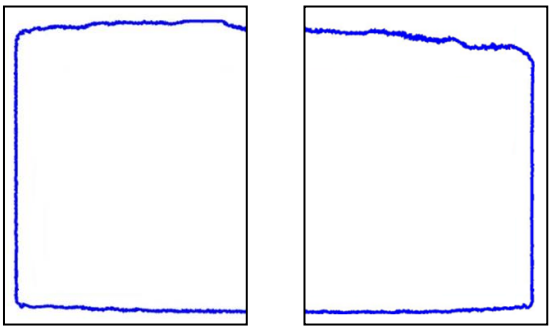

Figure 7-11: Separation of the left and right parts of the tablet

- ✓ The second step includes the creation of bins (thickness = 10 pixels) along the Y-axis (Figure 7-12). Each bin will contain the number of pixels with coordinates contained within the bins limits. As a result, a pixel frequency curve is obtained. This curve presents two main peaks corresponding to the tablets' top and bottom boundaries. The coordinates of the pixels contained in between these two peaks are of interest here. If one travels along this curve from its middle to the sides, then one would find two inflections at the start of the peaks. These two inflections are chosen to be the limits of the region of interest, Ymax and Ymin.

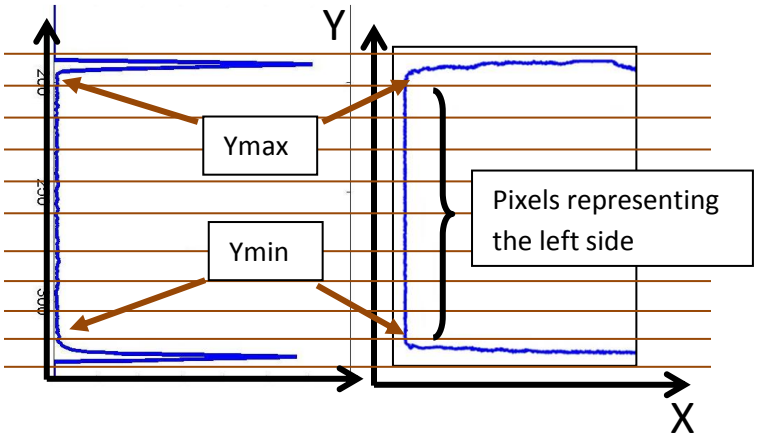

Figure 7-12: Plot of the pixel frequency curve along the Y axis to determine the left side boundaries, Ymax and Ymin

- ✓ The last step requires selecting the pixels whose coordinates lie in between the two limits and calculating their average value. This means that the average coordinate value of one of the side of the tablet is now known. If the same procedure is achieved on the opposite side of the tablet, an accurate length in between the two sides can be obtained along the X-axis. The determination of the difference in length of the two sides along the Y-axis is performed in the same manner.

The accurate determination of the diameter and thickness of the tablet during dissolution (as summarized in Figure 7-13) has never been obtained by authors in a systematic and automatic manner. In addition, the use of the average coordinates for each section of the tablet boundary ensures a more objective result compared to a manual determination. This approach could potentially be used for other systems.

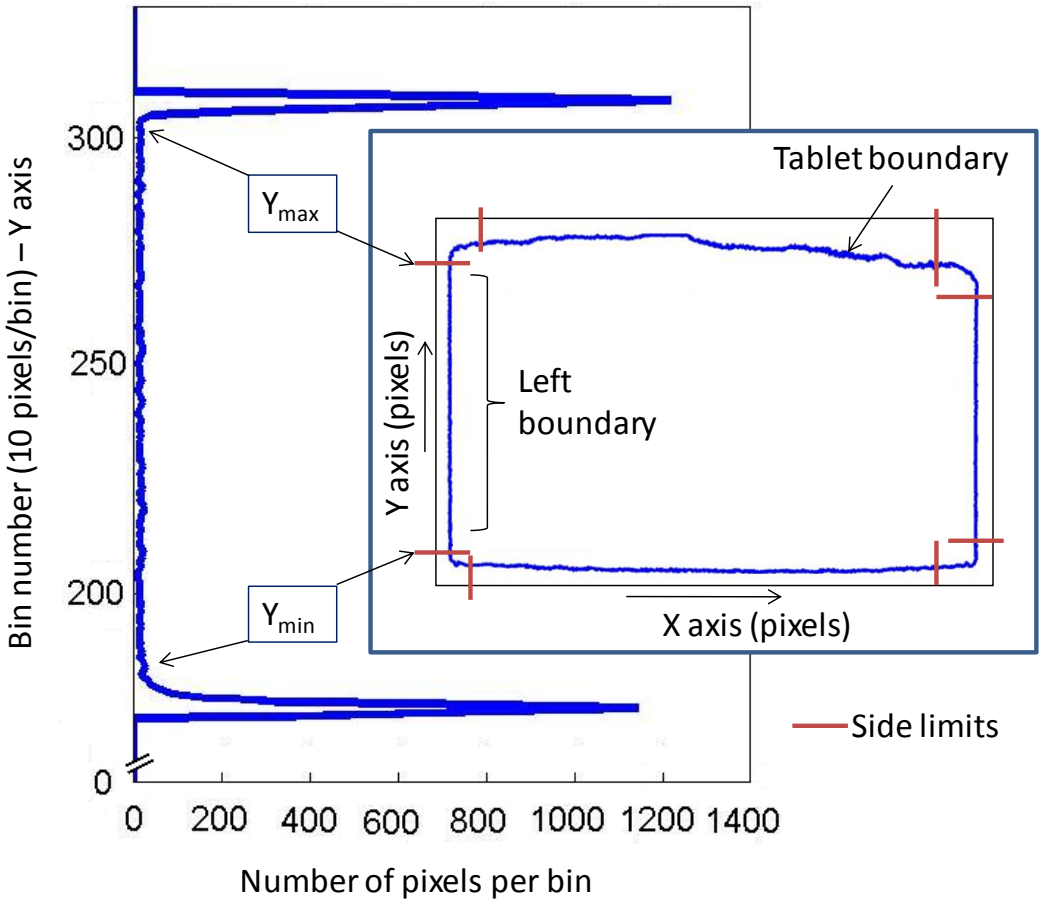

Figure 7-13: Description of the determination of the tablet sides limits with the frequency curve of the number of pixels along the Y-axis

7.5 Validation of the Matlab image analysis code

The image analysis code developed in this work needs to be validated by checking each output, particle size distribution and tablet dimensions.

Particle size distribution

Ceramic particles (non dissolving particles) were passed through the flow cell and images were taken. The resulting size distribution obtained after analysis of the images was compared with the size distribution of the same beads with a common particle size analyser QicPiC (Sympatec, Germany). The results are shown in Figure7-14. The results obtained show a strong similarity which validates the particle size measurement.

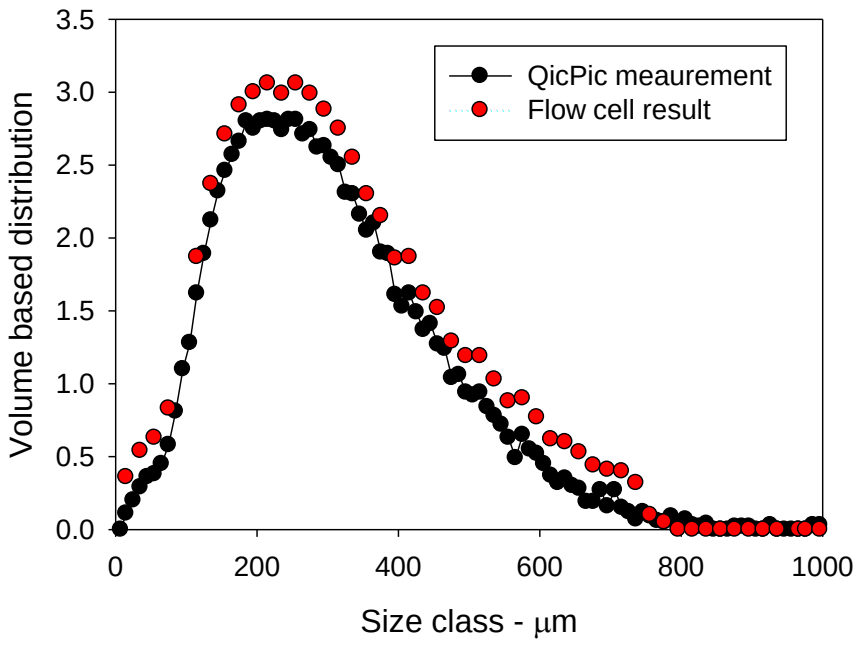

Figure 7-14: Size distribution of ceramic beads: similarities between the measurement by a commercial apparatus and the method developed in this work

Tablet dimensions

Unlike the particle size distribution, the tablet dimension determination is not based on a common approach. As a result, its validity has to be shown. A series of images obtained from the flow cell were both analysed by the code described above and by the open source image analysis software Image J (National Institut of health, USA). The diameter and thickness of the tablet were measured in pixels by the software ImageJ by drawing manually a segment on the image such as can be seen in Figure 7-15. The comparisons of the diameter and thickness obtained with the code described above and manual determination with the software ImageJ are shown in Figure 7-16 and Figure 7-17. It can be seen that the automated Matlab image analysis code delivers similar results to the one obtained manually by Image J; the diameter and thickness show similar values. In some cases, a small difference can be noticed, but this can mainly be imputed to the fact the code takes an average value for each section while the manual determination is more subjective. Similar work was repeated for several tablets at different porosities and in all cases the result is in agreement. It shows that the code written for this work is reliable. A more accurate and automatic determination of the tablets dimensions is then possible, compared with manual determination, image per image.

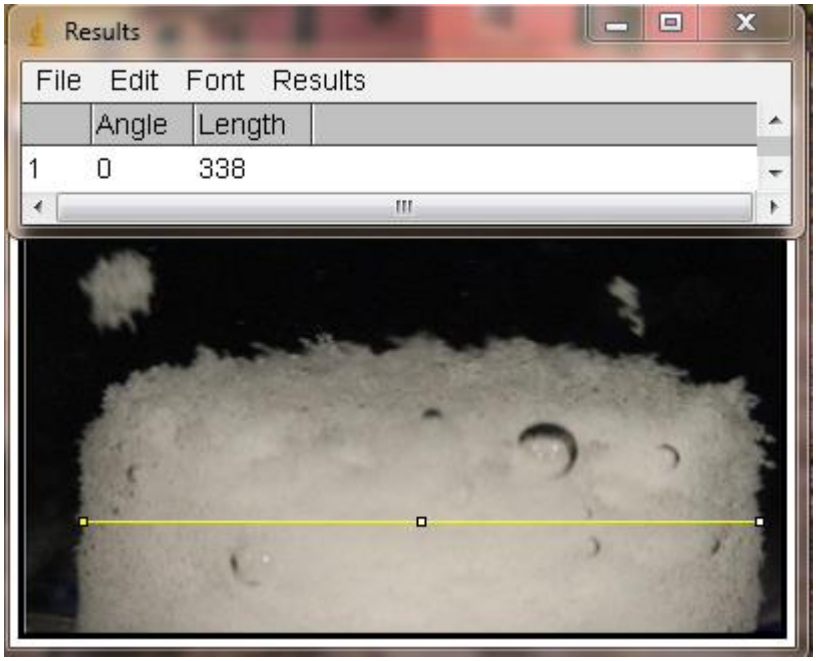

Figure 7-15: Measurement of the tablet diameter with the image analysis software Image J

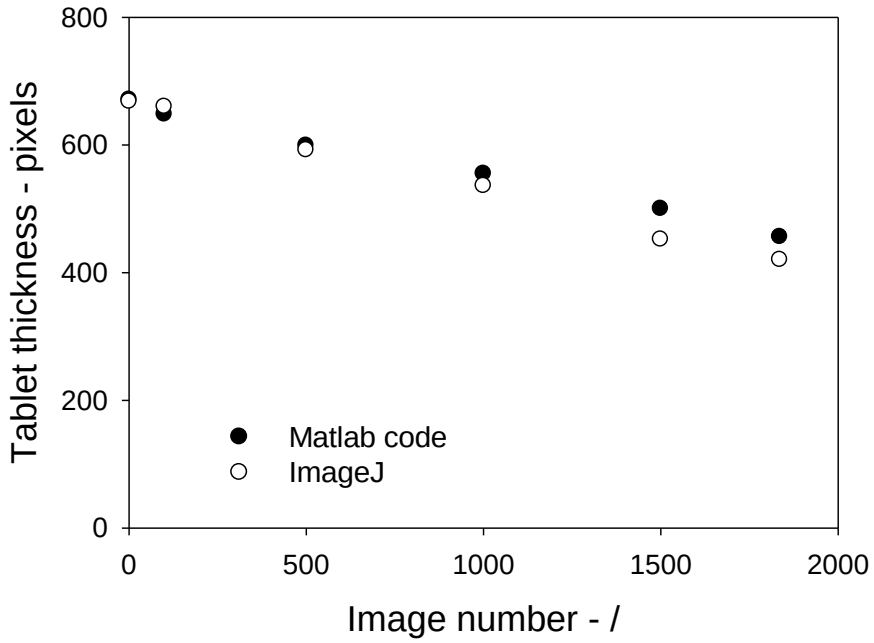

Figure 7-16: Comparison of the tablet thickness measured manually with Image J or calculated by the code in Matlab

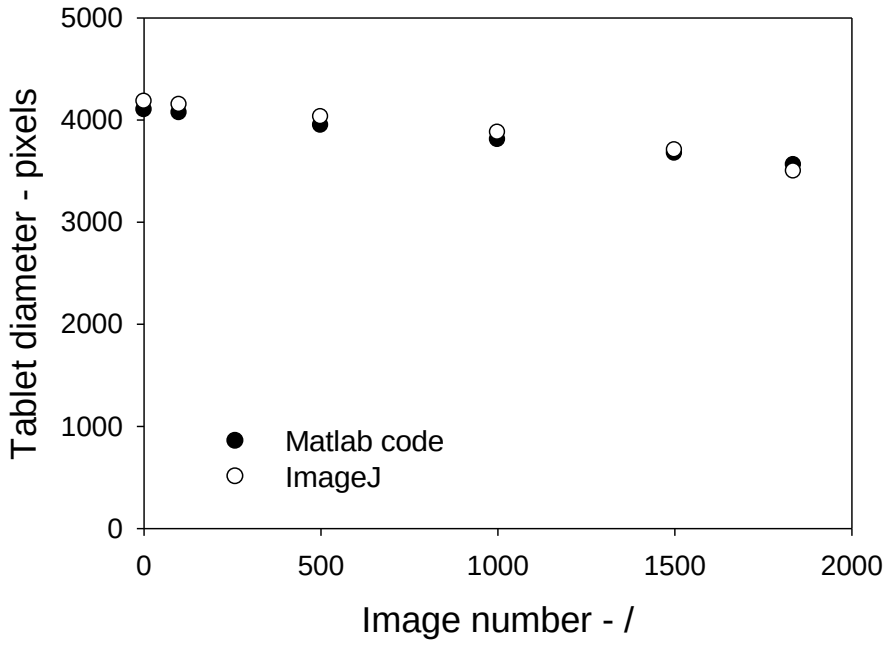

Figure 7-17: Comparison of the tablet diameter measured manually with Image J or calculated by the code in Matlab

7.6 Conclusions

In this chapter, a novel method to investigate the dissolution and disintegration of tablets is presented. This work focuses on the dissolution and disintegration of food tablets made of an amorphous material, however this method could be used for many types of disintegrating tablets. The author has successfully investigated the dissolution and disintegration of other amorphous and crystalline tablets (not presented in this PhD thesis) such as NaCl, microcrystalline cellulose, starch. There is a potential for great amount of data to be collected using this method to increase the general knowledge of tablet dissolution and disintegration.

The next chapter will introduce the main results obtained with this method.

CHAPTER 8 - FLOW CELL RESULTS

8.1 Introduction

In the previous chapters it was shown that the dissolution and disintegration of food tablets is not well understood. As a result, a novel method, described in Chapter 7, was developed to bring more knowledge of the two processes together. This method allows the following data to be obtained:

- Evolution of the tablet dimensions with time: projected surface area, thickness and diameter.
- Size distribution of the particles liberated from the tablet disintegration. The size distribution can be analysed for different times of the tablet dissolution.

In Chapter 4, the dissolution of maltodextrin tablets was found to behave according to two types of regimes: erosion and disintegration. The first part of this chapter will show and discuss that these regimes do really happen by analysing the tablets size evolution with time.

In Chapter 6, it was shown that the introduction of carrot fibres in maltodextrin tablets induces a reduction in the dissolution time. However, it could not be

concluded whether it was actually due to the disintegrant effect of the fibres or due to a reduction of the tablet tensile strength caused by the fibres. The effect of the concentration of the carrot fibres will be investigated in the second part of this chapter. The effect on the disintegration will be investigated by looking at the change in size and number of particles released in the presence of carrot fibres. Carrot fibres were chosen to further this work as they present the best activity in reducing the dissolution time compared to other disintegrants.

8.2 Erosion regime

The erosion regime is characterised by a low penetration of water within the tablet due to the low porosity. As a consequence, the dissolution and disintegration only occur at the surface of the tablet in contact with water. The finding of this regime was based on the fact that the initial tablet thicknesses could be linearly related to the dissolution time t_{90} for a constant porosity. It was then thought that the tablets would keep their shape along the dissolution time and that the change in size with time would be linear (cf. Chapter 4).

The method introduced in Chapter 7 allows the size of the tablets to be followed with time. This means that tablet's diameter and thickness can be obtained at any time. It is then possible to see whether the hypothesis developed in Chapter 4 about the existence of the erosion regime is valid. For this chapter, four different tablets of porosity 0.27 were chosen based on the linear relationship between tablet thicknesses – dissolution times shown in Chapter 4. The four different tablets all have a different initial thickness. They were placed in the flow cell and a flow rate of 15 $cm^3.s^{-1}$ was chosen because this was just strong enough to carry

the particles upwards in the flow cell. A water temperature of 25°C was chosen because it is easy to control and it is desirable to have a slow dissolution to capture all physical modifications of the tablets.

Figure 8.1 shows the evolution of the projected surface area of the four different tablets with time. The projected surface area corresponds to the area of the tablet marked in red on Figure 8.2; it is the area of the tablet from a side view. The results show the average value of 5 repetitions and the error bars represent the standard deviation in the results.

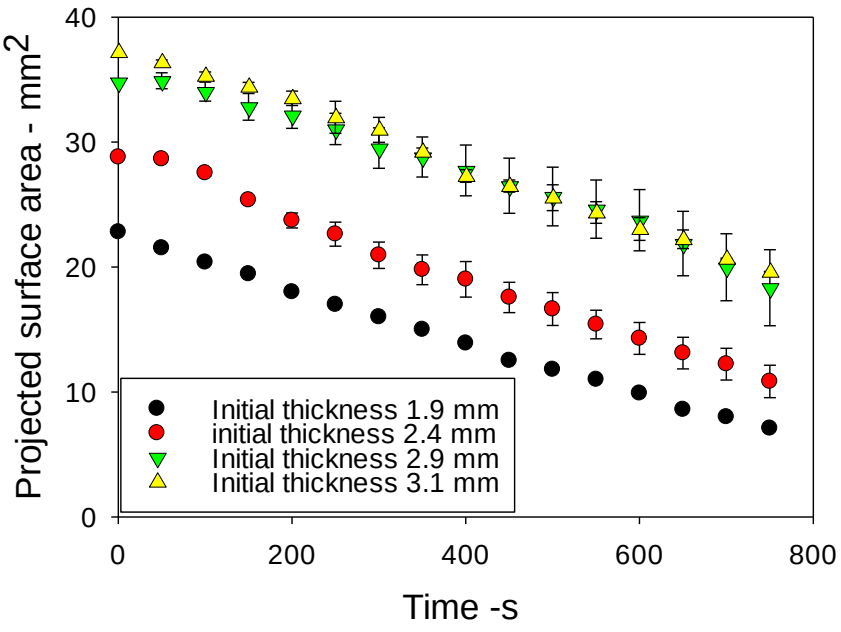

Figure 8-1: Evolution of the projected surface area of tablets of porosity 0.27. The four different types of tablets have a different initial thickness

Figure 8-2: Projected surface area of a tablet in red

It can be seen that for the four tablets, the evolution of the projected surface area is linear with time. It is logical that the tablets with a large thickness at the beginning have a larger projected surface area. In addition, the slopes of the four curves are parallel to each other showing that the rate of change in size does not depend on the tablet surface area. It means that the dissolution in this case is controlled by the external mass transfer, as shown in Chapter 4. The fact that the tablets surface areas are changing linearly with time means that the tablets shape remains the same during the dissolution process. It thus confirms that the dissolution can only occur at the surface of the tablets by erosion in this case.

Figure 8-3 and 8-4 give further insight into the change in dimensions of the tablets by looking at the evolution of the tablet thicknesses and diameter.

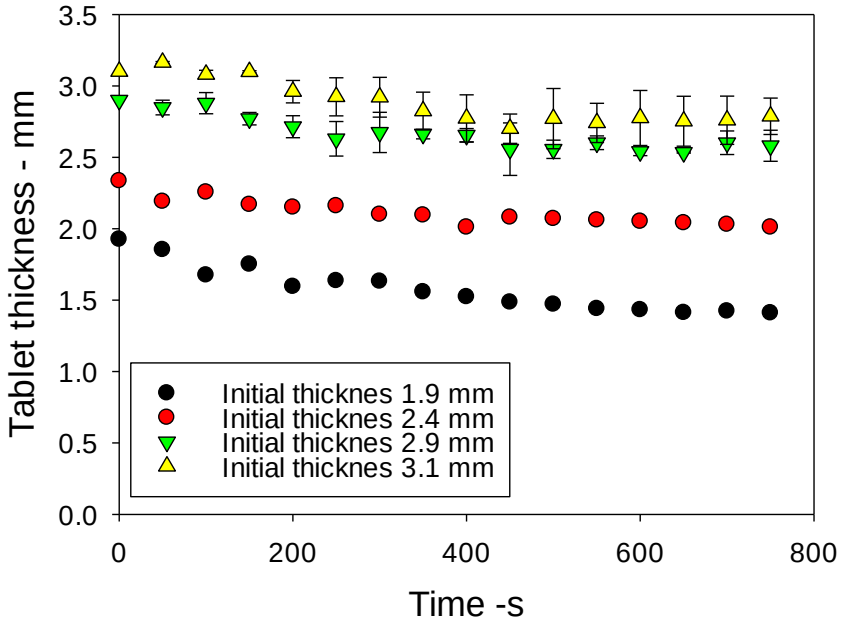

Figure 8-3: Evolution of the thickness with the dissolution time of tablets of porosity 0.27. The four different tablets have a different initial thickness

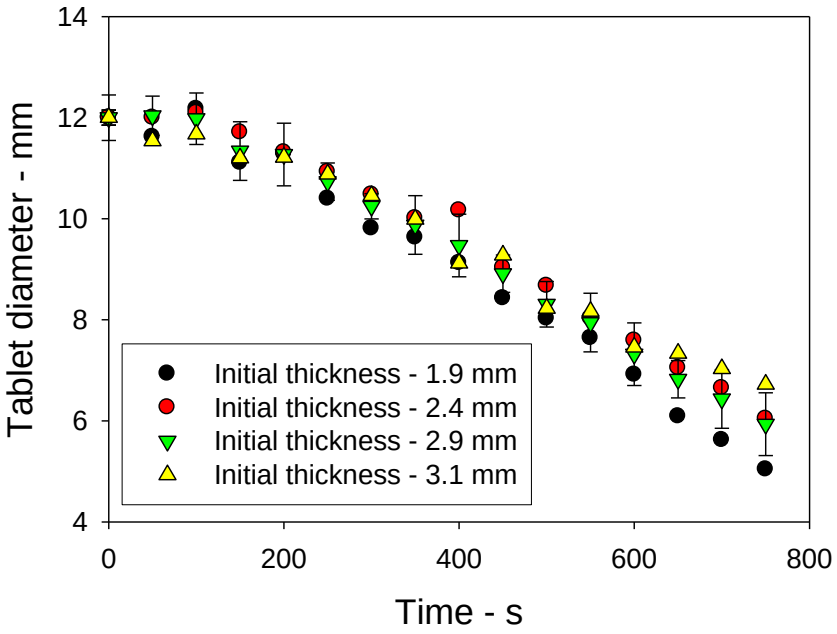

Figure 8-4: Evolution of the diameter with the dissolution time of tablets of porosity 0.27. The four different tablets have a different initial thickness. The error bars are only presented for one set of data for the clarity of the Figure

Both Figures 8-3 and 8-4 reinforce the conclusions drawn from Figure 8-1. In Figure 8-3 it can be seen that the thickness reduction is slow and the variations in time for the four tablets are similar. In Figure 8-4, it can be seen that the reduction in diameter is actually faster than the reduction in thickness. This can mainly be explained by the fact that in the flow cell the water is flowing around the tablet as demonstrated in Figure 8-5. Thus the water renewable around the tablet is faster on the sides than on the top and bottom. As the dissolution is limited by an external mass transfer depending on the water flow, dissolution is faster on the circular side of the tablets. However, this is just an hypothesis; a flow dynamics study could clarify this point.

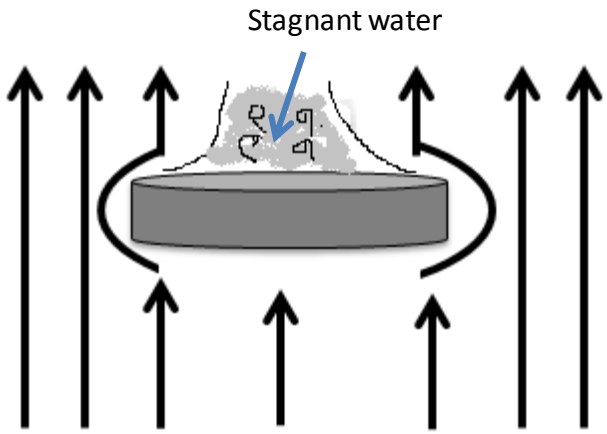

Figure 8-5: Possible explanation for the faster reduction in diameter than thickness of the tablets

If the measured tablet thicknesses and diameters are multiplied, then the results should be similar to the measured projected surface area. The projected surface area is obtained from an inbuilt function of the image analysis toolbox in Matlab, while the code for the determination of the thickness and diameter has been developed by the author. This provides an additional method to ensure that the measurements are accurate. Figure 8-6 shows the comparison of the results for tablets of porosity 0.27 and initial thickness of 2.4mm.

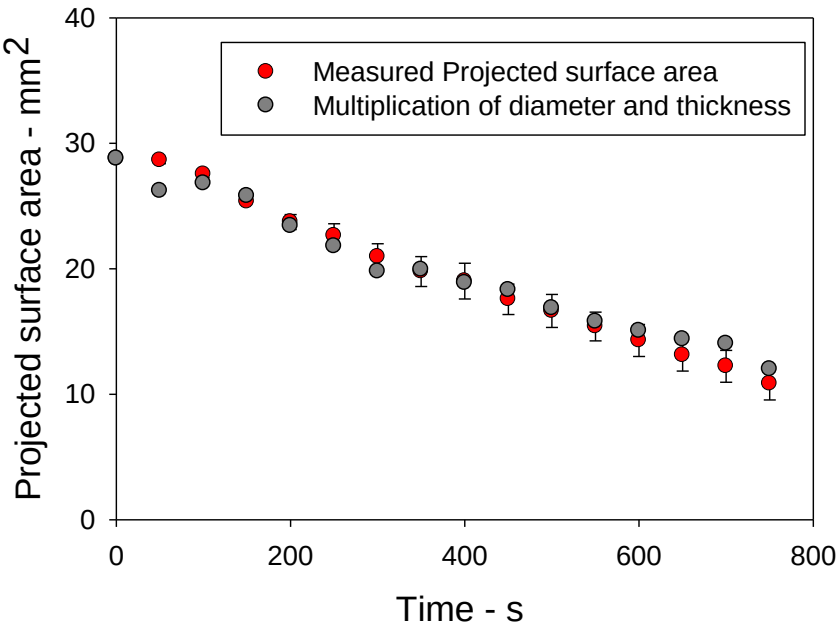

Figure 8-6: Comparison between measured projected surface area and the multiplication of the measured thickness and diameter

From the same experiments, the size distribution of the particles which are released during the tablet disintegration can be obtained. Even though it was shown that disintegration only appears at the surface of the tablet, it is interesting to see how large and numerous the solid fragments detached from the tablet are. For ease of comparison, only the median equivalent diameters based on the volume distribution are presented in Figure 8-7. It shows that the particles liberated have a median diameter of 320 µm for all the four tablets. It means that the same type of behaviour is happening for the four tablets. In addition, it is interesting to note that the median diameters of the particles released are larger to the one of the raw powder before compression. This can be possibly due to the creation of very strong bonds between primary particles during compression which are more difficult to break down during dissolution. An additional more plausible reason for this increase in size is the swelling of the particles in contact with water.

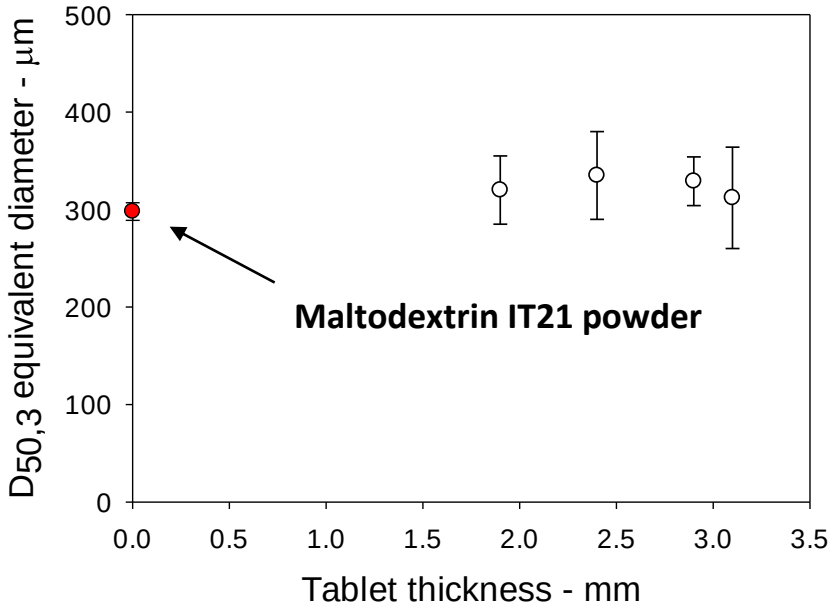

Figure 8-7: Median diameter of the total particles released during the dissolution during 800s for the four different tablets

It should be mentioned that the results presented in Figure 8-3 are based on a volume distribution, meaning that the median value is larger than if the results were based on the number of particles. It means that even though it seems that very large particles are detached from the tablets, in reality small particles are also detached from the tablets. Figure 8-8 show an example of a picture acquired during the dissolution of a tablet of porosity 0.27. Several particles can be seen leaving the surface of the tablet. It can be seen that fairly large particles (around 300 µm) for the large ones are detached but also smaller particles. The minimum size of particle which can be detected is of 20 µm.

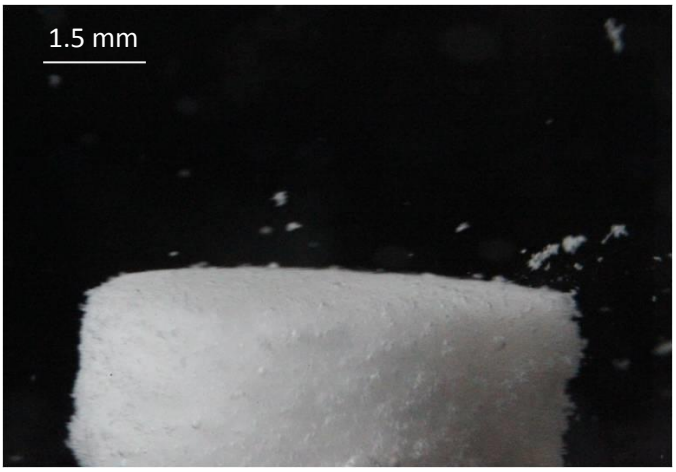

Figure 8-8: Example of an image obtained during the dissolution of a tablet of porosity 0.27 with the flow cell apparatus

Figure 8-7 provides the $D_{50,3}$ equivalent diameter after 800s, which is the time of interest for this study. However, it is possible to breakdown such data into several time scales. Figure 8-9 shows the median equivalent diameter for 200s time scales. It can be seen that the median diameter does not appear to change with time for the first 800s.

In addition to the size of the particles, it is also possible to extract the average number of particles which are released on each image taken. Figure 8-10 shows the average number of particles which are released with time for the four types of tablets. It can be seen that not only their size is similar (see Figure 8-7) but also their number is similar for the four tablets. It confirms that for one tablet porosity in the erosion regime, dissolution and disintegration behave the same.

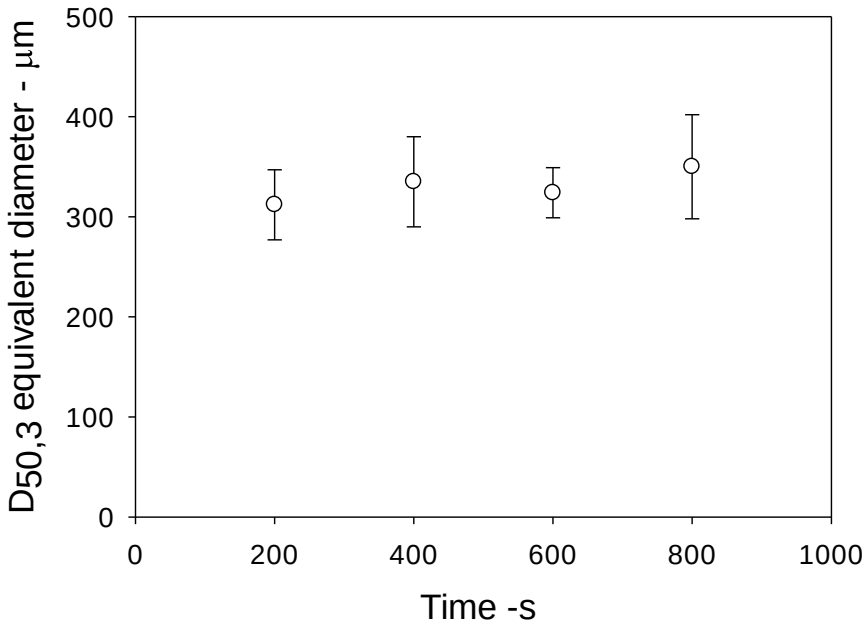

Figure 8-9: Median diameter of the particles released at different time scale: 0-200 s, 200-400 s, 400-600 s, 600-800 s. The results were obtained for tablet of porosity 0.27 and initial thickness of 2.4 mm

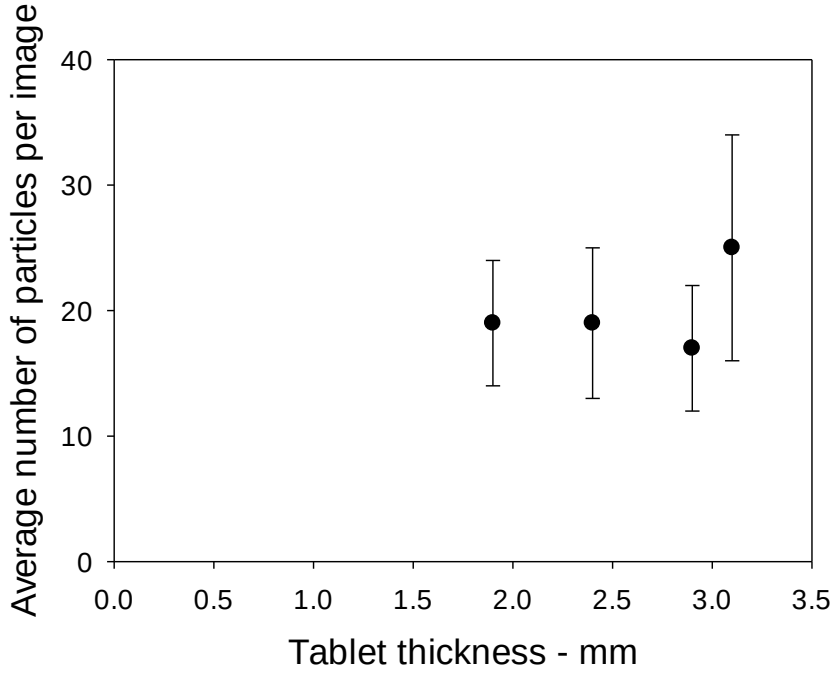

Figure 8-10: Average number of particles released per image of the total particles during the dissolution during 800s for the four different tablets

Likewise to Figure 8-9, it is possible to breakdown the number of particles released with time for the dissolution of one type of tablet. Figure 8-11 shows the evolution of the number of particles released with time for the same tablet studied in Figure 8-9. The results are interesting as they seem to suggest that with time more and more particles are released. This could be due to a difference in density within the tablet. It is well known that density is not uniform in a tablet (Sinka, Cunningham et al. 2004). The sides, top and bottom are usually denser than the central part of the tablet. This difference is the result of the force propagation within the tablet during the compression. It is possible that the increase in porosity or weaker inter-particles bonds result in more particles to be released once the more dense outer part of the tablets have dissolved. However, the increase in particle generated is only slight and the large error bars do not allow to conclude about the trend of the data points.

However, the results presented in Figure 8-11 do not seem to match the results obtained previously, mainly when comparing them to the evolution of the projected surface area. It can be thought that if more and more particles are being released with time, then the evolution of the tablets dimension should not be linear. More and more particles released should mean a faster decrease in thickness and diameter. The next paragraph should give us more insight into this matter as it will describe the ratio of volume lost by the tablet due to disintegration only.

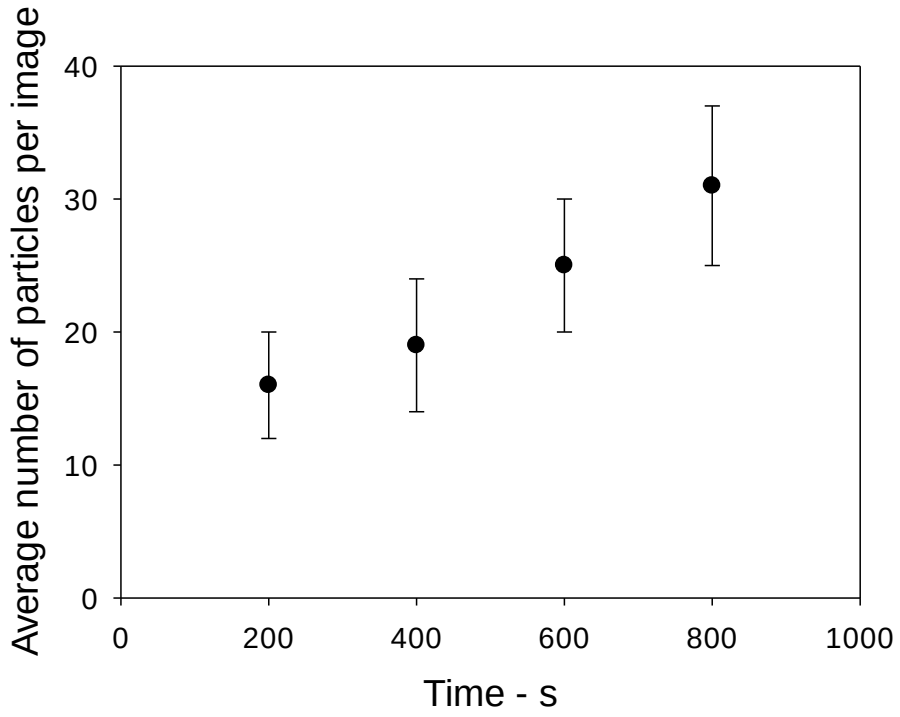

Figure 8-11: Average number of particles released per image at different time scale 0-200 s, 200-400 s, 400-600 s, 600-800 s. The results were obtained for tablet of porosity 0.27 and initial thickness of 2.4 mm

The results above have shown that the erosion regime described in Chapter 4 is certainly present at least for the porosity of 0.27. However, it is possible to further the discussion by separating the reduction of volume of the tablet due to dissolution and due to disintegration. The total reduction in size of the tablet is both due to dissolution and disintegration.

On one hand, the total number of particles and their volume are known from the particle size distributions. The addition of all the volume of all the particles corresponds to the reduction in volume of the tablet only due to disintegration. It is also possible to know the addition of the particles volumes at different times as well as suggested by Figures 8-9 and 8-11.

On the other hand, the dimensions of the tablet are known at any time (see Figure 8-3 and 8-4). Thus, if we compare the tablet dimensions at a given time, t, with the initial tablet volume, the volume lost by the tablet at that time can be obtained. This volume is lost by both dissolution and disintegration, however, the volume lost by disintegration is known. As a result, the disintegration and dissolution effect on the volume reduction of the tablet can be obtained (Mesnier, Althaus et al. 2013).

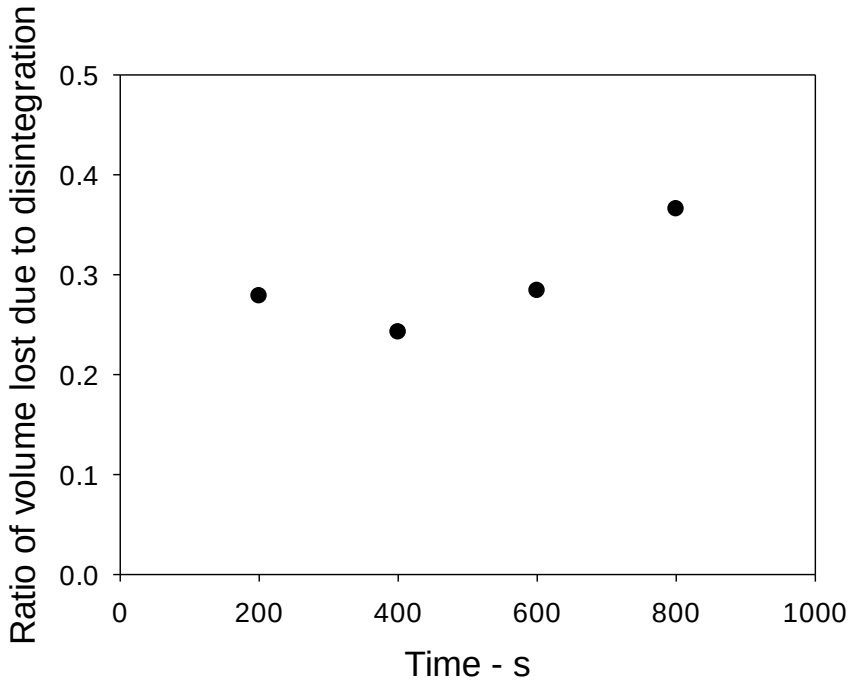

Figure 8-12: Ratio of tablet volume lost due to the disintegration process compared to the overall loss due to both dissolution and disintegration. The data represents the average value for the different time scales: 0-200 s, 200-400 s, 400-600 s, 600-800 s

Figure 8-12 shows that in general the ratio of volume lost by the tablet during its reconstitution is mainly due to dissolution. Indeed, the disintegration is only responsible for 30% of the volume reduction. It should mentioned that this result is based on the assumption that 100% of the particles which are liberated par erosion are captured by the camera system. However, it confirms the fact that there is an opportunity to promote the disintegration process. In addition, it should be noticed that a slight increase in disintegration can be noticed in the last two time scales studied. It could be the result of an increase in the number of particles released in the same time scale.

The work presented in this chapter shows that erosion take place at the peripheral surface of the tablet. This results is based on the specific type of flow occurring within the flow cell. It can be assumed that if the tablet was placed on the peripheral side within the flow cell, most of erosion would take place at both flat surface of the tablet. This remark is important in relation to the finding of Chapter 4. A model was derived on the basis that erosion takes place on the upper and lower surfaces, which contradicts the results from Chapter 8. However, it should be kept in mind that for the dissolution tests carried out in Chapter 3, the tablet was free to move within the basket and thus water could reach the tablet freely from every sides. In the flow cell, the tablet's position is controlled which thus influences the water flow.

To conclude, it means that both conditions are not comparable as the water flow conditions are very different. However, what is comparable is that in both cases the erosion regime was obtained. The experiments and model from Chapter 3, are more comparable to the conditions experienced by consumers in their kitchen where they drop the tablet in hot water and stir with a spoon.

In the next part of the chapter the same study is carried out on tablets containing different concentrations of carrot fibres.

8.3 Influence of the introduction of carrot fibres

The evolution of the projected surface area of tablets of maltodextrin containing different concentration of carrot fibres is shown on Figure 8-13. Carrot fibres were chosen for this study as it was pointed out in Chapter 6, they present the best dissolution time reduction capabilities. Only three concentrations are presented; 1, 5 and 10 % as no significant differences could be seen between 1 and 2%. Furthermore, the tablets containing 20% of carrot fibres have a very low tensile strength resulting in a rapid collapse of the tablet structure upon introduction of water in the flow cell, making it very difficult to obtain reliable data. The results are compared with a tablet of porosity 0.27 with an initial thickness of 2.4 mm.

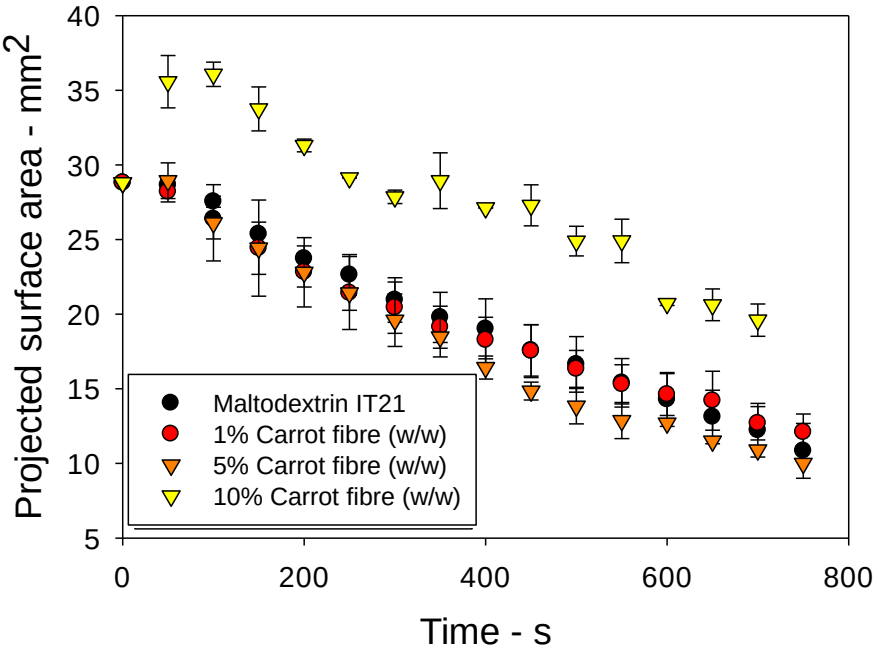

Figure 8-13: Evolution of the projected surface area of tablets of maltodextrin containing different concentrations of carrot fibres (w/w)

It is interesting to notice that the evolution of the projected surface areas is very similar for the tablets made of pure maltodextrin and the ones containing 1 and 5% of carrot fibres. However, it should be mentioned that the decrease in size is faster for tablets containing carrot fibres and the more concentrated, the faster, except for 10 % carrot fibres. However, the slope of the different curves is still parallel for the three types of tablets; this means that the disintegration regime was not reached by adding the disintegrants. The tablets still maintain their shape during the tablet reconstitution, at least for the first 800 seconds.

The projected surface area for tablets containing 10% of carrot fibres presents an interesting development, as an increase in size of the projected surface area can be noticed. The swelling of the tablet is the result of the swelling of the

individual particles of carrot fibres in contact with water. It can be seen that the maximum size is reached in a short time, 100 seconds, which may correspond to the time for all fibre particles to be wetted. This result is very interesting as it shows that even though a large quantity of swelling carrot fibres are present in the tablet, it does not induce the collapse of the tablet as Figure 8-16 shows later. More information on the tablet dimensions can be obtained from the study of the thickness and diameter in Figure 8-14 and 8-15.

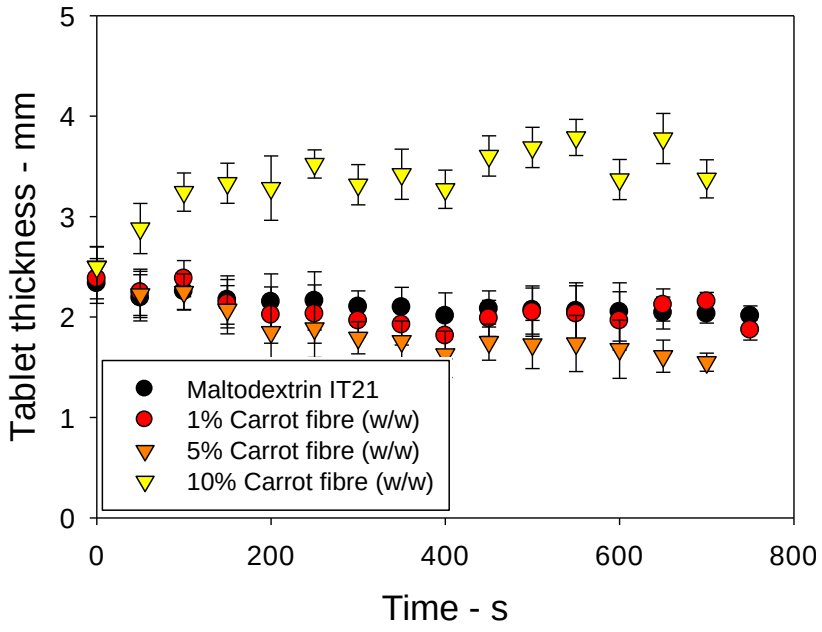

Figure 8-14: Evolution of the thickness of maltodextrin tablets containing different concentrations of carrot fibres (w/w)

Figure 8-13 and 8-14 show the evolution of the thickness and diameters of the different tablets under study. It is interesting to notice that the tablets at 0, 1 and 5% show similar trends and the same conclusion about the concentration effect can be made. The swelling of the tablet containing 10% of carrot fibres is even

more pronounced when examining at the increase in thickness. However, when looking at the diameter, it shows that the diameter increases at the beginning but then decreases rapidly. The reduction in diameter might be related to the flow of water around the tablet's side which may erode the swollen tablet sides. The swelling induces weaker inter-particle bonds, possibly causing an increase in tablet disintegration. More information should be obtained from the study of the size and number of particles released from the tablet.

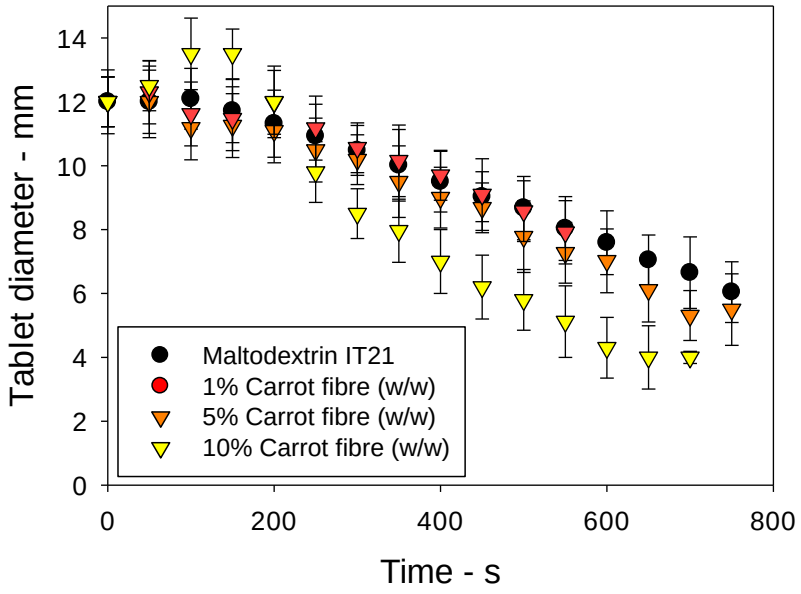

Figure 8-15: Evolution of the thickness of maltodextrin tablets containing different concentrations of carrot fibres (w/w)

Figure 8-15 shows a montage of several pictures taken every 10 seconds of the dissolution of a tablet containing 10% of carrot fibres. The increase in size can be clearly seen.

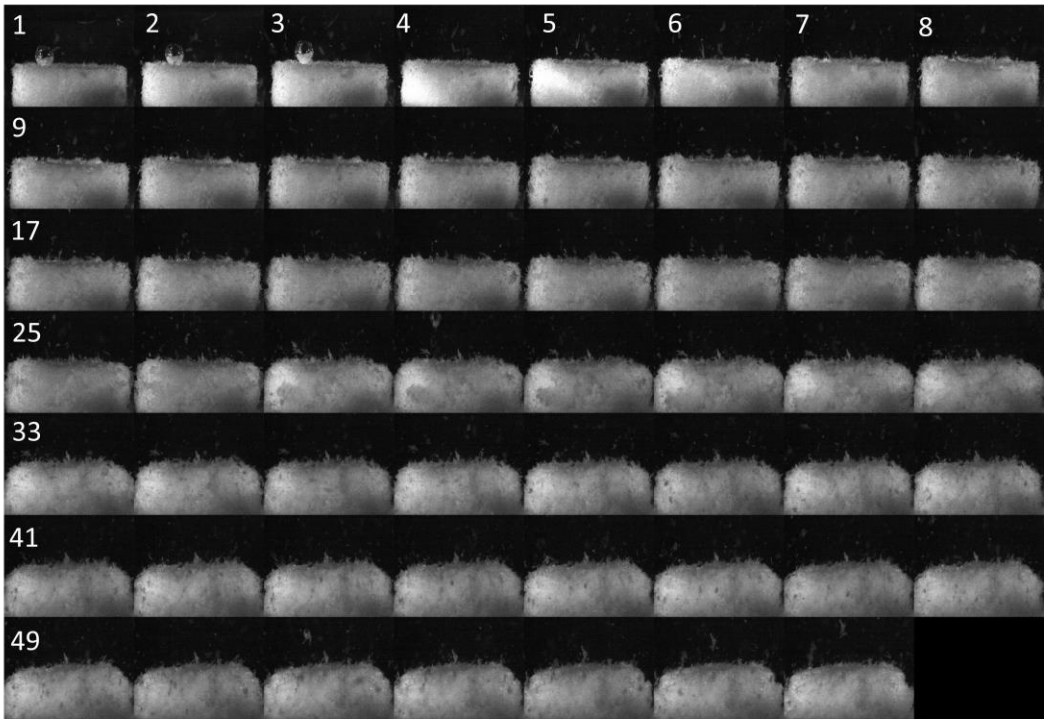

Figure 8-16: Increase in size of a tablet of maltodextrin containing 10% of carrot fibres in the flow cell. Each picture was taken at 1 second intervals

The study of the size distribution of the particles released in presence of carrot fibres is described in the next section.

Figure 8-17 shows the median value for the size of the particles released. It can be seen the size of the particles increases when a larger quantity of disintegrants are present in the tablet The increase in average size could be due to the action of disintegrants which help the breaking of larger aggregates of particles. Furthermore, it should be remembered that carrot fibre particles are larger than maltodextrin particles which would help increase the average size of the particles. Finally, the particles of carrot fibres will swell when exposed to water, which will result in the measurement of larger particles.

It is difficult to conclude on the effect of the disintegrant as swelling does impact the size of every set of data measured by image analysis. In the case of the tablet size, it could be seen that 5% of carrot fibres do not have a very large impact on size reduction. But it should be kept in mind that at this concentration, swelling might occur and thus the resulting tablet dimensions are the results of the competition between swelling and dissolution. Also it is very difficult to separate each process. However, Figure 8-18 gives us more insight on the effect of the carrot fibres on the disintegration of the tablets. It is indeed difficult to make a conclusion regarding the size of the particles; however, the number of particles released is not influenced by the particle swelling. Figure 8-18 shows that with increasing the concentration of disintegrants, the average number of particles released is increased. This can be linked with the swelling of the disintegrants causing the breakage of inter-particle bonds.

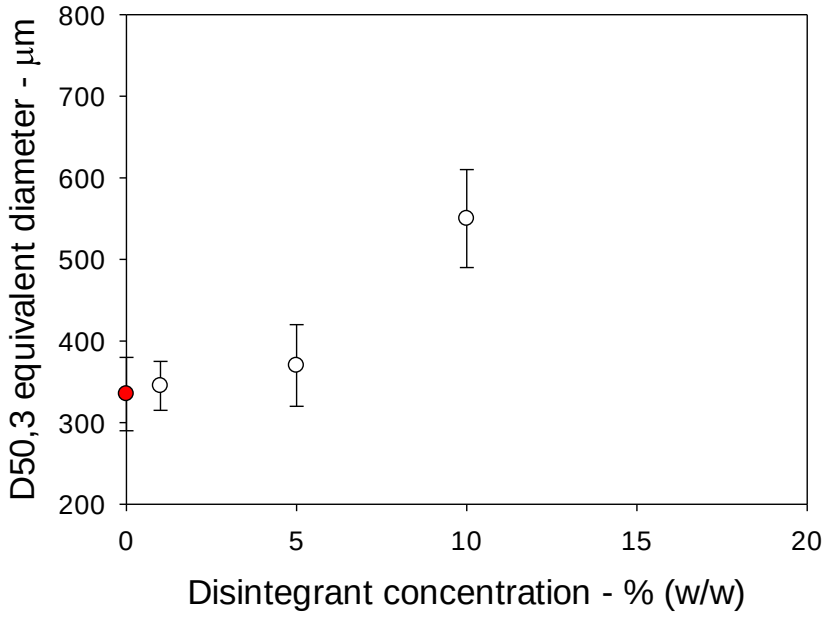

Figure 8-17: Median diameter of the total particles released during the dissolution after 800s for the tablets at different concentrations of carrot fibres

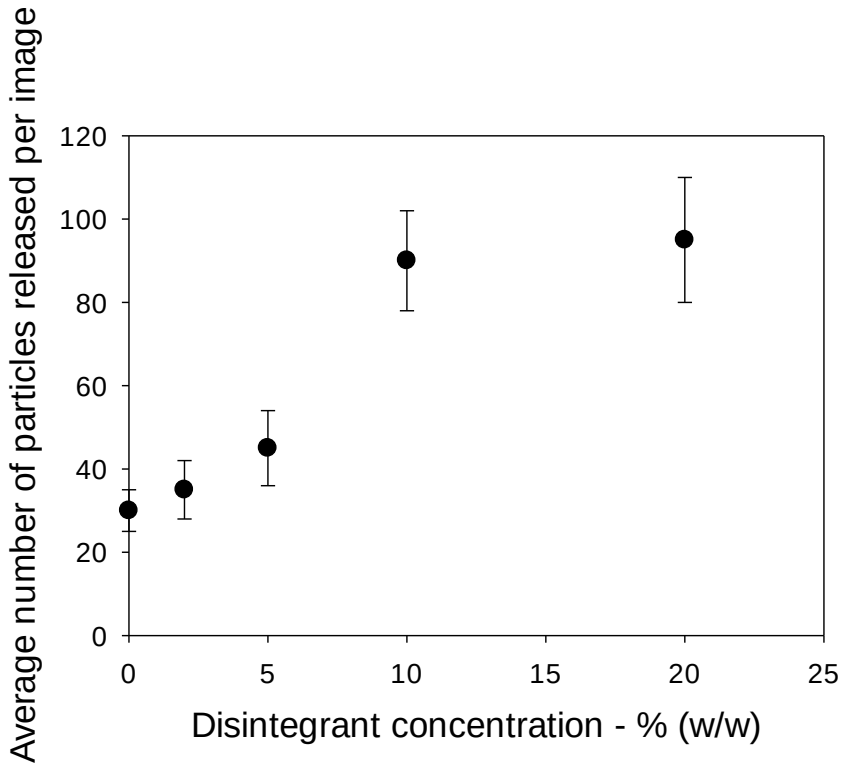

Figure 8-18: Average number of particles released per image of the total particles during the dissolution after 800s for the different tablets

It can be concluded that carrot fibres do actually have an impact on the disintegration as more particles are released with its presence. Unfortunately, the fact that the increase in particle size may not only due to the action of the disintegrants but also to their actual swelling, it is not possible to calculate the ratio of volume lost due to disintegration alone. The volume of the particles would as well be compared with the volume of the tablets which is also subject to swelling which would result in misleading data.

8.4 Conclusion

This chapter introduced the results obtained with the novel technique developed during this thesis.

In a first part, it allowed to confirm that the erosion regime hypothesized in Chapter 4 is valid. Futhermore, it was possible to quantify the part that disintegration takes into the overall reduction in tablet volume, showing that dissolution is the main process. However, it also highlighted that there is an opportunityto improve the disintegration of tablets of maltodextrin.

In a second part, it showed that the incorporation of carrot fibres does not change the dissolution regime from erosion to disintegration. The introduction of carrot fibres does have an impact on the disintegration as more and more particles are released, however it is difficult quantify it as swelling of the tablets and the particles meant that quantitative data were unreliable.

However, overall, it shows that the new method can provide numerous information about the dissolution and the disintegration of tablets. It can be potentially used to investigate the difference in dissolution of different types of materials; amorphous and crystalline. Furthermore, it could be used to investigate the difference in dissolution of different molecular weight polymers such as maltodextrin.

It should be mentioned that the work presented in this Chapter is based on tablet dissolving by erosion. When tablets dissolving by disintegration, i.e. complete disintegration of the structure from the inside upon penetration of water, the same data are not possible to obtain. First the tablet size cannot be measured as the code developed is based on the assumption that the cylindrical shape is kept during the dissolution. Secondly due to disintegration, very large fragments of the tablet are released. These large fragments are not carried upwards by the water flow but tend to sediment which means they are not captured by the camera. It is

one of the limitation of this novel method, but it could be argued that the already disintegrating tablets do not require the same attention as their dissolution is already very short.

CHAPTER 9 - CONCLUSIONS AND FUTURE WORKS

9.1 Conclusions

The aim of this thesis work was to investigate the potential use of disintegrants in food tablets. It was shown, in Chapter 4, that the reconstitution of food tablets in water followed two types of regimes as a function of their porosity; the erosion and disintegration regimes. At low porosities, the limited penetration of water within the tablet induces the erosion regime during where the dissolution and disintegration would only occur at the surface of the tablets. For high porosity tablets, higher than 35% for maltodextrin tablets, the disintegration regime predominates. The rapid liquid penetration induces the tablet disintegration and fast dissolution. These two regimes were highlighted because of the determination of the dissolution time t_{90} of tablets at different porosities and thicknesses. In the erosion regime, it was shown that the dissolution time can be linked linearly to the tablet initial thickness for a given tablet porosity. Such correlation can be explained by the fact that the shape of the tablets remain constant during dissolution and that the kinetics of dissolution are the same for a given porosity. It means that in this case dissolution was not limited by the surface area of the solid-liquid interface. However, such correlation was not found in the disintegration regimes.

To further the analysis, a model based on the Noyes and Whitney equation was develop to explain the interaction between the dissolution time, the tablets initial thickness and the dissolution of the solvent. Such models provide a rapid tool to predict the dissolution time of maltodextrin tablets based on easy to obtain characteristics such as porosity, tablet thickness, temperature. It allows saving a lot of experimental time. Further research into the effect of the stirring speed during dissolution with the Sherwood and Reynolds numbers showed that the dissolution was limited by the rate of the external mass transfer. It also showed that the disintegration regime can be obtained when the Reynolds number is increased further than a critical value at which the external mass transfer increases dramatically.

Several food fibres were chosen and their possible uses as disintegrants were studied in Chapter 5. It was found that carrot fibres are the best disintegrant to promote a shorter dissolution time. However it was found that its incorporation decreases the tablet tensile strength in Chapter 6. This is the result of an increase in tablet porosity promoted by a higher elastic re-expansion post compression. The trade-off between dissolution time and tensile strength was found to be possibly bypassed by the smart spatial distribution of the disintegrants within the tablet. This resulted in a more efficient channel of water into the tablet to target specifically the disintegrants and ensure their swelling.

Finally, a novel method based on a flow cell and image analysis was developed to provide useful information about the dissolution and disintegration of food tablets in Chapter 7. This method which allows the overall reconstitution of tablets to be analysed: dissolution and disintegration, can present information which has not been provided elsewhere previously. It confirmed, in Chapter 8, that the

hypothesis of the erosion regime, developed at the beginning of the thesis, is valid and also showed the swelling of the tablets in presence of disintegrants. It also concluded on the fact that disintegration is responsible for only 30% of the tablet volume reduction in water for maltodextrin at porosity of 0.27. Indeed, the addition of information collected about the tablet and the particles allow separating the contribution to overall reduction in tablet volume from dissolution and disintegration. This option offer many possibilities for the further understanding of both processes and their interaction.

9.2 Future works

The work carried out in this thesis could be furthered by considering the following points.

Firstly, this work is based on the use of a polymeric amorphous material, maltodextrin. Maltodextrin comes in different types according to the chain length of the polymers. It would be interesting to study the influence of the type of maltodextrin on the transition between erosion and disintegration regimes. Furthermore, a mono-carbohydrate such as glucose could also be investigated. This would widen our knowledge in the dissolution of carbohydrates. In addition, the influence of the water content in the tablets would also be interesting to investigate as this may influence the tabletting step and the strength of the inter-particles bonds.

Secondly, it would be possible to investigate the use of several other types of ingredients as possible disintegrants for the food industry. This study was based on five ingredients but many more could be studied. The sources of food fibres

are almost limitless and it is probable that more efficient compounds can be found.

Thirdly, the novel method developed in this work could be used to investigate the dissolution and disintegration of numerous other types of tablets, both amorphous and crystalline. In addition, as it was highlighted in Chapter 8, the size of the particles detached from the tablet might be a signature of the inter-particles bond strength. It would be interesting to deepen that relationship which would allow further knowledge into this field.

REFERENCES

Adebayo, S. A., E. Brown-Myrie, et al. (2008). "Comparative disintegrant activities of breadfruit starch and official corn starch." Powder Technology 181(2): 98-103.

Bele, M. H. and D. V. Derle (2011). "Brand to brand variation in the disintegrant functionality of Polacrilin potassium, NF." Journal of Excipients and Food Chemicals 2(3): 53-63.

Bettini, R., P. Colombo, et al. (1994). "Swelling and drug release in hydrogel matrices: polymer viscosity and matrix porosity effects." European Journal of Pharmaceutical Sciences 2(3): 213-219.

Bolhuis, G. K., K. Zuurman, et al. (1997). "Improvement of dissolution of poorly soluble drugs by solid deposition on a super disintegrant. II. The choice of super disintegrants and effect of granulation." European Journal of Pharmaceutical Sciences 5(2): 63-69.

BolthouseFarms, W. (2002). GRAS Notification for Hydrobind - Carrot fibre.

Brielles, N., F. Chantraine, et al. (2007). "Imbibition and Dissolution of a Porous Medium." Industrial & Engineering Chemistry Research 46(17): 5785-5793.

Brielles, N., F. Chantraine, et al. (2008). "Dissolution of a surfactant-containing active porous material." Journal of Colloid and Interface Science 328(2): 344-352.

Caramella, C., P. Colombo, et al. (1988). "A physical analysis of the phenomenon of tablet disintegration." International Journal of Pharmaceutics 44(1-3): 177-186.

Chang, R.-K., M. Shinwari, et al. (1998). "Evaluation of the disintegrant properties for an experimental, crosslinked polyalkylammonium polymer." International Journal of Pharmaceutics 173(1-2): 87-92.

Chirico, S., A. Dalmoro, et al. (2007). "Analysis and modeling of swelling and erosion behavior for pure HPMC tablet." Journal of Controlled Release 122(2): 181-188.

Chouk, V. (2010). Personal communication. University of Sheffield.

Chouk, V., B. Gururajan, et al. (2009). Effect of internal lubricant on granule and tablet properties. International Symposium on Agglomeration. Sheffield, UK.

Colombo, P., Bettini, R., Massimo, G., Catellani, P.L., Santi, P., & Peppas, N.A. (1995). Drug diffusion front movement is important in drug release control from swellable matrix tablets. Journal of Pharmaceutical Sciences 84(8): 991-997

Cooper, W. J., P. D. Krasicky, et al. (1985). "Effects of molecular weight and plasticization on dissolution rates of thin polymer films." Polymer 26(7): 1069-1072.

Costa, P. and J. M. Sousa Lobo (2001). "Modeling and comparison of dissolution profiles." European Journal of Pharmaceutical Sciences 13(2): 123-133.

Dhere, P. M. and S. L. Patwekar (2011). "Review on preparation and evaluation of oral disintegrating films." International Journal of Pharmacy and Technology, 3(4): 1572 - 1585.

Dokoumetzidis, A. and P. Macheras (2006). "A century of dissolution research: From Noyes and Whitney to the Biopharmaceutics Classification System." International Journal of Pharmaceutics 321(1–2): 1-11.

Efentakis, M. and K. Stamoylis (2009). "An investigation into the swelling properties, dimensional changes, and gel layer evolution in chitosan tablets undergoing hydration." Advances in Polymer Technology 28(1): 32-39.

Ferrero, C., N. Muñoz, et al. (1997). "Disintegrating efficiency of croscarmellose sodium in a direct compression formulation." International Journal of Pharmaceutics 147(1): 11-21.

Forny, L. (2010). Tablets in the food industry. Lausanne, Nestle Research Centre.

Forny, L., A. Marabi, et al. (2011). "Wetting, disintegration and dissolution of agglomerated water soluble powders." Powder Technology 206(1–2): 72-78.

Frenning, G., F. Fichtner, et al. (2005). "A new method for characterizing the release of drugs from single agglomerates." Chemical Engineering Science 60(14): 3909-3918.

Fukami, J., E. Yonemochi, et al. (2006). "Evaluation of rapidly disintegrating tablets containing glycine and carboxymethylcellulose." International Journal of Pharmaceutics 310(1-2): 101-109.

Gabbott, I. (2007). Designer Granules : Beating the trade-off between granule strength and dissolution time. . Chemical and Process Engineering. Sheffield, University of Sheffield. PhD: 171.

Gao, P. & Meury, R.H. (1996). Swelling of hydroxypropyl methylcellulose matrix tablets. 1. Characterization of swelling using a novel optical imaging method. Journal of Pharmaceutical Sciences 85(7): 725-731

Gao, P. and R. H. Meury (1996). J. Pharm. Sci. 85: 725.

Gianfrancesco, A., G. Vuataz, et al. (2012). "New methods to assess water diffusion in amorphous matrices during storage and drying." Food Chemistry 132(4): 1664-1670.

Gonnissen, Y., J. P. Remon, et al. (2008). "Effect of maltodextrin and superdisintegrant in directly compressible powder mixtures prepared via co-spray drying." European Journal of Pharmaceutics and Biopharmaceutics 68(2): 277-282.

Gordon and Taylor (1952). "Ideal copolymer and the second order transitions of synthetic rubbers. 1. Non-crystalline copolymer." Journal of Applied Chemistry 2: 493.

Gordon, M.S., Chatterjee, B., & Chowhan, Z.T. 1990. Effect of the mode of croscarmellose sodium incorporation on tablet dissolution and friability. Journal of Pharmaceutical Sciences 79(1): 43-47

Handbook of Pharmaceutical excipients , Ainley Wade and Paul J. Wedder eds, 2nd Ed, 1994

Hardy, I. J., W. G. Cook, et al. (2006). "Compression and compaction properties of plasticised high molecular weight hydroxypropylmethylcellulose (HPMC) as a hydrophilic matrix carrier." International Journal of Pharmaceutics 311(1–2): 26-32.

Herman, M. F. and S. F. Edwards (1990). "A reptation model for polymer dissolution." Macromolecules 23(15): 3662-3671.

Hogekamp, S. and H. Schubert (2003). "Rehydration of Food Powders." Food Science and Technology International 9(3): 223-235.

Iyad, R., A.-R. Mayyas, et al. (2008). "Chitin-silicon dioxide coprecipitate as a novel superdisintegrant." Journal of Pharmaceutical Sciences 97(11): 4955-4969.

Johnson, J. R., L.-H. Wang, et al. (1991). "Effect of formulation solubility and hygroscopicity on disintegrant efficiency in tablets prepared by wet granulation, in terms of dissolution." Journal of Pharmaceutical Sciences 80(5): 469-471.

Kachrimanis, K., M. F. Noisternig, et al. (2006). "Dynamic moisture sorption and desorption of standard and silicified microcrystalline cellulose." European Journal of Pharmaceutics and Biopharmaceutics 64(3): 307-315.

Kakhi, M. (2009). "Classification of the flow regimes in the flow-through cell." European Journal of Pharmaceutical Sciences 37(5): 531-544.

Kazarian, S. G. and J. v. d. Weerd (2007). "Simultaneous FTIR Spectroscopic Imaging and Visible Photography to Monitor Tablet Dissolution and Drug Release." Pharm. Res. 25(4):853-860

Koynov, A., F. Romanski, et al. (2013). "Effects of particle size disparity on the compaction behavior of binary mixtures of pharmaceutical powders." Powder Technology 236(0): 5-11.

Kravtchenko, T. P., J. Renoir, et al. (1999). "A novel method for determining the dissolution kinetics of hydrocolloid powders." Food Hydrocolloids 13(3): 219-225.

Lee, H.-R. and Y.-D. Lee (1991). "Mathematical models and experiments for swelling phenomena before dissolution of a polymer film." Chemical Engineering Science 46(7): 1771-1779.

Lee, P. I. and N. A. Peppas (1987). "Prediction of polymer dissolution in swellable controlled-release systems." Journal of Controlled Release 6(1): 207-215.

Luginbühl, R. and H. Leuenberger (1994). "Use of percolation theory to interpret water uptake, disintegration time and intrinsic dissolution rate of tablets consisting of binary mixtures." Pharmaceutica Acta Helvetiae 69(3): 127-134.

Lundqvist, Å. E. K., F. Podczeck, et al. (1997). "Influence of disintegrant type and proportion on the properties of tablets produced from mixtures of pellets." International Journal of Pharmaceutics 147(1): 95-107.

Malamataris, S. and T. Karidas (1994). "Effect of particle size and sorbed moisture on the tensile strength of some tableted hydroxypropyl methylcellulose (HPMC) polymers." International Journal of Pharmaceutics 104(2): 115-123.

Manuel, E. and S. Konstantinos (2009). "An investigation into the swelling properties, dimensional changes, and gel layer evolution in chitosan tablets undergoing hydration." Advances in Polymer Technology 28(1): 32-39.

Marabi, A. (2008). Dissolution of food powders Processes and modeling. Food and Environmental Quality Sciences. Jerusalem, Hebrew University of Jerusalem. PhD: 123.

Marabi, A., G. Mayor, et al. (2008). "Assessing dissolution kinetics of powders by a single particle approach." Chemical Engineering Journal 139(1): 118-127.

Melia, C. D. and S. S. Davis (1989a). "Review article: mechanisms of drug release from tablets and capsules. 2. Dissolution." Alimentary Pharmacology & Therapeutics 3(6): 513-525.

Melia, C. D. and S. S. Davis (1989b). "Review article: mechanisms of drug release from tablets and capsules. I: Disintegration." Alimentary Pharmacology & Therapeutics 3(3): 223-232.

Mesnier, X., T. O. Althaus, et al. (2013). "A novel method to quantify tablet disintegration." Powder Technology 238(0): 27-34.

Michrafy, A., Michrafy, M., Kadiri, M.S., Dodds, J.A. (2007) “Predictions of tensile strength of binary tablets using linear and power law mixing rules”. Int J Pharm. 333(1-2):118-26

Mikac, U., A. Demsar, et al. (2007). "A study of tablet dissolution by magnetic resonance electric current density imaging." Journal of Magnetic Resonance 185(1): 103-109.

Mikac, U., A. Sepe, et al. (2010). " A new approach combining different MRI methods to provide detailed view on swelling dynamics of xanthan tablets influencing drug release at different pH and ionic strength." Journal of Controlled Release 145(3):247-256

Miller-Chou, B. A. and J. L. Koenig (2003). "A review of polymer dissolution." Progress in Polymer Science 28(8): 1223-1270.

Mollan, M. J. and M. Celik (1993). "Characterization of directly Compressible Maltodextrins Manufactured by three different Processes." Drug Development and Industrial Pharmacy 19(17): 2335 - 2358.

Moore, T., S. Croy, et al. (2000). "Experimental investigation and mathematical modeling of Pluronic® F127 gel dissolution: drug release in stirred systems." Journal of Controlled Release 67(2-3): 191-202.

Moussa, I. S. and L. H. Cartilier (1996). "Characterization of moving fronts in cross-linked amylose matrices by image analysis." Journal of Controlled Release 42(1): 47-55.

Opota, D. O., H. Maillols, et al. (1997). "Effect of temperature on the dissolution of theophylline tablets containing three different molecular weights of hydroxypropylcellulose as binder." Pharmaceutica Acta Helvetiae 72(2): 87-93.

Palzer, S. (2005). "The effect of glass transition on the desired and undesired agglomeration of amorphous food powders." Chemical Engineering Science 60(14): 3959-3968.

Palzer, S. (2006). "Agglomeration of dehydrated consumer foods" In Salman, A. D., Hounslow M. J., & Seville, J. P. K. (First Edition) Granulation (Amsterdam, Elsevier) 591 - 672

Palzer, S. (2009). "Influence of material properties on the agglomeration of water-soluble amorphous particles." Powder Technology 189(2): 318-326.

Palzer, S. (2010). "The relation between material properties and supra-molecular structure of water-soluble food solids." Trends in Food Science & Technology 21(1): 12-25.

Papadimitriou, E., M. Efentakis, et al. (1992). "Evaluation of maltodextrins as excipients for direct compression tablets and their influence on the rate of dissolution." International Journal of Pharmaceutics 86(2-3): 131-136.

Peppas, N. A. and P. Colombo (1989). "Development of disintegration forces during water penetration in porous pharmaceutical systems." Journal of Controlled Release 10(3): 245-250.

Pesonen, T., P. Paronen, et al. (1989). "Disintegrant properties of an agglomerated cellulose powder." International Journal of Pharmaceutics 57(2): 139-147.

Patel, S. and Bansal, A.K. (2011). Prediction of mechanical properties of compacted binary mixtures containing high-dose poorly compressible drug. International Journal of Pharmaceutics, 403, 109-114

Pitt, K. and Sinka C. (2006). “Tabletting”. In Salman, A. D., Hounslow M. J., & Seville, J. P. K. (First Edition) Granulation (Amsterdam, Elsevier) 735 - 778

Rong, Y., M. Sillick, et al. (2009). "Determination of Dextrose Equivalent Value and Number Average Molecular Weight of Maltodextrin by Osmometry." Journal of Food Science 74(1): C33-C40.

Roos, Y. (1995a). "Characterization of food polymers using state diagrams." Journal of Food Engineering 24(3): 339-360.

Roos, Y. H. (1995b). Physical State and Molecular Mobility. Phase Transitions in Foods. San Diego, Academic Press: 19-48.

Roos, Y. H. and C. Benjamin (2003). WATER ACTIVITY | Principles and Measurement. Encyclopedia of Food Sciences and Nutrition. Oxford, Academic Press: 6089-6094.

Ryshkewitch (1953). Compression Strength of Porous Sintered Alumina and Zirconia. Journal of the American Ceramic Society 36 (2): 65-68

Schott, H. (1992). "Kinetics of swelling of polymers and their gels." Journal of Pharmaceutical Sciences 81(5): 467-470.

Siepmann J., and Siepmann F. (2013). Mathematical modeling of drug dissolution, International Journal of Pharmaceutics, 453 (1): 12-24

Sinka, I. C., J. C. Cunningham, et al. (2004). "Analysis of tablet compaction. II. Finite element analysis of density distributions in convex tablets." Journal of Pharmaceutical Sciences 93(8): 2040-2053.

Smallenbroek, A. J., G. K. Bolhuis, et al. (1981). "The effect of particle size of disintegrants on the disintegration of tablets." Pharmaceutisch Weekblad 3(1): 1048-1051.

Sriamornsak, P., N. Thirawong, et al. (2007). "Swelling and erosion of pectin matrix tablets and their impact on drug release behavior." European Journal of Pharmaceutics and Biopharmaceutics 67(1): 211-219.

Steendam, R., H. W. Frijlink, et al. (2001). "Plasticisation of amylodextrin by moisture. Consequences for compaction behaviour and tablet properties." European Journal of Pharmaceutical Sciences 14(3): 245-254.

Sugano, K. (2008). "Theoretical comparison of hydrodynamic diffusion layer models used for dissolution simulation in drug discovery and development." International Journal of Pharmaceutics 363(1–2): 73-77.

Thibert, R. and B. C. Hancock (1996). “Direct visualization of superdisintegrant hydration using environmental scanning electron microscopy.” Journal of Pharmaceutical Sciences 85(11):1255-1258

Tu, Y.-O. and A. C. Ouano (1977). "Model for the kinematics of polymer dissolution." IBM J. Res. Dev. 21(2): 131-142.

Ueberreiter (1968). The solution process. In: Crank J, Park GS, Diffusion in polymers. New York, NY: Academic Press: 219–57.

Villiers, A. (2003). "Effect of compression force, humidity and disintegrant concentration on the disintegration and dissolution of directly compressed furosemide tablets using croscarmellose sodium as disintegrant " Tropical Journal of Pharmaceutical Research 2(1):125-135

Weitschies, W., V. Hartmann, et al. (2001). "Determination of the disintegration behavior of magnetically marked tablets." European Journal of Pharmaceutics and Biopharmaceutics 52(2): 221-226.

Wilson, D., S. Wren, et al. (2012). "Linking Dissolution to Disintegration in Immediate Release Tablets Using Image Analysis and a Population Balance Modelling Approach." Pharmaceutical Research 29(1): 198-208.

Wu, C.-Y., S. M. Best, et al. (2005). "A simple predictive model for the tensile strength of binary tablets." European Journal of Pharmaceutical Sciences 25(2-3): 331-336.

Yamamoto, Y., M. Fujii, et al. (2009). "Effect of powder characteristics on oral tablet disintegration." International Journal of Pharmaceutics 365(1-2): 116-120.

Yunxia, B., Y. Yorinobu, et al. (1999). "Rapidly disintegrating tablets prepared by the wet compression method: Mechanism and optimization." Journal of Pharmaceutical Sciences 88(10): 1004-1010.

Zhao, N. and L. L. Augsburger (2006). "The influence of granulation on super disintegrant performance." Pharmaceutical Development and Technology 11(1): 47-53.

Zimmer, L., P. Belniak, et al. (2011). "Superdisintegrants in new solid dosageforms - A review." Annales Universitatis Mariae Curie-Sklodowska, Sectio DDD: Pharmacia 24(2): 75 - 81.

Zuleger, S., R. Fassihi, et al. (2002). "Polymer particle erosion controlling drug release. II. Swelling investigations to clarify the release mechanism." International Journal of Pharmaceutics 247(1-2): 23-37.

APPENDIX

Appendix A1: Dissolution profiles at different porosities

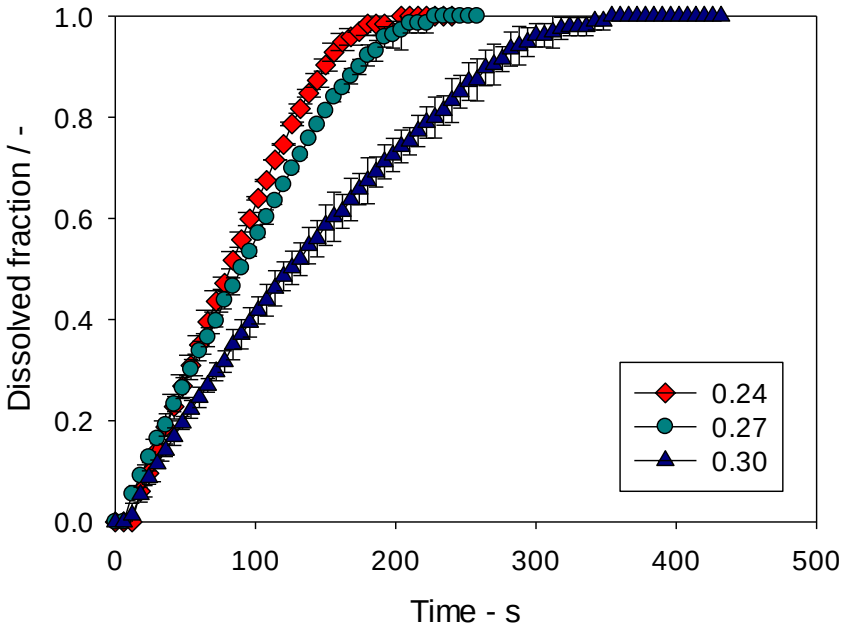

This graph shows examples of the full dissolution profiles of tablets of maltodextrin at different porosities.

Appendix A2: Dissolution profiles at different temperatures

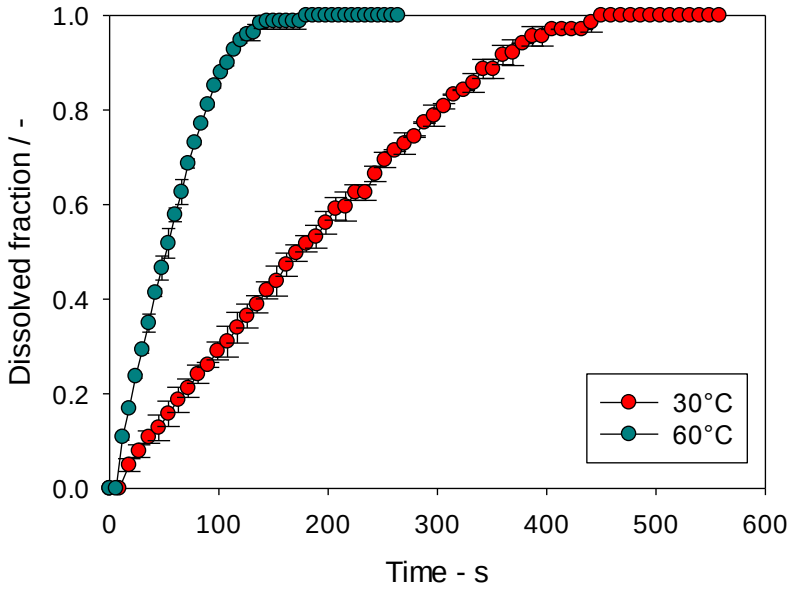

This graph shows examples of the full dissolution profiles of tablets of maltodextrin for different water temperature conditions.

Appendix A3: Dissolution profiles at different rotation speeds

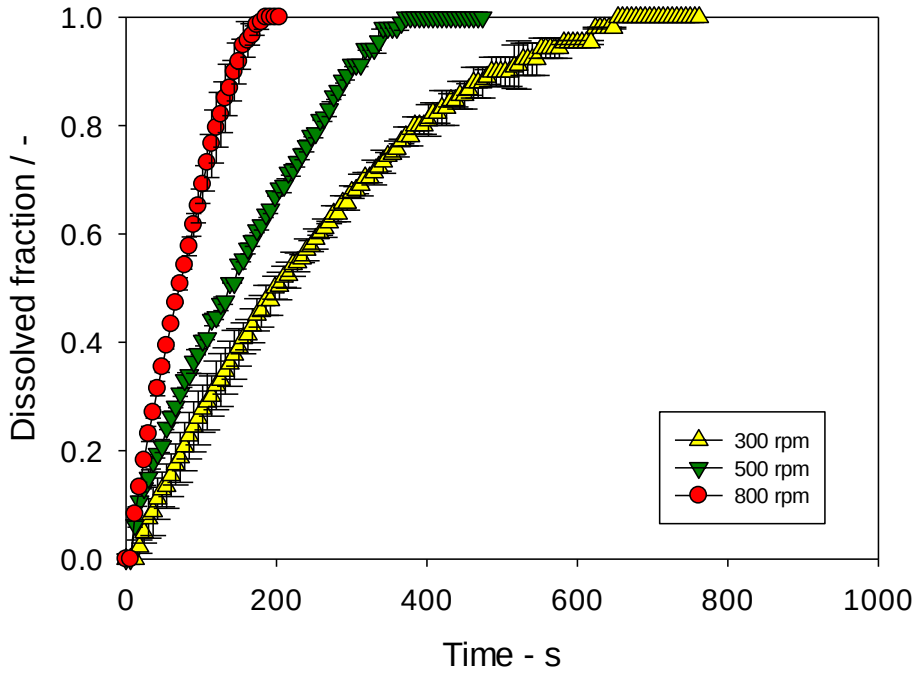

This graph shows examples of the full dissolution profiles of tablets of maltodextrin at different rotation speeds.

Appendix B: Matlab program for image analysis

```
clear all, close all;

%%

tic

pixelspermm=370;% correspondance pixels to mm, to be adjusted
Menan

sum_particles=0;

files = dir('*.JPG');

for i = 1:numel(files)

I=imread(files(i).name);

%I1=imcrop(I,[386.5 14.5 4236 3240]);

%% Convert into grey scale

I2 = .2989*I(:,:,1)...
    +.5870*I(:,:,2)...
    +.1140*I(:,:,3);

%% image contrats enhancing
I_imadjust = imadjust(I2);

%% binary image

%level = graythresh(I_imadjust);
bw = im2bw(I_imadjust,0.25); %replaced level by 0.09% to be
adjusted Menan

%% Image correction

% remove all object containing fewer than 50 pixels
ic = bwareaopen(bw,100); %% can improve this as it could be used
later after regionprops

% fill any holes, so that regionprops can be used to estimate
% the area enclosed by each of the boundaries
ic2 = imfill(ic,'holes');


%% Label objects

[labeled,numObjects] = bwlabel(ic2,8); % 8-connected

numpart=numObjects; %number of particles

RGB_label = label2rgb(labeled, @bone, 'b', 'shuffle'); %to show
the
```

```
%different regions in different colors (good for presentation but
not use
%during the analysis to reduce the processsing cost...)


%% sumparticles

sum_particles=sum_particles+numpart;

%% measurements area particles and tablet

particlesdata = regionprops(labeled,'area'); %'FilledArea',
'centroid','Perimeter'

allparticles = [particlesdata.Area];


max_area= max(allparticles); % Find the maximum area of all the
particles which thus corresponds to the tablet area


realparticles=find(allparticles<max_area); %gather all particle
different from tablet
arearp=[particlesdata(realparticles).Area];

% mean area of particles
Mean_areas_particles=mean(arearp);

% transform pixels2 to mm2
areas_m=allparticles./(pixelspermm*pixelspermm);
max_area_m=max_area./(pixelspermm*pixelspermm);
particles_area_m=arearp./(pixelspermm*pixelspermm);
Mean_areas_particles_m=Mean_areas_particles./(pixelspermm*pixelsp
ermm);

%% measurements tablet dimensions

I3=bwboundaries(labeled);

for x=1:length(I3); %first check the length of the cells in I3 or
it is equal to numobjects
    A(x,1)=length(I3{x,1});
end

B=max(A(:,1)); %Find the largest cell

for x=1:length(I3);
    A(x,1)=length(I3{x,1});

    if A(x,1)==B; % find which cell correspond to the largest and
select it as I4
        I4=I3{x,1};
    end

end

%% determination of the width
```

```
%separate in two parts left and right from the middle of the
image 2248
z=length(I4);
k=1;
l=1;

minx=min(I4(:,2));
maxx=max(I4(:,2));
meanx=(minx+maxx)/2; %determination of the middle of the tablet
on the x axis to seperate the tablet into 2.

% creation of I6 and I7 with, I6 contains coordinates of the left
part and
% I7 of the right part
for x=1:z
    if I4(x,2)<=meanx
        I6(k,1)=I4(x,1); I6(k,2)=I4(x,2);
        k=k+1;
    else I7(l,1)=I4(x,1); I7(l,2)=I4(x,2);
        l=l+1;
    end
end

% Determination of the ymin and ymax for the left part

%% I6

binsize=10;
bin=3300/binsize; %3300 is slightly larger than the photo size

jbin=zeros(bin,1); %create jbin to contain data

           % insertion of nbre of pixels per bin
for m=1:length(I6);
    for j=1:bin;
        if I6(m,1)>=(j-1)*binsize && I6(m,1)<j*binsize;
            jbin(j,1)=jbin(j,1)+1;
        end
    end
end



        % find the boundaries of the images, boundaries of jbin
to find out
        % its centre. boundaries are found by beeing the first
bin where
        % the values is different from 0
flag=0;

for p=1:bin
    if flag==0;
        if jbin(p,1)~=0;
        jleft=p;
        flag=1;
        end
    else flag=1;
        if jbin(p,1)==0;
```

```
        jright=p;
        flag=2;
        end
    end
end

jcentre=(jright+jleft)/2;
jcentre1=round(jcentre);

       %define whether the derivative is whitin the treshold
+10/-10

%bsup=10;
%binf=-10;

%Smoothjbin=smooth(jbin,10,'moving');

Difjbin=diff(jbin);

diffjbin=single(Difjbin); %convert to single precision

% plot(Diffjbin)

bsup=100;
binf=-100;

drapeau=0;

for w=jcentre1:-1:jleft
    if drapeau==0;
        if diffjbin(w)>=bsup || diffjbin(w)<=binf;
           ym=w;
           drapeau=1;
        end
    end
end

 ymin=ym*binsize;

 bandera=0;

 for q=jcentre1:1:jright
    if bandera==0;
        if diffjbin(q)>=bsup || diffjbin(w)<=binf;
           ymx=q;
           bandera=1;
        end
    end
end

 ymax=ymx*binsize;

 n=1;

for r=1:length(I6)
    if I6(r,1)>=ymin && I6(r,1)<=ymax;
        I8(n,1)=I6(r,1); I8(n,2)=I6(r,2);
        n=n+1;
```

```
    end
end

meanleft=mean(I8(:,2));

%% I7

binsize1=10;
bin1=3300/binsize1;

jbin1=zeros(bin1,1); %create jbin to contain data

           % insertion of nbre of pixels per bin
for a=1:length(I7);
    for j=1:bin1;
        if I7(a,1)>=(j-1)*binsize1 && I7(a,1)<j*binsize1;
            jbin1(j,1)=jbin1(j,1)+1;
        end
    end
end


flag1=0;

for d=1:bin1
    if flag1==0;
        if jbin1(d,1)~=0;
        jleft1=d;
        flag1=1;
        end
    else flag1=1;
        if jbin1(d,1)==0;
        jright1=d;
        flag1=2;
        end
    end
end

jcentre1=(jright1+jleft1)/2;
jcentre11=round(jcentre1);

       %define whether the derivative is whitin the treshold
+10/-10


Difjbin1=diff(jbin1);
diffjbin1=single(Difjbin1);


bsup1=100;
binf1=-100;

drapeau1=0;

for b=jcentre11:-1:jleft1
    if drapeau1==0;
        if diffjbin1(b)>=bsup1 || diffjbin1(b)<=binf1;
           ymr=b;
```

```
            drapeau1=1;
        end
    end
end

 yminr=ymr*binsize1;


 bandera1=0;

 for c=jcentre11:1:jright1
    if bandera1==0;
        if diffjbin1(c)>=bsup || diffjbin1(c)<=binf;
           ymrx=c;
           bandera1=1;
        end
    end
 end


 ymaxr=ymrx*binsize1;

 e=1;

for f=1:length(I7)
    if I7(f,1)>=yminr && I7(f,1)<=ymaxr;
        I9(e,1)=I7(f,1); I9(e,2)=I7(f,2);
        e=e+1;
    end
end

meanright=mean(I9(:,2));

width=meanright-meanleft;



%% determination of the thickness

%separate in two parts left and right from the middle of the
image 2248
z=length(I4);
k=1;
l=1;

miny=min(I4(:,1));
maxy=max(I4(:,1));
meany=(miny+maxy)/2;


% creation of I16 and I17 with, I19 contains coordinates of the
bottom part and
% I18 of the top part



for x=1:z
```

```
    if I4(x,1)<=meany %is it I4(x,1) and change value for
threshold: z axis/2
        I16(k,1)=I4(x,1); I16(k,2)=I4(x,2);
        k=k+1;
    else I17(l,1)=I4(x,1); I17(l,2)=I4(x,2);
        l=l+1;
    end
end



%% I16 for top

binsizeB=10;
binB=5000/binsizeB;

jbinB=zeros(binB,1); %create jbin to contain data

           % insertion of nbre of pixels per bin
for m=1:length(I16);
    for j=1:binB;
        if I16(m,2)>=(j-1)*binsizeB && I16(m,2)<j*binsizeB;
            jbinB(j,1)=jbinB(j,1)+1;
        end
    end
end



        % find the boundaries of the images, boundaries of jbin
to find out
        % its centre. boundaries are found by beeing the first
bin where
        % the values is different from 0
flagB=0;

for p=1:binB
    if flagB==0;
        if jbinB(p,1)~=0;
        jleftB=p;
        flagB=1;
        end
    end
end

for p=jleftB:binB
    if flagB==1;
        if jbinB(p,1)==0;
        jrightB=p;
        flagB=2;
        end
    end
end

jcentreB=(jrightB+jleftB)/2;
jcentre1B=round(jcentreB);
```

```
DifjbinB=diff(jbinB);

diffjbinB=single(DifjbinB);
bsupB=75;
binfB=-75;

drapeauB=0;

for w=jcentre1B:-1:jleftB
    if drapeauB==0;
        if diffjbinB(w)>=bsupB || diffjbinB(w)<=binfB;
           xm=w;
           drapeauB=1;
        end
    end
end

 xminB=xm*binsizeB;


 banderaB=0;

for q=jcentre1B:1:jrightB
    if banderaB==0;
        if diffjbinB(q)>=bsupB || diffjbinB(w)<=binfB;
           xmx=q;
           banderaB=1;
        end
    end
end

 xmaxB=xmx*binsizeB;

 m=1;

for r=1:length(I16)
    if I16(r,2)>=xminB && I16(r,2)<=xmaxB;
        I18(m,1)=I16(r,1); I18(m,2)=I16(r,2);
        m=m+1;
    end
end

meanbottom=mean(I18(:,1));

%% I17 for bottom part

binsize1B=10;
bin1B=5000/binsize1B;

jbin1B=zeros(bin1B,1); %create jbin to contain data

           % insertion of nbre of pixels per bin
for a=1:length(I17);
    for j=1:bin1B;
        if I17(a,2)>=(j-1)*binsize1B && I17(a,2)<j*binsize1B;
            jbin1B(j,1)=jbin1B(j,1)+1;
        end
    end
```

```
end


flag1B=0;

for d=1:bin1B
    if flag1B==0;
        if jbin1B(d,1)~=0;
        jleft1B=d;
        flag1B=1;
        end
    end
end

for d=jleft1B:bin1B
    if flag1B==1;
        if jbin1B(d,1)==0;
        jright1B=d;
        flag1B=2;
        end
    end
end

jcentre1B=(jright1B+jleft1B)/2;
jcentre11B=round(jcentre1B);

       %define whether the derivative is whitin the treshold
+10/-10


Difjbin1B=diff(jbin1B);
diffjbin1B=single(Difjbin1B);


bsup1B=100;
binf1B=-100;

drapeau1B=0;

for b=jcentre11B:-1:jleft1B
    if drapeau1B==0;
        if diffjbin1B(b)>=bsup1B || diffjbin1B(b)<=binf1B;
           xmb=b;
           drapeau1B=1;
        end
    end
end

 xminbB=xmb*binsize1B;


 bandera1B=0;

 for c=jcentre11B:1:jright1B
    if bandera1B==0;
        if diffjbin1B(c)>=bsup1B || diffjbin1B(c)<=binf1B;
           xmbx=c;
           bandera1B=1;
```

```
        end
    end
end

 xmaxbB=xmbx*binsize1B;

 e=1;

for f=1:length(I17)
    if I17(f,2)>=xminbB && I17(f,2)<=xmaxbB;
        I19(e,1)=I17(f,1); I19(e,2)=I17(f,2);
        e=e+1;
    end
end

meantop=mean(I19(:,1));

thickness=meantop-meanbottom;

%% write

widthmm=width/pixelspermm;
thicknessmm=thickness/pixelspermm;

dlmwrite('output_area.csv', areas_m, '-append','newline','pc');

dlmwrite('output_maxarea.csv', max_area_m, '-
append','newline','pc')

dlmwrite('output_partarea.csv',particles_area_m , '-
append','newline','pc')


dlmwrite('output_numparticles.csv', numpart, '-
append','newline','pc')

dlmwrite('output_sumparticle.csv', sum_particles, '-
append','newline','pc')


dlmwrite('output_thickness.csv', thickness, '-
append','newline','pc');

dlmwrite('output_width.csv', width, '-append','newline','pc');

dlmwrite('output_toc.csv', toc, '-append','newline','pc');

%%

%f = figure('Visible','off');

figure

subplot(3,3,1), imshow(I),title('Raw
Image','FontWeight','bold','FontSize',8);
subplot(3,3,2),
imshow(bw),title('Objects','FontWeight','bold','FontSize',8);
```

```
subplot(3,3,3),
imshow(RGB_label),title('Objects','FontWeight','bold','FontSize',
8);

subplot(3,3,4), plot(I4(:,1),I4(:,2)),title('tablet
contour','FontWeight','bold','FontSize',8);

subplot(3,3,5), plot(I8(:,1),I8(:,2)),title('left
part','FontWeight','bold','FontSize',8);
subplot(3,3,6), plot(I9(:,1),I9(:,2)),title('right
part','FontWeight','bold','FontSize',8);

subplot(3,3,7), plot(I18(:,1),I18(:,2)),title('top
part','FontWeight','bold','FontSize',8);
subplot(3,3,8), plot(I19(:,1),I19(:,2)),title('bottom
part','FontWeight','bold','FontSize',8);

filename = sprintf(files(i).name,i);

print('-dtiff',['analy' filename]);

close all;


toc

end
```

Appendix C: Example of data obtained after image analysis

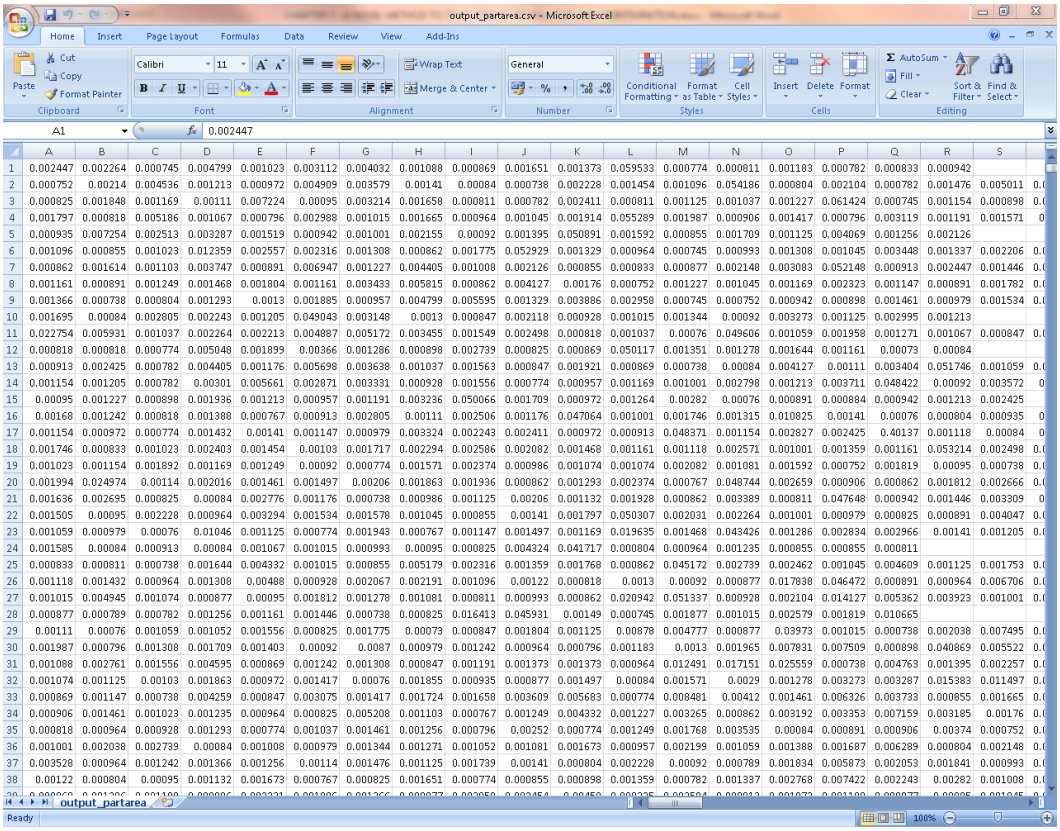

Appendix D: Fortran program to organise data from image analysis

psd_large.f

```
      implicit real*8(a-h,o-z)
      parameter(nx=2000,ny=5000,sizemin=0.0001,sizemax=1,ibin=100,
     &          imagestep=900)
      parameter(MAXLINE=50000,SMALL=sizemin*1d-5)
      dimension::psd(nx,ny)
      dimension::graph(ibin)
      dimension::sizeclass(ibin)

      character(MAXLINE) line

      open(unit=7,file='output_partarea.csv',status='unknown')
      open(unit=99,file='temp.txt',status='unknown')

      psd=0

      icount=0
  900 icount=icount+1
      read(7,'(A)',end=998) line
      read(line,*,end=999) (psd(i,icount),i=1,nx)

  999 continue
      write(6,*) icount
      Go to 900

  998 continue
      write(6,*) icount

      sizeincre=(sizemax-sizemin)/ibin
      do m=1,ibin
        sizeclass(m)=sizemin+(sizeincre*(m-1))
      end do

      idata=1

      do n=1,icount
        if(n.eq.1) then
          call OUTPUT(idata)
          graph=0
        end if
```

```
   do i=1,nx
     if(psd(i,n).gt.SMALL) then
       do m=1,ibin
         if((psd(i,n).gt.sizeclass(m)-sizeincre/2.).and.
&           (psd(i,n).lt.sizeclass(m)+sizeincre/2.)) then
           graph(m)=graph(m)+1
         end if
       end do
     end if
   end do

   if(n.gt.idata*imagestep) then
     idata=idata+1
     do m=1,ibin
       write (70,*) sizeclass(m),graph(m)
     end do
     close(unit=70)
     call OUTPUT(idata)
     graph=0
   end if
 end do

 do m=1,ibin
   write(70,*) sizeclass(m), graph(m)
 end do

 close(unit=7)
 close(unit=99)
 close(unit=70)

 stop
 end
```

```
************************
*  Making output file  *
************************

      subroutine OUTPUT(k)

      IMPLICIT NONE
      integer kk,kk2,kk1,kkk,extime,k,kk0
      double precision delt
      character*3 name
      common/TIME_STEP/delt

      extime=k-1

      kk=int(extime)

      kk2=kk/100
      kk1=kk-kk2*100
      kk0=kk1/10
      kkk=kk1-kk0*10

      name=''//char(kk2+48)//char(kk0+48)//char(kkk+48)//''

      write(6,*) name

      open(70,file='./output/output'//name//'.csv')

      return
      end
```